Joachim Schuster, BSc

Optimizing characterization methodology to test a low drug loaded oromucosal sustained release film at various levels: A core study on a clonidine paediatric oromucosal film formulation

MASTERARBEIT

zur Erlangung des akademischen Grades

Master of Science

Masterstudium Biochemie und Molekulare Biomedizin

eingereicht an der

Technischen Universität Graz

Betreuer

Univ. Prof. Dr. Andreas Zimmer

Institut für Pharmazeutische Wissenschaften

Graz, März 2017

EIDESSTATTLICHE ERKLÄRUNG

Ich erkläre an Eides statt, dass ich die vorliegende Arbeit selbstständig verfasst, andere als die angegebenen Quellen/Hilfsmittel nicht benutzt, und die den benutzten Quellen wörtlich und inhaltlich entnommenen Stellen als solche kenntlich gemacht habe. Das in TUGRAZonline hochgeladene Textdokument ist mit der vorliegenden Masterarbeit identisch.

Datum

Unterschrift

Table of contents

i. Acknowledgment

The present master thesis was performed at the Department of Pharmaceutics at UCL School of Pharmacy in London, UK in collaboration with the Department of Pharmaceutical Technology & Biopharmacy at the University of Graz and the Research Center Pharmaceutical Engineering (RCPE) in Graz. The thesis was supervised by Univ. Prof. Andreas Zimmer from the University of Graz, Dr. Mine Orlu Gul and Dr. Min Zhao from UCL School of Pharmacy and Dr. Amrit Paudel and Dr. Annalisa Mercuri from RCPE.

First of all I want to thank my academic supervisor, Prof. Zimmer for giving me the opportunity to work abroad and being part of his research group. I am extremely grateful to RCPE for funding this work and the great support throughout my studies. Thank you to all supervisors for their willingness to supervise this work and for making this collaboration possible in the first place.

I especially want to thank Dr. Mine Orlu Gul and Dr. Min Zhao for their time, helpful discussions, creating a great working atmosphere in London and overall scientific and non-scientific advice and guidance.

A special thanks to Dr. Simone Pival-Marko from RCPE for establishing the collaboration, advices and general helpfulness. Thank you to Mr. David McCarthy from UCL School of Pharmacy for the SEM images. Thanks to all my colleagues from UCL in London for their kindness and most importantly for providing a great working atmosphere and making me feel welcome.

Thank you to my parents Andrea and Heinz, my sister Nicole and my friends for your continuous support and encouragement over all these years.

Finally I want to thank Neira for your never-ending support, patience and love.

ii. List of abbreviations

AFM	atomic force microscopy
API	active pharmaceutical ingredient
ATR-FTIR	attenuated total reflection-fourier transform infrared
BCS	biopharmaceutics classification system
CUT	content uniformity test
DMTA	dynamic mechanical thermal analysis
DSC	differential scanning calorimetry
DVS	dynamic vapour sorption
E*	complex modulus (or dynamic modulus)
E'	storage modulus (or elastic modulus)
E''	loss modulus
ELSD	evaporative light scattering detector
EMA	european medicines agency
European Pharmacopoeia	Ph. Eur.
HPLC	high performance liquid chromatography
i.m.	intramuscular
i.v.	intravenous
IR	infrared
LTA	localized thermal analysis
MBF	mucoadhesive buccal film
MCG	membrane-coating granule
MS	mass spectrometry
MTDSC	modulated temperature DSC
NBE	new biological entity
NF-κB	nuclear factor kappa-light-chain-enhancer of activated B cells
NME	new molecular entity
NP	normal phase
ODF	oral dispersible film
OTF	oral thin film
P	partition coefficient
pI	isoelectric point
pKa	logarithmic acid dissociation constant
RH	relative humidity
RP	reversed phase
RSD	relative standard deviation
SD	standard deviation
SEM	scanning electrom microscope
SEM-EDS	scanning electron microscope - energy-dispersive X-ray spectroscopy
SOI	site of interest
T_g	glass transition temperature
TGA	thermogravimetric analysis
T_m	melting temperature
ToF-SIMS	time-of-flight secondary ion mass spectrometry
TTM	transition temperature microscopy
UV-Vis	ultraviolet-visible
WHO	world health organization
XRPD	X-ray powder diffraction

iii. List of figures

iv. List of tables

1 Abstract

Objective of this study was to develop a low dose oromucosal sustained release film. From a physiochemical and clinical perspective clonidine hydrochloride provides a perfectly suitable active pharmaceutical ingredient (API) for an oromucosal formulation. The developed film, loaded with 90 µg (F1), is applicable to treat paediatric patients with pre- and postoperative pain due to its sedative and analgesic effects. The study addressed difficulties in detecting and quantifying such low API concentrations, studying its solid state, thermal properties and uniformity of content. Chitosan, chosen as a film forming polymer, was extensively analyzed using several thermal characterization methods. The glass transition temperature (T_g) of chitosan (154.95 ± 0.47°C) and melting point (T_m) of clonidine hydrochloride (307.6 ± 4.8°C) were measured using dynamic mechanical thermal analysis (DMTA) and differential scanning calorimetry (DSC), respectively. Despite measuring moderately high shear viscosity and dealing with low drug load in F1, uniformity of content was achieved according to the European Pharmacopoeia (Ph. Eur.). Moreover, an analytical platform was established to detect and verify as well as map the homogeneity of such low dose drug distribution within the films developed. Therefore novel *in vitro* methodologies were used: among other things nano thermal analysis (TTM) and scanning electron microscope-energy-dispersive X-ray spectroscopy (SEM-EDS). Finally an *in vitro* drug release test confirmed the desired sustained release. Result of the study was a developed oromucosal film, which reached uniformity of content, displayed good mechanical and morphological properties and provided additional evidence for its applicability as alternative dosage form.

2 Zusammenfassung

Ziel dieser Studie war die Entwicklung eines niedrig dosierten oromukosalen Film mit verzögerter Wirkstofffreisetzung. Aus physiochemischer und klinischer Sicht bietet Clonidine Hydrochlorid einen geeigneten Wirkstoff für eine oromukosale Formulierung. Der entwickelte Film, dosiert mit 90 µg (F1), ist aufgrund seiner beruhigenden und analgetischen Wirkung für pädiatrische Patienten mit prä- und postoperativen Schmerzen anwendbar. Die Studie befasst sich mit der Schwierigkeit der Detektion und Quantifizierung derart niedriger Wirkstoffkonzentrationen durch die Analyse der Festkörperchemie, thermischen Eigenschaften und Einheitlichkeit des Wirkstoffgehaltes. Chitosan, ausgewählt als filmbildendes Polymer, wurde mittels mehrerer thermischer Charakterisierungs-Methoden umfangreich analysiert. Die Glasübergangstemperatur (T_g) von Chitosan (154.95 ± 0.47°C) und der Schmelzpunkt (T_m) von Clonidine Hydrochlorid (307.6 ± 4.8 °C) wurden mittels der dynamisch-mechanisch thermischen Analyse (DMTA) bzw. Differential-Scanning-Kalorimetrie (DSC) gemessen. Trotz der moderat hohen, gemessenen Scherviskosität und der niedrigen Arzneistoffkonzentration in F1, konnte die Einheitlichkeit des Wirkstoffgehaltes gemäß Europäischem Arzneibuch (Ph. Eur.) nachgewiesen werden. Weiters wurde eine analytische Plattform entwickelt, um eine derart niedrig dosierte Arzneistoffdistribution im Film zu detektieren und verifizieren sowie deren Homogenität abzubilden. Hierzu wurden innovative *in vitro* Methoden verwendet, u.a. eine nano thermische Analyse (TTM) und Rasterelektronenmikroskop-Energiedispersive Röntgenspektroskopie (SEM-EDS). Schließlich bestätigte ein *in vitro* Wirkstofffreisetzungs-Test die gewünschte, verzögerte Freisetzung. Ergebnis der Studie war die Entwicklung eines oromukosalen Films, der die Einheitlichkeit des Wirkstoffgehaltes erreichte, gute mechanische und morphologische Eigenschaften aufwies sowie weitere Beweise für die Anwendbarkeit als alternative Darreichungsform lieferte.

3 Introduction

3.1 Oromucosal films and their applicability

Oral thin films (OTFs) describe a fairly new dosage form which has gained a lot of research interest in the last decade. While early on predominantly common in the United States as over-the-counter products and breath-fresheners, the European market share has rapidly increased in the last couple of years [1]. Due to the plethora of publications on oral strip technology its terminology is somewhat confusing. Oral thin film, oral patch, wafer, strip, orodispersible film, oral soluble film, dissofilms, buccal film, mucoadhesive film and transmucosal film are the most common terms that can be found in the literature [2]. While some of these describe certain type of films, others are more general. OTFs or oromucosal preparations [3] are the most used general terms.

OTFs can be subdivided into orodispersible or oromucosal films, whether they are mucoadhesive or not. Given the relatively new research field, the European Pharmacopoeia has updated their monograph accordingly and added “Oromucosal Preparations” to it, in which mucoadhesive buccal films (MBFs) and orodispersible films (ODFs) are defined [4]. ODFs are developed to dissolve as fast as possible when placed on a wet surface, typically the tongue. While buccal administration is the most utilized route, the term MBF is somewhat misleading as these films are applicable for administration at all sites inside the oral cavity [3]. Oromucosal films are mostly prepared using hydrophilic polymers as these films are indented to adhere to the oral mucosa after wetting with saliva [5]. MBFs contain either dispersible or non-dispersible compounds. The ladder requires manual removal of the film after drug release. Permanent film formulations, that is non-dispersible, have been termed oromucosal or oral patch (ORP), although not specified by the European Pharmacopoeia [3]. If shorter residence times are desired the film is slowly eroding at the target site. These films are differentiated from ODFs due to differences in adhesive properties [3]. Both can be designated as oromucosal films though [6] and are intended for local or systemic action. Therefore the drug can be released through and into the oral mucosa or inside the oral cavity and is subsequently swallowed [3]. Those different administrations and several benefits of this novel dosage form allow addressing many research questions. One of which is the delivery to paediatric and geriatric patients.

3.2 Use for paediatric and geriatric patients

One of the main criteria for developing an oromucosal film formulation is drug loading as being limited to approximately 50% per dose weight or to 30 mg for orodispersible films [7, 8]. This restriction does not apply to drugs effective at lower therapeutic doses such as potent drugs and paediatric drugs. Additionally the possibility to bypass the GI tract and

consequently increasing the bioavailability leads to an even lower drug load [9]. Furthermore high drug load is more prone to recrystallization [10]. Due to these aspects the selection of an active pharmaceutical ingredients (APIs) is limited. In that regard oromucosal films are especially suitable for paediatric patients as lower dosages are needed. Moreover known difficulties of drug administration in paediatric and geriatric patients often require specific dosage forms such as oromucosal films [11, 12]. In this regard films provide numerous advantages: circumvention of swallowing, higher dose accuracy than syrups, enhanced paediatric population compliance (> 6 years), possibility of a local action, no need for water, better mouth feel, ease of handling and portability, difficult to spit out, minimized risked of chocking, termination of drug delivery by detachment, precludes hiding dosage form in the oral cavity, etc [3, 6, 7, 12–14].

The importance and need for adjusted medications for pediatric [15] and geriatric patients [11, 16] is based on the heterogeneity within both patient populations. Especially for pediatric patients oromucosal films provide numerous advantages over conventional dosage forms. Its need for pediatric patients has been covered recently [12]. The United States Government Accountability Office (GAO) reported in 2007 that two-thirds of drugs prescribed for children are neither labelled nor studied for pediatric use [17]. Moreover numerous considerations such as the technical feasibility and the patient's needs have to be considered - making this patient population particularly vulnerable [18]. In recent years it has been reported that about 90% of pediatric medicines are targeted for oral administration [19]. More specifically liquids have been considered as the most appropriate dosage form for children by the European Medicines Agency (EMA) [20]. It must be said, however, that liquids are more prone to stability and contamination issues [19] and its administration requires specific devices [12]. In 2008 the World Health Organization (WHO) proposed 'flexible solid dosage forms' as the most suitable dosage form, encouraging a shift of paradigm [21, 22]. Over the last couple of years different dosage forms such as the administration of powder in sachets, multiparticulates as well as orodispersible tablets and films have been investigated [18, 21]. In that regards films provide portability and also the advantage declared as 'ready to go' medicine.

In addition to paediatric patients oromucosal films might be a suitable dosage form for geriatric patients since not only young but also elderly patients suffer from difficulties swallowing dosage forms like tablets, capsules and bigger volumes of liquids [11, 23–25]. The need to focus on alternative dosage forms for elderly is confirmed by the demographic trend in developed and developing countries [16, 26]. Christensen et al predict that by the year 2050 30% of people in Germany are going to be 65 years of age or older [27] (Figure 1). This trend is based on the increase in life expectancy over the last century [27, 28] and the

so called “baby boomer generation” reaching 65 years of age or older [16]. This requires the pharmaceutical industry to address specific medication needs of elderly patients [16].

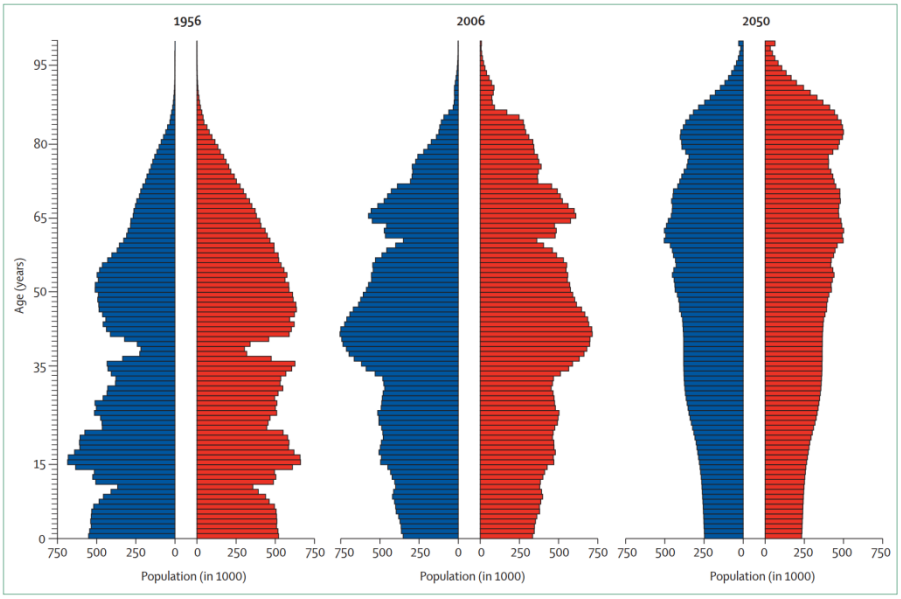

Figure 1: Demographic trend of Germany’s population by 2050. Data published by the Federal Statistical Office, Wiesbaden, Germany [28]. Reproduced from Ref [27]**.**

While oromucosal films are a promising dosage form for paediatric as well as geriatric patients, it appears more suitable for the former. Although applicable to elderly mostly due to circumvention of swallowing [3], impairment of motoric functions are especially critical when handling such thin, light and fragile dosage forms. Problems opening pharmaceutical packaging and handling dosage forms are impacted by cognitive impairment, diseases (Parkinson disease, stroke dementia, etc) and impaired vision [16, 29–31]. Moreover polypharmacy is common in elderly which in connection with poor vision increases the challenge of product identification. Although product identification might be enhanced using colouring agents, contributing to drug safety [32]. All these limitations have to be carefully addressed and remain obstacles to overcome for geriatric patients when handling their own medication. OTFs are more applicable when drug administration is supported by nursing homes or home care. For both patient populations, safety of excipients, palatability, handling of packaging, size of dosage form, etc are aspects to consider in regards of oromucosal drug therapy [11, 21]. Furthermore the EMA published guidelines for excipients, acceptability, container closure systems and measuring devices [33]. Overall OTFs provide a lot of advantages for a wide range of patients. For a large population the ease of administration, portability and the fact that no water is required make OTFs especially appealing.

3.3 OTFs applicability for other research interests and its disadvantages

While not further addressed in this work, it is worth noting that the delivery of macromolecules using MBFs has been thoroughly investigated[34]. Macromolecules are historically administered as parenterals but alternative routes of administration were investigated mainly due to high production costs and administration inconvenience associated with poor patient compliance. Alternative routes include pulmonary, nasal, transdermal, vaginal and transmucosal administration. In the oral cavity buccal administration seems the most promising route to deliver vaccines, peptides and even proteins [34]. MBFs are therefore considered a promising dosage form to administer macromolecules [35]. While overall a promising research field development of macromolecular drug delivery requires distinct expertise. The biggest problem involves poor permeability due to their size and hydrophilic as well as hydrophobic appendages. Moreover short biological half life, loss of tertiary/quatenary structure, immune response, costs, etc highlight the difficulties for macromolecular drug delivery [36–38].

The increasing market interest in new molecular entities (NMEs) and new biological entities (NBEs) [39] underlines the importance to administer highly potent APIs. In that regard MBFs are particularly of interest as highly potent APIs require lower dosages. Poorly water soluble drugs are another research area applicable for OTFs. Benet [40] highlighted the importance for new development strategies as 54% of NMEs are declared as Biopharmaceutics Classification System (BCS) class II drugs. These drugs are characterized with poor solubility and good permeability. In that regard the development of OTFs has been recently used as one of many possibilities to incorporate BCS class II drugs in a dosage form [41]. Moreover OTFs can be produced via 3D printers, which offer the possibilities of personalized medicines. This fact contributes to the patent-centricity [6, 42–44]. In conclusion OTFs address a wide variety of state of the art research questions which highlights its market potential [1, 7].

The main disadvantages of OTFs are their susceptibility to humidity and consequent changes in mechanical properties which can results in tackiness (humid conditions) or brittleness (dry conditions) [45]. To ensure stability and shelf life, adequate packaging is required. At the moment there are several different packaging variants available [46]. Airtight packaging like aluminium sachets protect films from environmental moisture and can be opened directly before administration [45]. Although overall film flexibility is its main disadvantage, in terms of fragility during transportation it is advantageous in comparison to oral disintegration tablets (ODTs) [7]. Other disadvantages include inadequate uniformity of content [47–49] and its novelty which comes with a disagreement of non-standardized characterization methods (e.g. dissolution test [50]) as they are neither clearly defined by

authorities nor biorelevant [46]. The young history of OTFs is also reflected in a limited number of publications covering the galenic development which is especially critical consideration a vast number of polymers to choose from [2].

3.4 Oromucosal drug delivery

3.4.1 Anatomy and physiology of oral mucosa

The total surface area of the oral mucosa (214 cm^2 [51]) is relatively small in comparison to the skin (20,000 cm^2) and GIT (350,000 cm^2) [52, 53]. Within transmucosal drug delivery the buccal mucosa provides the biggest surface area with 50.2 ± 2.9 cm^2 [51]. The oral cavity is an attractive route of administration and includes among others the soft and hard palatal, sublingual and buccal mucosa. Each mucosa is characterized by a different number of layers which each include the epithelium, separated from the connective tissue (lamina propria and submucosa) by the basement membrane (Figure 2). The connective tissue comprises a thickness of 150 - 500 µm [54]. The buccal epithelium is composed of 40 - 50 cell layers with a thickness of 150 - 250 µm [54]. Cumulated this sums up to a total thickness for the buccal mucosa of 500 - 600 µm [55, 56]. The epithelium consists of four morphological layers, which are named starting from the basement membrane: basal layer, prickle cell layer, intermediate layer and superficial layer. The basement membrane consists of three layers, namely lamina lucida, lamina densa and lamina fibroreticularis (not seen in Figure 2). In the keratinized oral mucosa such as hard palatal, the epithelium composition differs in the two outermost morphological layers. The layers starting from the basement membrane are termed: basal layer (stratum basale), prickle cell layer (stratum spinosum), granular layer (stratum granulosum) and keratinized layer (stratum corneum). It is noteworthy that the terms basal lamina and basement membrane are not interchangeable as the basal lamina constitutes a portion of the basement membrane.

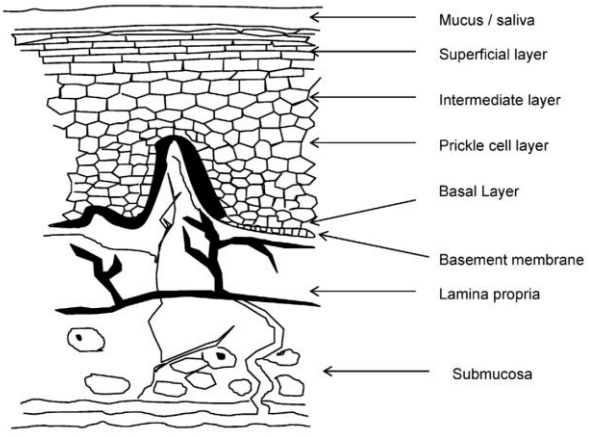

Figure 2: Structure of the buccal mucosa (non-keratinized). Epithelial surfaces are coated by a mucus / saliva layer. Epithelium consists of four layers: superficial, intermediate, prickle cell and basal layer. Deeper layers include the basement membrane and connective tissue (lamina propria and submucosa). Reproduced from Ref [22].

The epithelial surfaces are coated by a mucus / saliva layer with an estimated thickness of 70 - 100 µm [51]. The mucus is an intercellular ground substance and mainly composed of glycoproteins called mucins [57]. Those huge molecules occupy a molecular weight of 0.5 - 20 MDa [58] and provide due to its sulfhydryl groups and sialic acid residues a negative charge at physiological pH. This enables the interaction with the film polymer and is responsible for the mucoadhesion (e.g. buccal adhesion) providing the advantage of a strong interaction and consequently long residence time [59].

Additionally to thickness differences in the oral mucosa the epithelia chemical composition varies as there are keratinized and non-keratinized lining existing within the oral cavity [60]. In the stratum granulosum keratinocytes differentiate into nonvital surface cells or squames which lead to the formation of stratum corneum. Fully keratinized epithelial cells, that is stratum corneum, are located upon the mucus layer [55]. Furthermore the lipid composition varies depending upon the keratinization profile and functions as main permeation barrier (3.4.3). The oral cavity represents three different types of mucosae, namely the masticatory, lining and specialized mucosa [61]. The masticatory mucosa comprises the hard palate and gums whereas the specialized mucosa describes the dorsal surface of the tongue, which is a keratinized epithelium. The lining mucosa comprises non-keratinized epithelia which is one of the reasons that sublingual (under the tongue and on the floor of the mouth) and buccal tissue (located on the inner lining of the cheek) are the most utilized for drug administration within the oral cavity [34]. Additionally the soft palatal comprises also a non-keratinized mucosa [55] (Figure 3). In simplified terms, more flexible and soft tissues are typically non-keratinized epithelia.

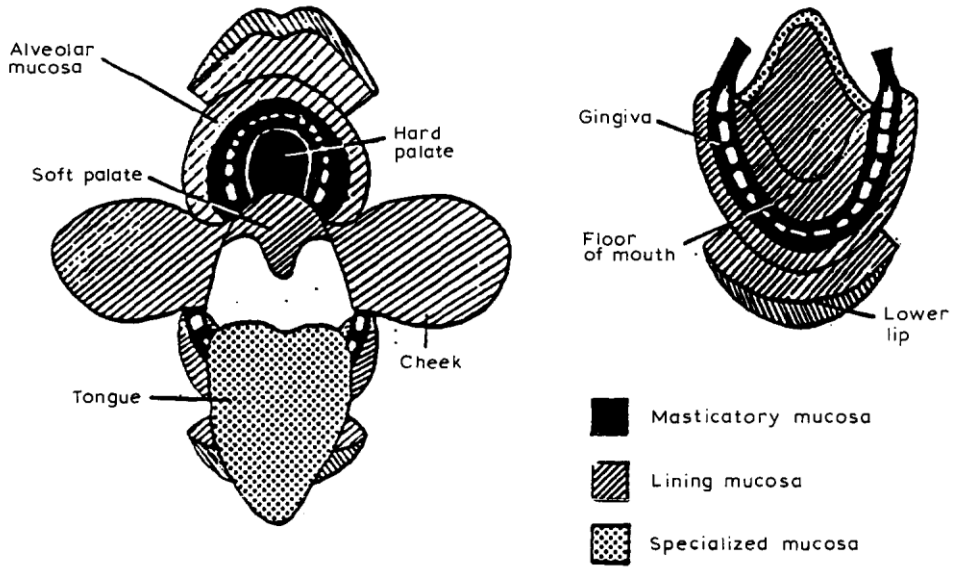

Figure 3: The oral cavity displaying regions occupied by masticatory, lining and specialized mucosa. Reproduced from Ref [62].

Another important aspect in the oral cavity is saliva itself. First and foremost its main role is to lubricate the oral cavity. Lubrication assists at swallowing, movement of food and speaking. Saliva also helps to maintain the integrity of teeth, digest carbohydrates and maintain the oral pH which is essential for enzymatic activity [58, 63, 64]. The mucus / saliva layer purpose is also to concentrate secretory immunoglobulins and reduce the attachment of microorganisms [7]. There are three major salivary glands (parotid, submandibular (also referred to as submaxillary) and sublingual) and minor salivary or buccal glands secreting saliva and mucus [63]. Under unstimulated conditions the glands contribute as follows to the total salivary secretion: 65 - 70% submandibular, 20% parotid, 7 - 8% sublingual and < 10% minor salivary glands [65]. This contribution changes greatly upon salivary flow stimulation with parotid glands contributing over 50% [65].

Saliva consists mainly of water (95 - 99% (w/w)) and only 1% of organic and inorganic materials which includes enzymes (e.g. lysozyme), immunoglobulines, inorganic salts, lipids and mucus (glycoproteins) [66–68]. Saliva is also rich in electrolytes, namely potassium, bicarbonate, calcium, phosphorous, chloride, thiocyanate, urea and sodium) [67, 69]. Its composition is highly influenced by its flow rate which on the other hand depends upon four factors: the time of day, the type of stimulus (type of food, smell and taste), the duration as well as the degree of stimulation [57, 64, 65, 70]. Other factors influencing the composition and saliva flow are medications, type of secretion, relative contribution of salivary glands, physical exercise, systemic diseases, nutritional deficiencies, etc [65]. Under normal

physiological conditions the flow rate of the total whole saliva varies between 1 and 2 mL/min [71]. The total daily saliva volume is in the range of 0.5 - 2L with 1.1 mL being constantly present in the mouth which in comparison to the GIT is a very low volume [70, 72]. This aspect is particularly important for *in vitro* drug release studies which at this point are not clearly defined by the European Pharmacopoeia and are considered a challenge [50, 73, 74]. At a high flow rate sodium and bicarbonate are less absorbed, consequently their concentrations and saliva pH increase [64]. Moreover saliva functions as a weak buffer in the pH range of 5.5 - 7.0. At rested state saliva's pH is slightly acidic (6.6) and increases up to 7.4 [75]. Disparities in saliva pH are due to different methodology determining the pH as well as the flow rate occurring while testing [64, 66].

3.4.2 Mechanism of oromucosal drug transport (e.g. buccal drug delivery)

Permeation through the membrane of the oral mucosa is driven by passive diffusion, carrier-mediated diffusion, active transport and pinocytosis or endocytosis [66]. Passive diffusion can be subdivided into paracellular and transcellular transport. The mechanism of transport is impacted by the drug's lipophilicity. While some hydrophilic molecules are delivered through the buccal mucosa by a carrier-mediated transport [76], the main role is associated with passive diffusion. Paracellular describes the transport between the cells whereas transcellular refers to an intracellular route in which molecules are crossing the cell membrane and enter the cells [55, 66] (Figure 4). Consequently hydrophilic compounds are thought to permeate the buccal mucosa via the paraceullar route since those molecules are more soluble in aqueous fluids which are located in intercellular spaces [55, 77]. Hydrophilic molecules have to pass through tight junctions which block intracellular gaps [69]. It is a general consensus in the literature that both routes coexist but each drug prefers the route that offers less resistance [79].

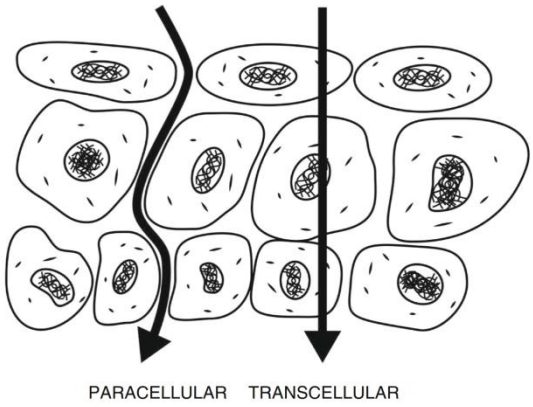

Figure 4: Passive diffusion through the oral mucosa (e.g. buccal mucosa). Paracellular transport describes the transfer of a molecule between cells. In transcellular transport a molecule travels across cell membranes, entering cells. Both routes can coexist and are driven by passive diffusion. Reproduced from Ref [34].

Finally if a molecule manages to permeate through the buccal mucosa and overcomes all potential barriers (3.4.3) it enters the connective tissue which contains a network of capillaries and drains directly into the jugular vein [80]. Molecules are subsequently delivered to the systemic circulation by avoiding the first pass metabolism [54].

3.4.3 Permeation barriers of oromucosal drug delivery (e.g. buccal drug delivery)

Studies on dextran 4,000 and benzylamine across rabbit buccal mucosa and amphetamine across dog buccal mucosa demonstrated a presence of permeability barriers. The obtained range however is still considered to be 4 - 4,000 times more permeable than the skin [55, 81] but less permeable than the intestine [9, 82, 83]. Additional studies compared the oral mucosa to the skin in terms of its permeability and reached similar conclusions [84, 85]. From a physiological point of view the biggest barriers in the buccal drug delivery are intercellular lipids and to some extent saliva, mucus and enzymatic degradation [55, 64]. The lack of stratum corneum (the major barrier of absorption across the skin) in the buccal mucosa is considered to play a major part in those conclusions. However it is not the keratinisation level of the epithelia itself that functions as the main permeation barrier [86, 87]. So called membrane-coating granules (MCGs) are thought to be primarily responsible [55, 62]. MCGs, spherical or oval shaped with a diameter of 100 - 300 nm, are located in the upper part of the prickle layer (stratum spinosum) [88] of nearly all stratified epithelia [89–91] (Figure 5).

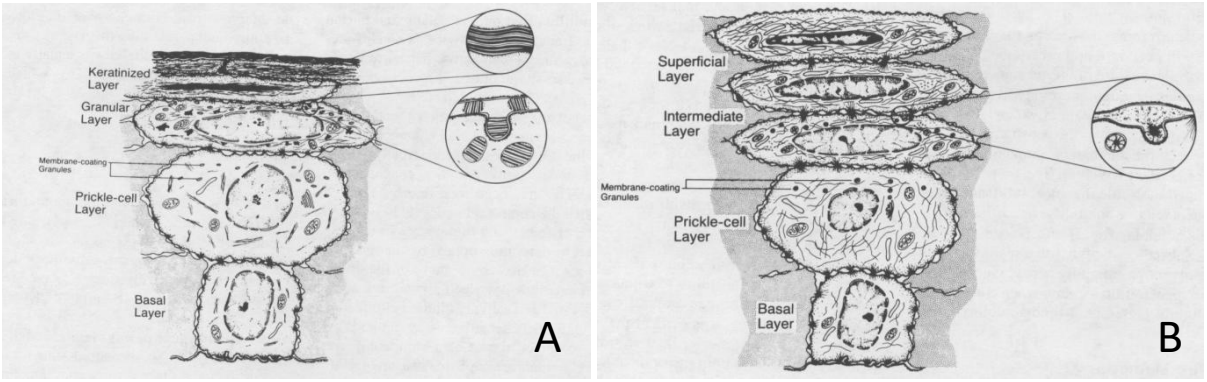

Figure 5: Keratinized (A) and non-keratinized epithelia (B). Both epithelia contain all four morphological layers and display membrane-coating granules (MCGs). A: Keratinized epithelium contains the basal layer (stratum basale), prickle cell layer (stratum spinosum), granular layer (stratum granulosum) and keratinized layer (stratum corneum). B: Non-keratinized epithelium contains the basal layer, prickle cell layer, intermediate layer and superficial layer. Reproduced from Ref [92].

During differentiation MCGs move from the prickle layer towards the superficial layer. When they reach the upper third quarter of the epithelium (superficial layer) their lipid content is discharged into intercellular spaces, a process driven by exocytosis [60]. MCG membranes are then fused with cell membranes [62, 93]. It is precisely this discharged intercellular

material which is considered the primary permeation barrier of oromucosal drug delivery for various compounds [63, 66, 94]. Permeability studies using topically and subepithelially applied tracers demonstrated that the presents of MCGs in the superficial membrane is the determining factor for penetration. When applied topically the tracers did not penetrate beyond the first 1 to 3 cell layers whereas subepithelially applied tracers reached the prickle cell layer [62, 87, 95, 96]. MCGs are present in keratinized and non-keratinized epithelia [89, 97, 98] and the same results were observed with both epithelia, which led to the conclusion that the keratinization level in itself is not believed to be a major penetration barrier [62, 87, 99]. These results are particularly interesting as a study by Tavakoli-Saberi et al confirmed that only the outermost layer of the epithelium present a barrier for permeation [100]. The presence of MCGs is not dependent on the keratinization level but their quantity depends on the body region and also differs within sites of keratinized and non- keratinized epithelia [62, 101].

Moreover MCGs in keratinized and non-keratinized epithelia contain a different lipid composition which explains the disparity in intercellular lipid properties present in these epithelia. While keratinized epithelia contain neutral lipids (ceramides and acylceramides), non-keratinized epithelia contain only small amounts of ceramides and mostly neutral polar lipids (cholesterol sulphate and glucosyl ceramides) [102–104]. Therefore keratinized epithelia are known to be less water permeable than non-keratinized epithelia [103]. Additionally these epithelia are also distinguished by their histological properties. Keratinized epithelia comprise flat superficial cells in their keratinized layer (stratum corneum) which devoid organelles [55]. Superfical cells in non-kertanized epithelia are less flattened and retain some cytoplasmic function as well as their nuclei [55]. Furthermore in non-keratinized epithelia lipids are structured in a more amorphous like state with occasional short stacks of lipid lamellae [105]. This configuration provides less of a barrier to the diffusion of molecules [34]. In keratinized mucosa lipids are aligned in a ordered, lemellar state, which hinders the possibility to diffuse through the membrane [34, 80, 105]. In essence non-keratinized epithelia have a better permeability due to the absence of organized lipid lamellae in its intercellular spaces [60]. Additionally the intracellular lamellae is thought to play a relevant role in the drug permeability through the human buccal mucosa [106].

The enzymatic activity in the oral cavity is described as moderate [63] but has to be taken into consideration. It is especially important for drug delivery of macromolecules as they might be converted into their inactive form [107–109]. For small molecules enzymatic degradation is considered less of a challenge. However, there is a variety of enzymes active in the oral cavity, namely esterases (mainly carboxylesterases) [110–116], carbohydrases and phosphatases but it does virtually not contain any proteases [34, 63, 117]. Moreover

studies could not determine any endopeptidases and carboxypeptidases [79] as well as no dipeptidyl peptidase IV activity in porcine buccal mucosa [118]. Proteases, namely trypsin, chymotrypsin and pepsin are responsible for enzymatic degradation of macromolecules via oral route. Due to the enzymatic composition in the oral cavity ester groups in APIs are a concern. Esterase activity is positively correlated with the pH and is at its highest after fasting and decreases postprandial [119]. Saliva also contains α-amylase, lysozyme and lingual lipase [69]. α-amylase breaks 1-4 glycosidic bonds, lysozyme breaks bacterial cell walls and functions as a general protective barrier whereas lingual lipase breaks down fats. Saliva composition is also influenced by diseases and age [67]. Additionally during permeation the drug is exposed to enzymes located within the cytosol, membrane and intercellular [34, 79, 120]. Aminopeptidases are thought to have the biggest impact in buccal drug delivery [63, 79, 118, 121]. These enzymes are divided into aminopeptidase N and A which are plasma membrane-bound peptidases and aminopeptidase B which is a cytosolic enzyme [108, 122]. Those enzymes are thought to be able to convert macromolecules into its inactive form resulting in low bioavailability. Examples are insulin, proinsulin, enkephalin analogues, thyrotropin realising hormone, calcitonin and substance P [34]. Additional research has to be conducted in order to determine if degradation occurred due to intracellular or extracellular action [34]. Some papers suggest peptides and proteins are most likely not affected by intracellular enzymes if their primary absorption route is paracellularly. Due to the potential degradation enzyme inhibitors are an important factor to consider during formulation design. Since enzymes are substrate specific its degradation property on a given API has to be carried out in *in vitro* and *in vivo* experiments which again is particularly important for peptide and protein delivery [34]. Within the buccal mucosa enzymes are differentially distributed between the mucus, epithelium and the connective tissue which presents a task for permeability studies. Particularly intraindividual and interindividual differences between dogs, rats, guinea-pigs and rabbits in enzyme activities are important aspects in the selection of a suitable animal model [123].

Finally the API may bind specifically or non-specifically to the mucus layer which is yet another permeation barrier. A high molecular weight mucin called MG1 comprises disulfide-linked subunits which are responsible for its ability to adhere to the surface of the oral epithelium. This layer itself acts as a physical barrier [124].

3.5 Physiological and pharmaceutical considerations

3.5.1 Selection of site of administration and dosage form

As described above there are a lot of permeability barriers involved in oromucosal drug delivery which have to be considered carefully to justify the selection of an API, polymer, type of dosage form and site of administration. Mucosa and drug properties are key aspects in the

formulation design of oromucosal drug delivery [55, 63]. Key mucosa properties include the keratinization level, mucosa thickness, mucus turnover time, surface area, residence time, blood flow, enzymatic activity and its overall permeability. Main drug properties include the partition coefficient (P), molecular size and its ionization state.

The biggest benefit of conventional routes like buccal and sublingual administration lies in the potential to bypass the GI tract which provides several advantages, mainly increasing the bioavailability. This is a consequence of avoiding the first pass metabolism, presystemic elimination (enzymatic degradation) and/or the harsh acidic environment in the stomach (chemical degradation). In general this is relevant to drugs reaching low bioavailability when administered orally [88]. Due to higher bioavailability lower drug load might be required which in turn can reduce possible side effects. Finally possible GI irritation by drugs can be circumvented. The oral mucosa is highly vascularised and its blood flow rate is considered substantial and not a rate-limiting factor for the absorption [63]. In particular the buccal mucosa contains a blood flow of 2.4 mL/min/cm^2 which is higher than the blood flow of the sublingual mucosa with 1.0 mL/min/cm^2 [72]. The buccal mucosa distinguishes itself due to its higher surface area [51] and thickness [125] in comparison to the other oral mucosae [63]. Moreover it is quite robust and not nearly as mobile as other mucosae which is particularly important if a systemic effect through the oral mucosa or a local effect is desirable as both require a longer residence time [55, 79]. Its thickness results in a lower onset of action, intermediate permeability and makes it less prone to irritations which suits this route of administration for a controlled / sustained release formulation as well as the potential to administer macromolecules like peptides and proteins [34]. This is based on the migration of cell layers from the basal layer to the superficial layer which protects the underlying tissue against fluid loss and more importantly xenobiotics [34, 60, 80]. Administration to the buccal mucosa is generally highly accepted by patients due to its ease of accessibility, robustness, convenient administration and small number of Langerhans cells which potentially lower the risk of immune responses caused by allergens [41, 53]. Especially for oromucosal films its large surface area and more importantly its moist environment which allows rapid wetting, underline the buccal mucosa as a perfect route of administration [7]. It is worth noting that sublingual and buccal are the most utilized routes of administration of oromucosal drug delivery. The permeability within the oral cavity is ranked as follows: sublingual>buccal>palatal [53, 92, 126].

The sublingual mucosa is thinner and therefore more permeable which leads to a fast absorption and higher bioavailability. Therefore sublingual administration is desirable for smaller molecular weight APIs which require an immediate onset of action (e.g. glyceryl trinitrate) [55]. The soft palatal provides a lot of advantages too, and therefore represents

another attractive route [53]. One disadvantage of soft palatal drug delivery is its location. Administration of films potentially lead to discomfort for the patient as it is located deep inside the oral cavity, close to the uvular. Moreover it is difficult to find an area with a mucosal layer that enables bioadhesion and its permeability which is characterized as poor. Moreover buccal and sublingual routes are more thoroughly researched than gingival and hard palatal drug delivery [72]. Other challenges to overcome in oromucosal drug delivery include saliva, enzymatic acitivity and salivary mucin as they all affect the dosage form [127].

The biggest disadvantage associated with buccal drug delivery is the low flux which might result in low drug bioavailibility [122]. The cellular turnover in the buccal mucosa is slower (4 - 14 days [128]) than in the GIT but faster than the skin [129]. In theory this allows dosage forms to adhere at the site of action for a longer time [34] and more importantly makes the mucosa less susceptible to damage or irritation [41, 79]. However the duration of bioadhesion is largely affected by the short turnover time of the mucus layer [79] (12 - 24 h in humans [130], 47 - 270 min in rats [131]). Additionally a change in the pH value in the oral cavity which causes changes in the chemical composition of the polymer could eventually lead to a loss of mucoadhesion [66]. As previously mentioned the buccal mucosa is relatively immobile which is favourable as normal functions such as swallowing, talking, eating and drinking present already a task in hand for the residence time [66]. Therefore a specific time span is often recommended [132]. According to the literature buccal patches were reported to be administered for a maximum of 4 - 6 h [133] or 5 - 6 h [134] for general oromucosal drug delivery due to patients behaviours like eating, drinking, etc. Possible irritations or other inconveniences to the patient have to be thouroghly observed. The saturated solution of the film formulation should have a pH in the range of 5 to 9, so that the final film does not irritate the skin (Table 1). Film surface pH values < pH 4 or > pH 8 might cause irritations [135–137].

One of the key aspects in order to achieve a systemic effect is the residence time which is highly affected by the saliva flushing effects. As the name suggests saliva could potentially displace and/or completely detach the dosage form which could lead to involutary swallowing [138]. Additionally the saliva can dilute the drug concentration and will essentially reach the GI tract which would lead to very complex pharmacokinetic profiles [139]. This process is often refered to as saliva-wash-out effect [63]. This is yet another reason to favour the buccal over sublingual epithelium when longer residence times are required as the latter is constantly washed by a considerable volume of saliva [140]. To avoid this effect altogether multilayer mucoadhesive films with non dispersible backing layer can be used [3]. These films offer the advantage of protecting the drug loaded layer from saliva and provide an unidirectional release into the oral mucosa. To summarize in short, within the oral cavity the

buccal mucosa is generally the route of choice seeking a local or systemic effect through the oral mucosa and/or a controlled release.

3.5.2 Selection of drug and polymer

The selection of API is especially critical for numerous reasons which are discussed in this section. In that regard clonidine hydrochloride (from now on named clonidine) was chosen as API and compared to recommended physiochemical drug properties for oromucosal drug delivery systems (Table 1).

The molecular weight of an API is a very critical aspect as the rate of absorption is a function of molecular size [55]. According to the literature the buccal epithelium's molecular weight cut-off lies at around 500 - 1000 Da [35]. These aspects highlight the importance of formulation design and more specifically for permeation enhancers. Harris et al. [55] suggest that small molecules < 75 - 100 Da are capable of crossing the mucosa rapidly. Due to the molecular weight cut-off of the buccal mucosa literature recommendations are a molecular weight < 500 Da. Bioavailability of APIs decreases heavily if molecular weight increases beyond 700 Da [141–144]. As discussed earlier transport might take place trans- or paracellular depending upon its lipophilicity or hydrophilicity, respectively. The paracellular route is thought to be restricted to small molecular weight APIs (< 200 Da) [141–144]. Camenisch et al. [145] estimated this particular molecular weight restriction to be even less than 100 - 200 Da. This is based on the limited space of 10 and 30 - 50 Ångström which hinders large molecules to permeate via the paracellular route [38]. It is a general agreement that most macromolecules show a more hydrophilic nature [36, 37, 141, 142] which favours the paracellular route. This permability obstacle highlights one of many difficulties for formulation scientist dealing with oromucosal drug delivery of macromolecules [36–38].

Secondly the lipophilicity, often expressed as logP or P, impacts the permeability. Due to the lipophilic nature of the phospholipid bilayer an ideal drug should possess high P values [146]. Furthermore Becket et al. found a positive correlation between P and the buccal absorption [147] and according to the literature P values in the range of 40 – 2,000 [148] or 10 – 1,000 are desirable.

Table 1: Recommended physiochemical drug properties for oromucosal drug delivery systems. Modified from Ref [149]. *Recommendations exclusively for buccal administration.

Formulation considerations	Recommended range [35, 64, 70, 148, 150–153]	Clonidine HCl [154–157]
Aqueous solubility	> 0.1% w/v	7.7% w/v
Lipophilicity, Partition coefficient (P)	10 - 1000 or 40 - 2000*	38.9 (logP: 1.59)
Molecular weight	< 500 Da or 500 - 1000 Da*	266.6 Da
Melting point	< 200°C	305°C
pH of saturated aqueous solution	pH 5 - 9 or 7.0 ± 1.5*	4.0 - 5.0 (2% w/v chitosan: pH 4.3)
Required dose deliverable	< 10 mg/day and ≤ 30 mg/film	90 µg/film
pK_a	≥ 9.0	8.2

The third major aspect of drug properties is its ionization degree which is dependent upon the pH as shown below by the Henderson-Hasselbalch equation ((1) and (2)). Handerson-Hasselbalch equations are used to calculate the ratio of ionized and non-ionized species at certain pH values [158].

$$\mathrm{pH} = \mathrm{pK_a} + \log_{10}\left(\frac{[\mathrm{A^-}]}{[\mathrm{HA}]}\right) \quad \textbf{(1)}$$

$$\mathrm{pH} = \mathrm{pK_a} + \log_{10}\left(\frac{[\mathrm{B}]}{[\mathrm{BH^+}]}\right) \quad \textbf{(2)}$$

HA and A^- describe the non-ionized and ionized species of a weak acidic drug, respectively. B and BH^+ are the non-ionized and ionized species of a weak basic drug, respectively. pK_a is the negative logarithm of the acid dissociation (or ionization) constant K_a. The pK_a value describes the acidic strength of a given molecule in solution. pK_a can also be used to calculate the protonation of weak bases.

The permeability is at its highest if the molecule is in its unionized state. This is based on the fact that drugs in their non-ionized state exhibit greater lipid solubility which is particularly important for the transcellular route [159]. It is assumed that molecules which are slightly more hydrophobic but contain both a hydrophobic and hydrophilic nature (amphiphilic) permeate the fastest [54]. As previously mentioned, at rested state the pH of saliva is known

to be in the range of 6.6 and increases up to 7.4. If the pH is two pH units away from a drug's pK_a the molecule is almost completely ionized or non-ionized [160]. Assuming the pH of saliva is located at an average of 7.0 a pK_a value of ≤ 5.0 for weak acidic drugs or ≥ 9.0 for weak basic drugs would be desirable as the molecule would appear in an unionized state [88]. It is worth noting that the pH is also likely to change during permeation. The solubility limit according to Rathbone et al. [88] is > 1 mg/mL. In conclusion the pH at the absorption site and, the dosage form and the choice of pK_a of a drug are absolutely key considerations for formulation design.

3.5.2.1 Clonidine as post-operative sedative and pain medication

Pediatric patient are widely regarded as a heterogenic and vulnerable patient population represented by the lack of approved formulations. In that regard clonidine is particularly interesting as it was listed in 2012 by the EMA in their 'Revised Priority List' [161].

Clonidine hydrochloride (Figure 6) is mainly used to treat hypertension by stimulating α2 adrenergic receptors in the brain. The α2 agonist lowers the blood pressure by decreasing the cardiac output and peripheral vascular resistance. More specifically it has a high selectivity towards presynaptic α2 receptors which lower calcium levels and inhibit catecholamine release (especially noradrenalin) into the adrenal medulla. This negative feedback loop is responsible for a lower heart rate and blood pressure [162]. It has also been proposed that clonidine binding the imidazoline receptor I_1 lowers blood pressure via the sympathoinhibition of imidazolines [163].

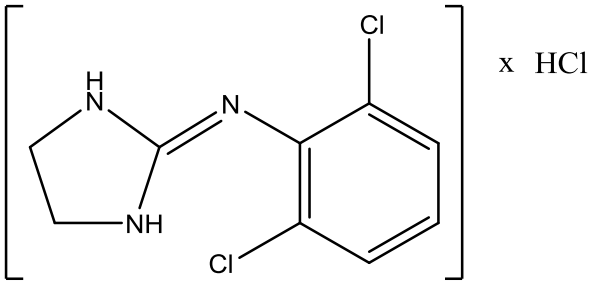

Figure 6: Chemical structure of clonidine hydrochloride.

Clonidine was also reported to cause several side effects including sedation, anxiolysis and maintaining hemodynamic stability during stress [164]. These effects are based on α_2 agonists acting through the central nervous system [165]. Its mild sedative and analgesic properties are particularly beneficial as pre- and postanesthetic medication, in both paediatric

patients and adults [166–170]. While all these properties are the basis of an ideal pre- and postanesthetic medication [164] these indications are restricted to off-label use as there is no licensed age appropriate oral dosage form for this particular purpose.

Other off-label uses in children include treatment of sleep disturbance, aggression and attention-deficit hyperactivity disorder (ADHD) in children [171]. These indications are most likely based on clonidine's ability to bind to postsynaptic α_{2a} adrenergic receptors [172]. Overall available pharmaceutical products of clonidine are not appropriate for paediatric patients. The required dosage for regional anaesthesia and post-operative analgesia in children aged 5 years-old (18 kg) has been proven successfully at a minimum of 18 µg and maximum of 90 µg per dosage form (1 - 5 µg/kg) [173, 174]. Clonidine is available in numerous dosage forms such as tablets, extended-release tablets (as base), suspensions (as base), tansdermal patches and injectables to be administered i.m., i.v., or epidurally (Table 2). The need for an oromucosal clonidine film for paediatric patients has been previously addressed in studies on different dosage forms including lollipops, orally-disintegrating tablets [175] and sublingual tablets [164].

Table 2: Available dosage forms of clonidine in the US, Europe and UK.

Dosage forms	Indication	US	Europe	UK
Eye drops	Elevated intraocular pressure	X	X	
Tablets	Migraine and recurrent vascular headache	X	X	X
Injectables (i.v., i.m, epidurally)	Treatment hypertensive crises	X	X	X
Transdermal film	Hypertension	X		
Suspension, extented release (base)	Hypertension	X		
Tablets, extented release (base)	Hypertension	X		
Transdermal film extented release (base)	Hypertension	X		
Buccal tablet	Mucositis	Phase II clinical trial		

Above all clonindine's mechanism of action as agonist of α_2 adrenergic receptors in the brain reduces the pro-inflammatory mechanism and releases an anti-inflammatory cytokine [176].

In particular NF-κB (nuclear factor kappa-light-chain-enhancer of activated B cells) activation has been reduced by topically applied clonidine [177]. In a phase II randomized trial Giralt et al. administered 50 and 100 µg clonidine lauriad buccal tablets (Validive®) to prevent severe radiomucositis caused by chemoradiation therapy in head and neck cancer patients [177]. The treatment strongly reduced severe oral mucositis and was tolerated by patients. This study reinforces the need of an oromucosal film aiming for a local effect as buccal tablets were administered for a duration of at least 6 hours. Severe mucositis is accompanied by pain and mouth dryness, preventing patients from drinking and eating which often leads to treatment breaks and longer hospitalization [176]. Besides evidence suggests that cancer patients undergoing chemotherapy experience adverse affects on food liking and appetite changes [178–181]. These inconveniences are often accompanied by dysphagia, nausea and vomiting. Those symptoms raise the demand of an easy to swallow oral dosage form. The developed oromucosal film in this study fulfills this requirement as clonidine is known to treat post-operative pain and vomiting [175]. From a chemical point of view, clonidine is a well suited API for oromucosal drug delivery [148, 149]. Moreover when administered orally its bioavailability has been reported in the range of 75 to 88% [164] making it also well suited for orodispersible films as developed in a previous study [174].

3.5.2.2 Chitosan as film forming polymer

Chitosan (poly [β-(1-4)-2amino-2-deoxy-D-glucopyranose) is undoubtedly one of the most investigated polymers for the development of oromucosal films. Chitosan (Figure 7) is a natural product as it is derived from chitin using deacetylation. Its molecular weight (MW) ranges from 3800 to 2,000,000 with a degree of deacetylation (DD) of 66 to 95%. There are also different types of salts available including acetate, citrate, glutamate, hydrochloride and lactate [41, 182, 183]. Chitosan has been used as a film forming polymer due to its high mucoadhesiveness, low price, suitability for chemical modification, biocompatibility, biodegradability, low toxicity, antimicrobial activity and most importantly its water insolubility [184, 185]. Due to its pk_a value of ~ 6.3 chitosan is insoluble in aqueous solution [63]. Its high mucoadhesive force is based on interactions of its primary amino groups and the negative functional groups of mucus or epithelial cells [189]. Thiolated chitosan, often referred to as second generation polymer, functions also as a penetration enhancer because it is often used to enhance the delivery or larger molecules across the buccal mucosa [34]. As polymers are widely considered not be absorbed into the systemic circulation from the oral cavity, multifunctional polymers are generally regarded as more popular than distinct excipients [34]. Overall while being often used in combination with polycarbophil and/or hydroxypropyl methylcellulose (HPMC) it possess excellent film forming properties on its own, making it a polymer of choice for oromucosal film preparations [3].

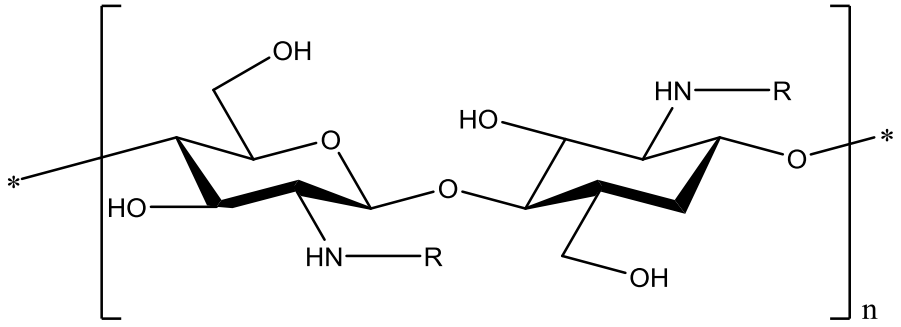

Figure 7: Chemical structure of partly deacetylated chitosan. R = H or CH_3CO.

3.6 Theory of used methods

3.6.1 Solvent casting

Solvent casting is the most utilized technique for OTF preparation in research. Alternatives are hot melt extrusion and 3D printing [6]. Solvent casting is an easy technique which does not require specialized equipment. The biggest problems concerning solvent casting are long processing times and thickness fluctuations due to surface tension and other aspects which are addressed below in this study.

3.6.2 Rheology

Rheology is the study of flow and deformation of materials exhibiting solid and fluid characteristics. Flow describes continuous deformation of a material in response to force [190]. Viscosity is the measure for internal friction of a liquid resisting to flow. In other words viscosity can be described as a tendency to flow [190]. Viscosity measurements are done using μ rheometers. By plotting shear stress (Pa) as a function of shear rate (1/s) different types of viscous behaviour can be determined. If a material's viscosity is independent of strain rate it can be characterized as a Newtonian fluid. Its viscosity coefficient η is constant and often denoted with μ. The majority of materials though display non-newtonian behaviour which changes upon strain rate. Non-newtonian fluids are subdivided into pseudoplastic, dilatants and Bingham plastic materials. An effect called "shear-thinning" obtained by pseudoplastic fluids describes a decrease in viscosity upon an increase in shear strain. Dilatant fluids obtain "shear-thickening" which is characterized by an increase in viscosity upon an increase in shear strain. Both fluids do not show a direct proportional correlation between viscosity and shear stress. Bingham plastics are interestingly because their behavior at low stresses is similar to a solid whereas at high stresses it behaves as viscous fluid. Therefore a certain yield stress has to be exceeded so that flow occurs. The flow typically follows a Newtonian behavior. Another interesting behavior can be seen in thixotropic materials in which viscosity decreases over time at constant shear rate [191].

Viscosity is of high importance in pharmaceutical sciences as it influences the spreading property of ointments, physical stability of suspensions, sedimentation in suppositories, etc. In oromucosal film formulation the viscosity of casting solution is a key aspect as it highly influences the feasibility of developing films [6]. Moreover viscosity influences the uniformity of content greatly [6].

3.6.3 Scanning electron microscope (SEM)

SEM provides high-resolution images with a wide range of magnifications. A thermionic cathode is heated up by high electric current. Electrons are accelerated into a high vacuum due to a strong electric field between cathode and anode. The beam consisting of primary electrons is focused by an electromagnetic lens and subsequently hits a small spot on the specimen's surface. The narrow beam allows for three-dimensional appearance. So called secondary electrons of the specimen are knocked out and measured by a secondary electron detector. A high number of secondary electrons lead to a bright image point while a low number leads to a dark image point. A raster scan generator guides the electron beam. Essentially upon deflection of the beam in x and y axes, surfaces are scanned in a raster fashion providing high resolution images [192].

3.6.4 *In vitro* disintegration and drug release studies (dissolution test)

For oromucosal films a disintegration test can be applied to verify its insolubility although it is not a prerequisite. Increase in size due to surface wetting can be observed as well. Authorities have updated their respective guidelines due to the vastly rising interest on OTFs. However to this day disintegration and dissolution tests are still not clearly defined nor address some concerns regarding the lack in biorelevance [46, 50]. Disintegration is used to verify solubility of orodispersible films. Films are visually observed until the beginning of breakage which is generally defined as time point where the film starts to break as measured by several studies [49, 193]. According to Ph. Eur. monograph ODTs require disintegration times < 180 s [194]. FDA define disintegration times < 60 s [195]. Generally disintegration as fast as possible is desirable [46] but its inverse relationship with mechanical properties have to be considered [196]. Disintegration times within 5 to 30 s for ODFs have been reported [197]. Since disintegration time requirements for ODTs have been set at 30 [195] and 180 s [194], these criteria have been adopted for ODFs to differentiate between fast, intermediate and slow dissolving films [3].

Firstly there is no clearly defined disintegration or dissolution medium for oromucosal film preparations. To simulate saliva which has a pH range of 6.6 to 7.4 [75], media with comparable pH values should be used. Based on saliva's composition distilled water is the most used disintegration medium [46]. Fluctuations of water pH due to carbon dioxide have to be observed though. Another popular medium is simulated saliva solution at an adjusted

pH of 6.75 [198] containing Na_2HPO_4, KH_2PO_4 and NaCl. Phosphate buffer pH 6.0 is defined as dissolution medium for medical chewing gums and has been used for OTFs as well [46]. While the temperature should be set to 37 ± 1°C the volume is another critical value. Only 1.1 mL of saliva are constantly present in the mouth. Besides low volumes, saliva contains enzymes [66–68] which might affect disintegration time as well. Disintegration tests have been adapted specifically for OTFs known as slide frame and petri dish method [49, 199]. Several other disintegration tests have been reported as well [46]. Moreover contact angle measurements and thermomechanical analysis of swelling behaviour have been implemented due to unsatisfying relevance of disintegration tests [46, 200]. Tongue movements, pressure and humidity are additional aspects which confirm difficulties for biorelevant *in vitro* tests. Generally, it can be argued that results obtained from *in vitro* disintegration and dissolution tests are more relevant for preformulation studies and quality control than for biorelevant purposes.

3.6.5 Attenuated total reflection-Fourier transform infrared (ATR-FTIR)

Basically in attenuated total reflection (ATR) pressure is applied to the sample using a clamp. An IR beam is directed through a crystal of high refractive index [201]. This accessory of FTIR allows direct sample measurements and does not require specific sample preparation. Generally in Fourier transform spectroscopy a beam containing different frequencies of light is used. The IR beam is also modified in order to obtain different frequencies. One essential part of any FTIR is its interferometer, the Michelson interferometer being the most used one [202]. The IR beam is sent to an interferometer which splits the light into two beams and leads them to different directions. The two light beams are recombined into one and then leave the interferometer. An interferometer contains, among other parts, a collimating mirror and beamsplitter [203]. The collimating mirror causes light in parallel rays. A beamsplitter transmits and reflects light - transmitted light travels to a fixed mirror while reflected light is directed to a moving one. The ladder leads to differences in length in comparison to the stationary mirror. Free movement at a constant velocity of the mirror is critical as the wavenumber depends on the mirror speed. Once these two light beams are directed back to the interferometer their amplitudes will add together and form a single wave. In other words these differences in length lead to a constructive and destructive interference which is expressed in an interferogram [203]. The recombined IR light will eventually travel to the sample which absorbs wavelengths characteristic for its properties. After interacting with the sample light will reach the detector which reports energy variation over time for all wavelengths. To obtain a spectrum of intensity (absorbance or % transmission) as a function of frequency (cm^{-1}) mathematical functions named Fourier transform are applied. Spectra are typically obtained in mid-infrared range (4000 to 400 cm^{-1}). The obtained spectrum contains the wavenumber in cm^{-1} on the x axes and either absorbance or transmission on the y axis.

While both are used for qualitative analysis, absorbance must be used for quantitative analysis since peaks are linearly proportional to concentration [202]. Overall FTIR provides several advantages such as its fast and easy feasibility. Moreover it can be applied to nearly all molecules, is relatively inexpensive, sensitive and the obtained spectra are rich in information [204]. One disadvantage includes hydrogen bonds affecting peak widths and therefore might overlap certain areas in the spectrum.

3.6.6 X-Ray powder diffraction (XRPD)

Typically diffractometers can be applied in two different ways. Either to determine spacing d of various planes or to measure the radiation wavelength. The former is determined by applying monochromatic X-rays of a given wavelength λ and measuring 2θ. To measure the wavelength, crystal planes of known spacing d are utilized [205]. Additionally XRPD can be used to determine crystallize size, residual strain, orientation, twinning, etc. The basic principles underlying this technique are quintessential differences in solid state properties of materials and their behaviour to scatter X-rays. Solids can be crystalline, liquid crystalline or amorphous. Crystallinity is characterized by its long-range order in all 3 dimensions. Liquid crystallines possess long-range order in 3, 2 or 1 dimension whereas amorphous materials do not exhibit long-range order at all. In other words atoms are periodically arranged in a 3 dimensional space forming lattice planes in crystals. In 3 dimensional spaces there are essentially 14 possible crystal lattices (Bravais lattices). Atoms in amorphous materials on the other hand are randomly distributed in all dimensions. Essentially depending upon these differences, monochromatic X-rays are scattered in different ways. From a mathematical point of view monochromatic X-rays are diffracted in specific angles of incidence which are according to Bragg's law. Constructive interference of X-rays scattered by atoms on all planes form diffracted beams in a certain direction [205]. Therefore crystalline materials hit by X-rays diffract these in distinct directions. This leads to high intensity in signals and gives diffraction patterns. The latter provides information on the atomic arrangement within the crystal. To put it another way different arrangements of atoms of chemically identical materials can be distinguished due to differences in their diffraction pattern. Amorphous materials do not produce diffraction patterns due to their lack of periodically arranged atoms and broad scattering peaks are obtained instead. Scattered intensity is typically plotted as function of 2θ. In crystalline materials typically almost no intensity is observed except for certain angles providing sharp distinct peaks indicating diffracted beams. Amorphous materials show a scattering curve containing usually one or two broad maxima [206].

Essential parts of a diffractometer include a X-ray tube, incident-beam optics, receiving-side optics, goniometer, sample and its holder as well as the detector. X-rays are produced via photoelectric effect using tungsten filament striking the target anode placed inside X-ray

tubes. At this point X-rays consit of several wavelengths determined by the anode material used. To eliminate unwanted wavelengths monochromators are used. Additionally β-filters are utilized to reduce the intensity of K-α and K-β radiation. X-rays emitted from a X-ray tube are conditioned by incident-beam optics. Then these X-rays hit the sample and are again conditioned by receiving-side optics before counted by the detector. The goniometer is basically the platform holding and moving several parts including the sample and detector. The positions of the X-ray source and sample as well as the incident beam and detector are key aspects in XRPD as the incident angle ω and diffraction angle 2θ are defined by the position of these parts, respectively. Bragg-Brentano geometry is one of the most utilized geometries in XRPD:

Disadvantages in XRPD include variations in particle size and orientation. Too small particle sizes lead to broadering of peaks and may appear amorphous whereas large particle sizes may cause non-random orientation. Plate- or needle-shaped particles may cause parallel aligninment to the specimen axis. This increases the possibility for some planes to reflect X-rays. To minimize this effect samples can be rotated. As with all analysis to decrease statistical errors the scanning speed should be set to low speed.

3.6.7 Dynamic vapour sorption (DVS)

Dynamic vapour sorption uses varying vapour concentrations to measure how much solvent is absorbed over a certain period of time. This is done by measuring changes in mass. Samples are subjected to different concentrations of relative humidity for certain intervals. DVS also allows to test desorption behaviour by decreasing relative humidity (RH) [207]. Moreover samples can be dried by applying 0% RH until constant weight is reached. This has been used to determine initial water content [208]. Amorphous content can also be determined using DVS [209]. Overall DVS is applied to understand hygroscopic behaviour of samples which is especially important for stability and microbiological activity. Water content or moisture is a very critical aspect in pharmaceutical sciences as water sorption is known to affect crystallinity, storage modulus, melting temperature (T_m), glass transition temperature (T_g), etc [210]. It is particularly important to analyze certain storage conditions and to evaluate stability. Water content can be determined using several techniques such as TGA, loss-on-dry, Karl-Fischer titration or Near-infrared reflectance spectroscopy [211]. The biggest advantage of DVS over other techniques determining water content is the fact that it allows evaluating maximum water sorption capacity under extreme RH conditions. This helps setting and justifying certain specifications for storage conditions and stability studies [210].

3.6.8 Thermogravimetric analysis (TGA)

TGA, Karl-Fischer titration, etc have been used for measuring moisture levels in pharmaceuticals. In addition, TGA predicts the thermal stability of materials, characterization

of samples due to decomposition patterns and gives information of reaction kinetics, etc [212]. In TGA the sample is placed inside a pan and weighed by a high precision balance. Samples are then exposed to a temperature program and changes in mass are measured as function of time (constant mass loss and/or constant temperature) or temperature (constant heating rate) [213]. Temperature programs are controlled by a programmable furnace equipped with a thermocouple to monitor the temperature. Moreover to obtain a stable environment a purge gas (usually N_2) with an optimized flow is used [212]. Essentially weight loss is related to decomposition, evaporation, reduction and desorption. Weight gain is based on oxidation and absorption. So called high resolution TGAs offer the advantage to distinguish between bound and “free” surface water. A combination of DSC and TGA is particularly insightful for thermal characterization of samples. A main disadvantage of TGA is the fact that weight loss is affected by volatile solvents and moisture. Moreover drugs sensitive to high temperatures are problematic as degradation occurs and does not allow water content determination.

3.6.9 Modulated temperature differential scanning calorimetry (MTDSC)

DSC measures the heat flow that is required in order to increase the temperature of a reference and sample. Measurements of both are done independently from one another. A sample is placed inside a pan while an empty pan functions as reference. Both reference and sample are placed each on a thermocouple inside a furnace. The temperature difference between sample and reference is measured directly from the developed voltage of the pair. The heat flow (dQ/dt) is given by (3).

$$\mathrm{dQ/dt} = \Delta \mathrm{T/R} \qquad \textbf{(3)}$$

Q is heat, t stands for time, ΔT is the temperature difference between the pan and furnace and R describes the thermal resistance of the heat path between the furnace and the pan [212].

This equation demonstrates the direct correlation of temperatures differences measured between sample and reference and their differences in heat flow as the sample is placed inside the pan. Essentially changes in temperature and energy associated with thermal events (melting, crystallisation, glass transition and decomposition) can be measured [212]. For instance melting is an endothermic phase transition absorbing heat and therefore requiring more heat to increase its temperature than the reference. Differences in heat flow allow for measurements of amounts of heat absorbed during melting. Therefore this transition can be seen as distinct endothermic peak in DSC. The furnace is purged with an inert gas (e.g. N_2) to remove residual moisture or volatile compounds stemming from the sample due to heating. This can influence the analysis and even damage the furnace [212].

To measure heat flow and changes in heat capacity (C_p) simultaneously, modulated temperature differential scanning calorimetry (MTDSC) can be applied (4).

$$dQ/dt = Cp(dT/dt) + f(t,T) \quad \textbf{(4)}$$

f (t,T) is a function of time and temperature. This demonstrates the response associated with chemical or physical transformations.

MTDSC describes a versatile extension of conventional DSC in which a sinusoidal modulation is superimposed over the linear temperature ramp. Additional mathematical procedures are applied which allow separation of different types of sample behaviour (deconvolution) [212]. Heat capacity of a sample represents the required energy to increase the sample temperate by 1 K. MTDSC allows the separation of total heat flow signal into heat capacity and kinetic. In other words in a single MTDSC run three signals are obtained, namely heat flow, reverse heat flow (heat capacity) and non-reverse heat flow (kinetic). The glass transition temperature is obtained from the reversing heat flow [4]. Whereas crystallization occurs from the non-reversing heat flow as it is a non-reversing process which liberates heat. In conventional DSC sensitivity can be increased by higher heating rates which in turn decrease the resolution. Heating rates are limited when using MTDSC to allow enough modulations, to enable a separation of cycles and their underlying processes. MTDSC offers high sensitivity due to low heating rates and large modulation amplitudes without compromising resolution. Basically MTDSC offers a combination of high resolution and high sensitivity. Therefore it is often used in pharmaceutical sciences to determine T_g [214, 215]. MTDSC has also been used to measure the effect of water content lowering the T_g of amorphous materials [216] It is worth noting that MTDSC requires an additional calibration of heat capacity. This is usually done by measuring a material with a known heat capacity (e.g. sapphire).

3.6.10 Dynamic Mechanical Thermal Analysis (DMTA)

Dynamic mechanical analysis (DMA) is mostly applied to study viscoelastic behaviour of polymers as physical changes are usually accompanied by changes in mechanical modulus [217]. Viscoelastic modulus of materials are measured over time, temperature and/or relative humidity [217]. DMA has also been applied to quantify the rate of crystallisation in amorphous materials using orodispersible films [217]. DMA measurements have been described as study of relaxation of polymer chains [218] or changes in free volume of polymers [219, 220]. In DMA materials, such as oromucosal films, will exhibit strain γ or deformation when applying stress [220]. The modulus of a material (its stiffness) depending

on applied stress and temperature is measured. DMA results provide a complex modulus (or dynamic modulus, E*), storage modulus (or elastic modulus, E') and loss modulus (E'') [221]. These moduli allow to describes the material's ability to lose (E'') and to return energy (E'). In other words E'' gives information on the elastic and E' on the viscous behaviour of polymers [220]. In simple terms, in DMA a sample's response to an oscillating force is measured.

An interesting application of DMA, often abbreviated DMTA, allows for measurements of glass transition temperatures. In DMTA the material's dimension are measured, when subjected to temperature and transitions. The basis of these measurements are changes in the free volume of the polymer [220, 222]. At the T_g more energy is absorbed leading to an expansion of the free volume of a polymer. This allows for greater chain mobility measured by thermal expansion. Basically DMTA utilizes the fact that materials exceeding their T_g will become rubbery due to an increase in viscosity and especially vast decrease in stiffness. This results in a drastic decrease in E' whereas E'' reaches its maximum. T_g can be determined in two different ways. Either measuring the signal maximum of tan δ (quotient of E' and E'') [223] or by assessing the inflection point of E' decrease [223]. For T_g determination of a sample measurements are done at a constant temperature ramp and its modulus is measured as function of temperature. T_g is depending on both temperature and strain rate. Essential parts of a DMA include an analytical train, furnace, heat sink, thermocouple and clamps holding the sample.

3.6.11 High Performance Liquid Chromatography (HPLC)

Chromatography is one of the most utilized techniques in science. It comprises physical techniques in which analytes are separated by their distribution between a stationary phase and mobile phase. As the name high performance liquid chromatography (HPLC) suggests it falls in the category of liquid chromatography. It can be further subdivided into column chromatography and more precisely adsorptions chromatography [224]. In HPLC a stationary phase is packed into a column hence its affiliation to column chromatography. Mobile phases are pumped under high pressure (typically in the range of 50 to 400 bar) through the column [224]. All components interact varyingly strong with the stationary phase and are subsequently retained for different durations leading to variable retention times. Essentially there are two methods of HPLC: normal phase (NP) and reversed phase (RP) chromatography. These methods are characterized by different polarities of their columns. In NP polar column materials are used such as silica, diol, cyanpropyl, etc. In this method adsorption is based on polar interactions (hydrogen-bonding or dipole-dipole interaction) between the permanent dipole of the column's silanol group and dipole of analyte. A higher polarity of an analyte leads to higher affinity and hence longer retention times. Mobile phases used in NP are typically nonpolar such as pentan or hexan. If a stronger mobile phase is

required more polar solvents such as chloroform, dichlormethan, propanol and methanol are used. This leads to a stronger interaction between solvent and column in comparison to the analyte and column.

RP is the counterpart to NP and characterized by nonpolar columns. Silica gel modified with immobilised alkyl rests such as octadecyl (C18), octyl (C8), ethyl (C2), etc serve as stationary phase. Adsorption is based on relatively weak Van-der-Waals interactions [225]. Separation is therefore strongly influenced by the used mobile phase. Typical polar mobile phases are water, methanol and acetonitrile. If required stronger mobile phases such as chloroform or more nonpolar solvents can be used. For both methods mobile phases can be composed of a single or several components. Chromatographic separation can be distinguished between isocratic and gradient separation. The ladder consists of a variable mobile phase meaning its composition changes over time. As a result peaks are more distinct and overall separation is better. This method is often used to find ideal conditions for isocratic separation. It requires re-equilibration of the column which takes more time. Isocratic separation is more efficient and the method of choice if separation is adequate. This becomes increasingly difficult with a higher number of compounds. Independent of the method samples are detected using evaporative light scattering detector (ELSD), UV-Vis (ultraviolet-visible), IR (infrared) or MS (mass spectrometry), which are listed in ascending order of selectivity. Most HPLC set ups for pharmaceuticals use an UV-Vis detector and allow controllability of column temperature and sometimes autosampler.

Overall HPLC allows for qualitative and quantitative conclusions of samples. An adequate separation of an analyte and interfering matrix is a prerequisite, reinforcing the importance of an efficient separation method. Qualitative information requires a comparison between the retention time of a known substance (standard) and analyte. Quantitative analysis is based on a proportional correlation between injection volume and peak area. In other words unknown sample amounts can be determined by a comparison to known concentrations. Therefore calibration curves must be carried out primarily to confirm a linear relationship over a certain concentration range. This relationship is termed “linear dynamic range” and represents direct proportionality between the signal and concentration of analyte. If calibration curves are carried over a wide concentration range they also allow determining non-linear relationships called “analytical or dynamic range”. This range may include non-linear response of concentration and signal changes especially observed at higher concentrations [226]. Essentially it is expressed as the ratio of the maximum usable indication and minimum usable indication (detection limit) [226]. Another interesting interval is called “working or calibration range” which spans from the LOQ to deviation of sensitivity

[227]. Overall calibration curves provide informative content, represented in LOQ and LOD form of precision, accuracy and response function [228].

3.6.12 Scanning electron microscope - Energy-dispersive X-ray spectroscopy (SEM-EDS)

SEM-EDS, sometimes also abbreviated EDX or XEDS, allows an elemental analysis of a sample. Essentially electrons of each atom occupy certain electron shells labelled K, L, M, N, O, P and Q (or 1 to 7) with each possessing discrete energy levels. Energy levels increase from the innermost (K) to outermost (Q) shell. Electrons are capable of changing their energy level upon excitation from a so called “ground or unexcited state” to an “excited state”. This technique exploits this feature by treating samples with X-rays of coherent energy. The created energy beam usually occupies a diameter of micro- or nanometers and ranges from 5 to 30 keV [192]. As a result, electrons from an inner shell may excite and get ejected creating a hole in the shell. An electron from an outer shell (higher energy shell) will essentially fill this hole. The energy difference between these shells will be released in form of X-rays and detected by an energy-dispersive spectrometer (EDS). Energy differences of two shells and therefore atom configurations are characteristic and allow for specific elemental analysis. This technique is based on inelastic scattering of secondary electrons [192]. EDS detection allows for quick, versatile and cheap analysis. Although quantification of heavy metals can be measured without a standard, when analysing lighter elements such as oxygen, standards for calibrations are required. Moreover topography and surface roughness influence intensities. Therefore flat and polished samples are a prerequisite for high precision and accuracy. Finally chemical analysis is carried out by sophisticated calculations of the computer.

3.6.13 Transition temperature microscopy (TTM)

TTM describes an extension of localized thermal analysis (LTA) using a probe as in atomic force microscopy (AFM) [229]. Its diameter of 13 µm and resolution of up to 1 µm allow for site-specific thermal analysis which can be carried out over different sites of interests (SOIs). This probe is applied to the sample’s surface and can be heated at a controlled rate. Moreover a scanning voltage profile is applied and simultaneously monitors the probe deflection. As the probe temperature increases the sample expands which is recorded by the probe as upward deflection [230]. This continues until the material softens due to melting, glass transition or degradation and therefore the probe penetrates deeper into the sample. Once this downward deflection occurs the temperature is recorded, the probe stops, retracts and moves on to the next measuring point. Once the temperature is cooled down to the start temperature the next measurement begins. Measurements are taken in a grid pattern. In this fashion TTM provides a live-map of the measurements taken and assigns colors to certain

transition temperatures. This provides the possibility to essentially map the distribution of drug within a dosage form or in a mixture with pharmaceutical additives. In the end all measurements are displayed as a histogram with the number of measurements (y-axis) versus the corresponding measured temperatures (x-axis). The mean value obtained can be assigned as transition. When measuring several compounds TTM detects single and multi phases. Single phases are indicated by a Gaussian distribution of the measured temperatures displayed in the histogram. When analyzing mixtures results have to be observed carefully as different concentrations will influence the results. Moreover TTM will stop after measuring one transition, irrespective of whether or not several transitions occur. Comparisons to obtained DSC data are difficult as the underlying principles of measuring a transition temperature are completely different.

4 Material and Methods

4.1 Preparation of oromucosal films

Oromucosal films were prepared using conventional solvent casting/evaporation method. Drug loading of F1 was based on calculations for sedation of 5 year old patients with a desired amount of 90 µg clonidine per film [174](Table 3). F2 contains 1200 µg clonidine per film which corresponds to a theoretical concentration of 11.3% (w/w) in solid state. This film was developed to ensure LOD and LOQ of several methodologies in this study are reached. Drug free films are termed F3. To ensure API solubility calculated amount of clonidine hydrochloride (Sigma, MO, USA) was stirred in 15 mL 1% (v/v) acetic acid (Fisher Scientific, UK) for 60 min. 0.3 g chitosan was added to the solution. Chitosan with a molecular weight (MW) of 100 - 300 kDa and a degree of deacetylation (DD) of ≥ 90% (free amine groups)) was purchased from Acros organics (NJ, USA). The solution was stirred vigorously over night. Centrifugation (Sigma 3-16KL) at 9500 rpm for 5 min was used in order to separate chitosan impurities and expedite the removal of entrapped air bubbles. The whole solution (15 mL) was then transferred into a polystyrene petri dish (diam. H 90 mm × 15 mm, vented) and left to stand overnight at room temperature to remove entrapped air bubbles [231]. The resultant solution was measured to have a pH of 4.4. Solvent casting was carried out on a levelled hot plate (IKA® RH basic 2) at 40°C for 24 h at ambient temperature. All film characterizations were performed immediately after solvent casting. Additional films were packed in aluminium foil and stored in a climate chamber at 25°C and 60% RH according to ICH guidelines for pharmaceuticals.

Table 3: Composition of the developed oromucosal clonidine films. F1 contains the desired drug load of 90 µg clonidine per film. F2, containing 1200 µg clonidine per film, was developed as standard for several methods. F3 stands for the drug free film (placebo).

Formulation	Composition of film in solid state % (w/w)		Clonidine (µg) per film
	Clonidine	Chitosan	
F1	0.9	99.1	90
F2	11.3	88.7	1200
F3 (placebo)	-	100.0	-

4.2 Rheology

To measure the solution viscosity an AR 1000-N Rheolyst Rheometer (TA Instruments, UK Ltd.) equipped with a 60 mm standard steel parallel plate was used. Experiments were

conducted at a constant temperature of 25°C and 40°C. To avoid over and under filling 0.9 mL of solution was pipetted onto the rheometer plate. Experiments were carried out on at least triplicates with a shear rate of 1 to 100 s^{-1}. Equipment was calibrated before usage. Shear viscosity was calculated from the intercept obtained by plotting shear stress (Pa) as a function of shear rate (1/s).

4.3 Preformulation studies

Films were visually examined for impurities, bubbles or any other surface irregularities. In addition films were folded and compared in terms of their stickiness or brittleness. Thickness measurements of 10 films were done at two points of each film and performed by using Mercer Precision Dial Gauges (Type 130/8, 0.01 mm). Weight measurements of 10 films were performed using an analytical balance (Mettler Toledo XS205). SEM analyses of films were done using FEI Quanta 200 FEG ESEM. Films were arranged onto a 25 mm stub by attachment with an adhesive carbon membrane. Films were coated with 25 nm of gold using a Quorum sputter-coater.

4.4 Disintegration

Disintegration test was carried out using three different disintegration media with a volume of 15 mL, i.e. water (pH: 5.5), deionised water with a pH of 6.8 and a simulated saliva solution [198]. The simulated saliva solution was made of Na_2HPO_4 (2.38 g), KH_2PO_4 (0.19 g) and NaCl (8 g) in 1 L deionised water and the pH was adjusted to 6.75 using phosphoric acid (Sigma-Aldrich, MO, USA). Films were placed centrally onto a glass petri dish with a diameter of 7 cm and wetted with medium to prevent curling and in order to attach the film to the petri dish. In all tests petri dishes were constantly shaken (100 times per min) and kept at a temperature of 37 ± 1°C using a water bath (Fisher Scientific, UK). Films were visually observed until breakage of film (n = 3).

4.5 Attenuated total reflection-Fourier transform infrared (ATR-FTIR)

ATR-FTIR studies were conducted to identify molecular interactions between clonidine and chitosan using Perkin Elmer Spectrum™ 100 Optica FT-IR Spectrometer. Measurements were undertaken on individual raw materials as well as each film formulation (F1, F2 and F3). FTIR spectra were collected at a range of 4000 to 600 cm^{-1} at ambient conditions. Each sample (and background) was analyzed using: 64 scans with a resolution of 1 cm^{-1}. Spectra were analyzed using Spectrum Express software (application version 1.02.00.0014, 2008).

4.6 X-Ray powder diffraction (XRPD)

XRPD was performed to analyze the physical state of various individual raw materials as well as each film formulation (F1, F2 and F3). Rigaku MiniFlex 600 (RigaKu, UK) XRPD instrument was used. Operated with Cu Kα radiation (λ = 1.5418 Å) at a voltage of 40 kV and

a current of 15 mA. Data was collected with a step size of 0.01°, speed of 10°/min over a range of 3 to 40° 2θ. Samples were placed onto circular sample holder which obtained no background noise. Data was analyzed using Xpert data viewer software (PANalytical B.V, Netherland) and Origin® 8.7 software (OriginLab Corporation, USA).

4.7 Dynamic vapor sorption (DVS)

Investigation of water sorption and desorption of F1 using dynamic vapour sorption (DVS, Q5000 SA TA Instruments) was performed at ambient pressure and at a constant temperature of 25°C. Films were cut into small pieces (around 13 mg) and dried down to 0% RH for 120 min to equilibrate. RH was increased up to 90% in 10% steps. Every step was kept until change in weight was less than 0.01% before increasing to the next step.

4.8 Thermogravimetric analysis (TGA)

TGA (Hi-Res TGA 2950, TA Instruments DE, USA) analyses were used to measure water content and degradation onset temperatures of raw materials, F1 and F3. Samples (5 to 10 mg) were equilibrated at 30°C and heated at a rate of 2°C/min using a nitrogen gas purge flow of 20 mL/min. Experiments were carried out in TA Standard pinholed aluminium pans and repeated at least in triplicates. Water loss was measured in the temperature range from 30 to 125°C. Data collection and analyses were performed using TA Instruments Universal Analysis 2000 (Version 4.5A). Mass loss in % (w/w) and onset temperature were calculated and reported as mean ± SD.

4.9 Differential scanning calorimetry (DSC)

DSC (Universal Analysis 2000, TA instruments DE, USA) analyses were used to measure T_g and T_m of raw materials, F1 and F3. Samples were analyzed using conventional DSC and modulated temperature DSC (MTDSC). Samples (5 to 10 mg) were equilibrated at 0.0°C. Conventional DSC experiments were carried out using a heating rate of 10°C/min. MTDSC conditions were set at a heating rate of 2°C/min, amplitude of ±0.212°C over a period of 40 s. A nitrogen gas purge flow of 50 mL/min was used. Experiments were carried out in TA high sensitive pinholed aluminium pans and repeated at least in triplicates. An empty TA high sensitive pinholed aluminium pan was used as reference. Temperature calibration was done using indium, n-octadecane and tin.

4.10 Dynamic mechanical thermal analysis (DMTA)

DMTA measurements were performed using a Q800 TA instruments (TA Instruments) to determine the T_g of F1, F2 and F3. Films were fixed under constant preload force of 0.01 N using film tension clamps. Experimental parameters were set at a static force track of 125% and strain of 0.1% was set as limit. Oscillating frequency was set at 1 Hz. According to a previous study, experiments were carried out from 30°C to 200°C and 250°C for the

plasticized form and non-plasticized form of each film, respectively [232]. A heating rate of 2°C/min and a soak time of 5 min were used. Data collection and analyses were performed using TA Instruments Universal Analysis 2000 (Version 4.5A). Experiments were repeated in triplicates.

4.11 Chromatographic separation and content uniformity (drug assay)

The casted film was visually examined, peeled off using tweezers and cut into 1 x 2 cm (2 cm^2) pieces. To ensure the dimensions of 1 x 2 cm film pieces a reference sized carton was fixed onto the film using mini magnets. 10 individual casted film pieces (1 x 2 cm) were weighed as described in section 4.3 to verify possible variations generated by thickness fluctuations. Thickness measurements were done as described in section 4.3. All films were placed in 5 mL specimen glass tubes filled with 2 mL 1% (v/v) acetic acid. Films were sonicated for 60 min to dissolve at a temperature below 30°C. Samples were filtered through a mixed cellulose esters (MCE) filter with a pore size of 0.45 µm before HPLC injection. Solutions were transferred into 1.5 mL (diam. 6 mm) transparent vials. Chromatographic separation was performed using Agilent Technologies 1200 series (Germany) set-up with an UV-diode-array detector. The stationary phase was a Phenomenex SynergyMax C-12 column (250 mm x 4.6 mm x 4 µm; Phenomeney SynergyMax, USA). The mobile phase comprised 0.1% (v/v) trifluoroacetic acid (Sigma-Aldrich, MO, USA) in water (Fisher Scientific, UK) and acetonitrile (Fischer Scientific, UK) (80:20). Flow rate was set at 1.0 mL/min with an injection volume of 10 µL. Column temperature was set at 40°C. Absorption was measured at 220 nm. All solvents were at least HPLC grade. According to ICH Harmonised Tripartite guideline Q2(R1) (Validation of Analytical Procedures: Text and Methodology) a linear relationship was evaluated across the range of 120 to 0 µg/mL. 1% (v/v) acetic acid was used as solvent. Water was purified using the Elga Option 4 Water Purifier system (ELGA LabWater, Marlow, UK). Content uniformity was tested according to uniformity of dosage forms guidelines of the European Pharmacopoeia (Ph.Eur. 2.9.40). Content uniformity is determined by calculating the acceptance value (AV)(5):

$$|M - \bar{X}| + ks \quad \textbf{(5)}$$

M is the reference value depending on target drug content. $\bar{X}$ denotes the mean of the individual content in percent. k is the acceptability constant whereas s is the sample standard deviation. The value of k is depending on the number of dosage units (10 or 30) used. The acceptability constant k is 2.4 or 2.0 for 10 or 30 dosage units, respectively.

4.12 Scanning electron microscope – energy-dispersive X-ray spectroscopy (SEM-EDS)

SEM-EDS analyses were performed using a Hitachi S-3400N operated at 20 kV. The instrument was equipped with an Oxford Instruments INCA energy dispersive X-ray spectrometer, standardized in the laboratory with pure elements and oxides. Instrumental drift was corrected by the frequent analyses of metallic cobalt. EDS analyses were performed at 20 kV, 10.0 mm working distance and 100 s counting time. Experiments were carried out on at least triplicates.

4.13 Transition temperature microscopy (TTM)

TTM was performed using a VESTA system set up with an AN-200 ThermaLever probe both from Anasys Instruments (Santa Barbara, CA, USA). A NikonCFI Plan Fluor 10x: N.A. 0.30 objective was used. This technique provides a neat extension of localized thermal analysis (LTA) used with the same set up in a previous study [230]. The applied voltage of the probe was calibrated in the temperature range up to 250°C as described by Dai et al. [229]. Three standard polymeric samples namely, polycaprolactone, polyethylene and polyethylene terepthalate, with melting temperatures of 55°C, 116°C and 235°C, respectively, were used. Experiments were performed from 30 to 350°C at a heating rate of 10°C/s (600°C/min). Engage force was set to 2 V and Max(Peak-Average) was set at 0.2 V. Measurement were carried out on several sites of interest (SOI) comprising an area of 300 x 300 µm each. Measurements were done with a resolution of 6 µm. Samples were glued on stainless steel magnetic pucks.

4.14 *In vitro* Drug release (dissolution)

In vitro dissolution tests were carried out in glass petri dishes (diameter: 7 cm). 5 mL deionised water (pH: 6.8; 37 ± 1°C) was used as the dissolution medium. Sample volumes of 2 mL at time intervals of 1, 5, 15, 30, 60, 120, 180, 240, 300 and 360 min were collected. Volume was replaced with fresh medium (37 ± 1°C). Petri dishes were constantly shaken (100 times per min) and kept at a temperature of 37 ± 1°C using a water bath (Fisher Scientific, UK). Films (n = 3) used for dissolution test weighed 17.17 ± 1.72 mg with a thickness of 71.67 ± 4.51 µm. Samples were filtered through a MCE filter with a pore size of 0.45 µm before HPLC injection. Solutions were transferred into 1.5 mL (diam. 6 mm) transparent vials. Chromatographic separation was performed in accordance to the method used for content uniformity test. According to ICH Harmonised Tripartite guideline Q2(R1) (Validation of Analytical Procedures: Text and Methodology) a linear relationship was evaluated across the range of 120 to 0 µg/mL. Deionised water (pH: 6.8) was used as solvent. Water was purified using the Elga Option 4 Water Purifier system (ELGA LabWater, Marlow, UK).

5 Results and discussion

5.1 Rheology measurements

F1, basically a 2% (w/v) chitosan solution, displayed Newtonian behavior at 25°C. This was verified by its linear correlation by plotting shear stress (Pa) as a function of shear rate (1/s) (Figure 8). At 40°C, F1 exhibited non-newtonian behavior as highlighted by its increase in function by increasing shear rate. This effect is known as “shear thickening”. F1 displayed a shear viscosity of 123.5 ± 4.9 mPa s and 141.5 ± 7.5 mPa s at 25°C and 40°C, respectively. 1% (w/v) chitosan solutions are known to obtain viscosities over a broad range of 10 to 1,000 mPa s [233]. Chitosan solutions at concentrations of 1 - 2% (w/w) are known to display Newtonian behaviour while at higher concentration non-Newtonian behaviour has occurred due to shear thinning [234]. Additionally viscoelastic behaviour has been observed [235, 236]. Its viscosity is affected by numerous factors such as DD, MW, concentration, solvent, temperature, etc [237, 238]. Krampe et al highlighted the importance of viscosity by stating too low viscosity might lead to insufficient drug content uniformity whereas too high viscosity would be unsuitable for film casting due to entrapped air bubbles [6]. Values of 123.5 ± 4.9 mPa s and 141.5 ± 7.5 mPa s can be classified as moderately high in comparison to other measured viscosities used in oromucosal film formulations [6].

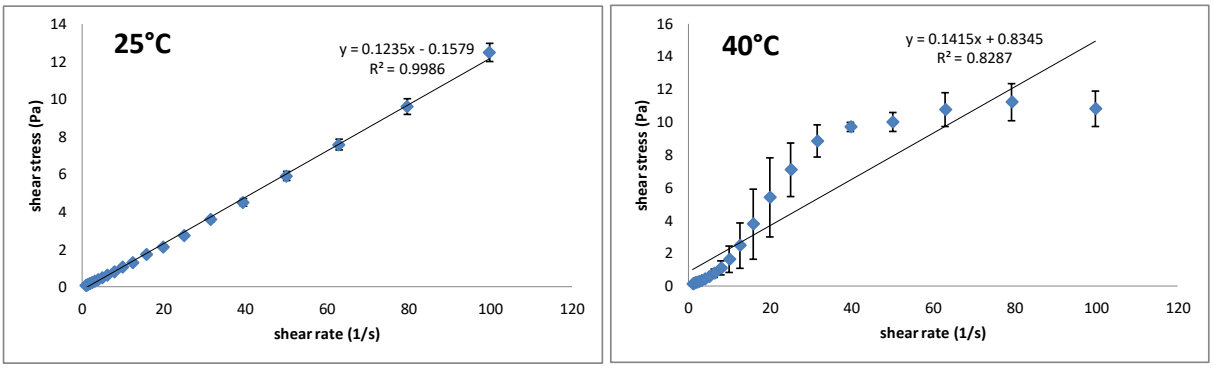

Figure 8: Shear viscosity measurements of F1 solution at 25°C and 40°C. 0.9 mL solution measured with a shear rate of 1 to 100 s^{-1}. n = 3.

5.2 Preformulation studies

Preformulation experiments were carried out using different types of chitosan and glycerol as plasticizer at a concentration ranging from 0.10% to 10% (w/v). Moreover KollicoatIR® was used as a film forming polymer in combination with chitosan with and without glycerol. These concentrations were used in several previous studies using chitosan as film forming polymer [137, 239, 240]. Films containing glycerol concentrations of 5% (w/v) and more displayed “gel-like” behavior. Even at glycerol concentrations of 2.5% (w/v) films were not easy to handle due to their stickiness. The addition of KollicoatIR® did not improve handling

properties in comparison to films made solely of chitosan. These films displayed extremely good handling properties, transparent appearance as well as suitable morphological characteristics as seen by SEM (Figure 9). F1 and F2 displayed clear morphological differences as F1 contained a uniform surface whereas F2 showed convex patterns. F2 appeared to be non-transparent as these patterns were also slightly visible by the naked eye. Abruzzo et al. reported quite similar convex patterns in chitosan films when loaded with an excessive amount of gelatine [241]. F1 showed some irregularities which most likely emerged from peeling the film off the petri dish or due to handling.

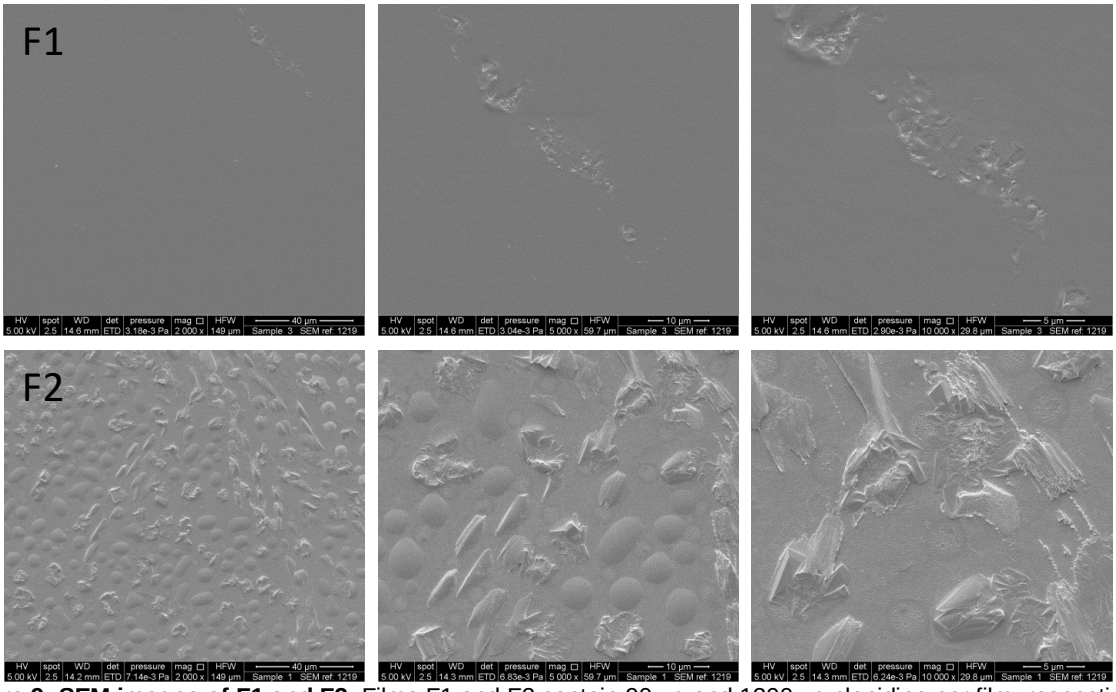

Figure 9: SEM images of F1 and F2. Films F1 and F2 contain 90 µg and 1200 µg clonidine per film, respectively. Prior to SEM imaging films were gold coated.

Overall great handling properties of obtained films might be based on intrinsic film forming properties of chitosan and moderate moisture content by improving the mobility of its polymer chain [242]. Great mechanical properties are particularly important for handling, packaging and storage [196]. For ODF it is up to the formulation scientist to find a compromise between a fast dissolving film while remaining good mechanical properties [46]. This is less of an issue for oromucosal films although room conditions while casting should be carefully observed. Casting below 50% RH has been recommended for ODFs [42]. Moreover films were bubble free which was also verified by its uniform thickness of 54.80 ± 2.53 µm and weight of 13.41 ± 0.80 mg.

This confirmed the sufficiency of deaeration steps used. Sometimes additional deaeration steps such as storage in refrigerator, vacuum equipment, etc are imperative. This is particularly important for highly viscous formulations [3]. Clear appearances of films were achieved by separating solution impurities before casting. This is especially critical when dealing with high viscosity solutions. Therefore chitosan solutions have been filtered through gauzes instead of conventional filters to separate impurities [137]. To lower the risk of losing solution and in turn influencing content uniformity, centrifugation was used instead.

Handling is obviously absolutely key for OTFs but arguably even more important for oromucosal films since patients are required to place the film precisely to the site of administration. Any damage done to the film could lead to insufficient mucoadhesiveness and detachment of the film as well as inadequate drug absorption. Casted films were cut into 1 x 2 cm pieces as preferred sizes are known to range from 1 - 3 cm^2. Patches up to 10 - 15 cm^2 have also been judged as acceptable [243]. Thickness for buccal devices is limited to a few millimetres [244] while ellipsoid-shaped was reported as most acceptable overall [243]. While not tested in this study chitosan films have measured surface pH values of 5 in the past [245, 246]. A pH of 7 ± 1.5 is generally considered as non-irritant for buccal films [153]. Moreover lower pH values (4.5 - 6.5) did not cause irritations in the past [6, 247]. Granted patients already suffering from mucositis or any skin irritations are even more susceptible to any possible pH changes caused by films. In that regard the pH of chitosan films is particularly important and should be thoroughly tested *in vivo*.

5.3 Disintegration

Disintegration was performed to verify chitosan's water insolubility. For ODFs disintegration time limit is set at 180 s. Disintegration time is not a critical aspect for oromucosal films designed for sustained release [3]. Due to the low drug concentration film properties are almost solely based on chitosan therefore disintegration tests confirmed its inability to dissolve in deionised water (pH: 6.8) and simulated saliva solution. Although it is important to note that water with pH 5.5 led to disintegration within 30 min. Chitosan's low water solubility stems from its amine groups with a pK_a value of 6.3 requiring a pH below its pK_a for quaternisation. Chitosan's water solubility is therefore depending on its DD and the solution pH. Thus chitosan used in this study (DD ≥ 90%) is only readily soluble in acidic solutions with a pH below 6.0 [186–188].

5.4 FTIR

Figure 10A demonstrates the FTIR spectra for chitosan, F1 and F3. A peak at 887 cm^{-1} indicates aliphatic aldehydes and in conjunction with 1055 cm^{-1} these peaks are characteristic for chitosan's saccharide structure [248, 249]. 1149 cm^{-1} indicates primary or secondary alcohol. Amide II peak range comprises 1515 - 1570 cm^{-1}. 1593 cm^{-1} and 1301

cm^{-1} were reported as amide I and III peaks, respectively [250]. Those peaks are characteristic of chitin and chitosan. 1371 cm^{-1} and 1420 cm^{-1} are corresponding to CH_3 symmetrical deformation mode [251, 252]. 1019 cm^{-1} assigns to C-O stretching vibration in chitosan. 3450 cm^{-1} indicates N-H symmetrical vibration and can be used in conjunction with 1650 cm^{-1} for quantitative analysis of chitosan's DD. In this study N-H symmetrical vibration was observed at 3365 cm^{-1}. 2940 - 2840 cm^{-1} are typical C-H stretch vibrations [253]. Broadering in peaks from 3500 to 2800 cm^{-1} seen in chitosan powder, F1 and F3 are due to presence of residual moisture content [240]. Since F1 and F3 spectra are nearly identical it can be concluded that clonidine concentration present in F1 is too low for detection using FTIR. This was already reported by Buanz et al at higher concentrations [174]. Analyses of spectra were done according to previous studies [253, 254]. F2 and clonidine spectra exhibit very similar spectra (Figure 10B). Significant reductions in transmittance were found at 540 to 1100, 1300 to 1600 and 2800 to 3600 cm^{-1}. Chemical interactions between the drug and polymer were confirmed by FTIR data. Broadening of peaks are noticeable at 864, 1017 and 1073 cm^{-1}. Peaks found in clonidine powder and F2 were in accordance with previous analyses [174]. Similarities in patterns between F1 and F3 as well as clonidine powder and F2 are displayed in Figure 10C.

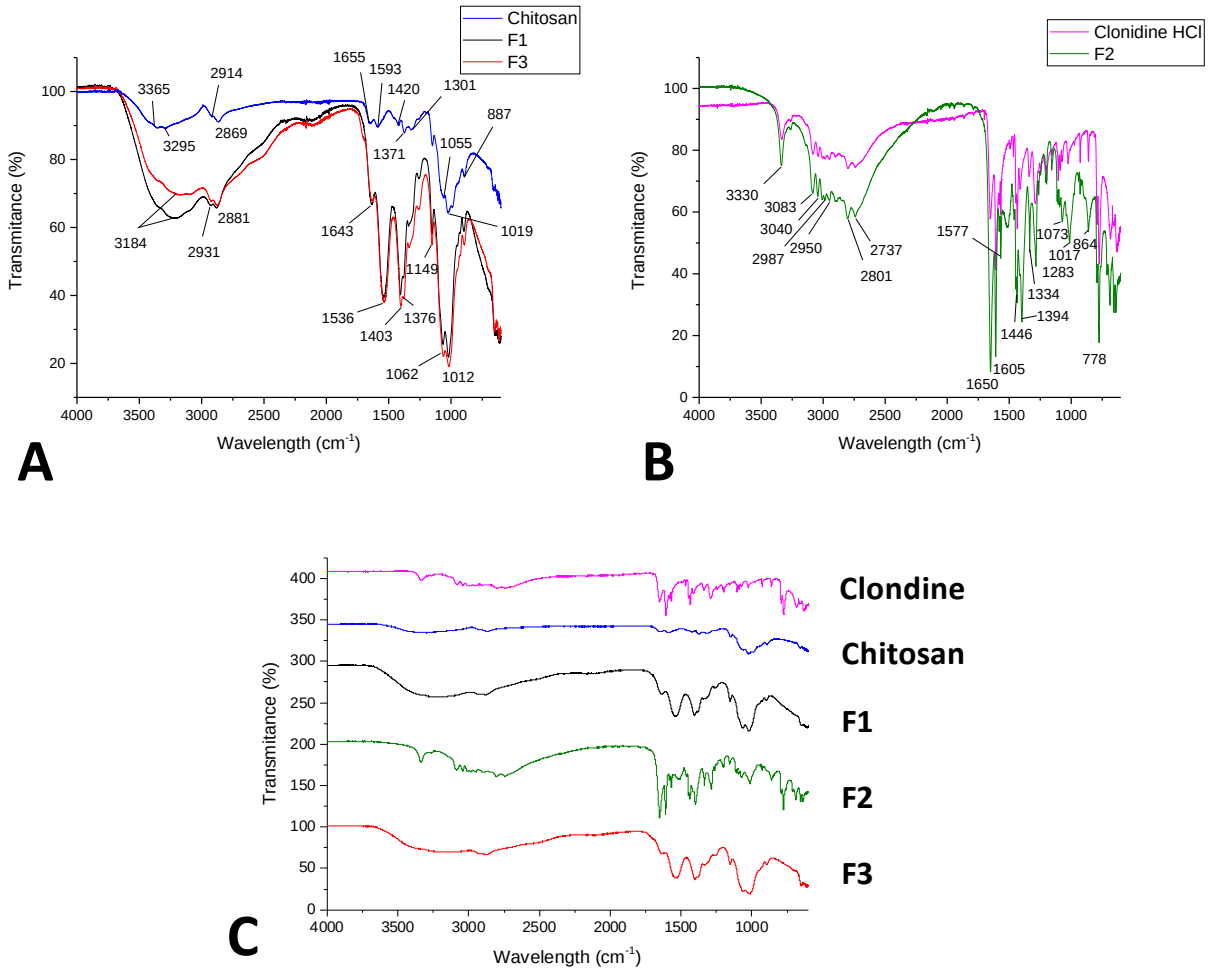

Figure 10: FTIR analyses of raw materials clonidine, chitosan and films termed F1, F2 and F3. A: similarity of patterns between chitosan, F1 and F3 can be contributed to the low drug load in F1. B: Similar spectra between clonidine and F2 verified higher drug load in F2. C: Clonidine, chitosan, F1, F2 and F3 are stacked by y offsets.

5.5 XRPD

Chitosan powder displayed its characteristic peaks at 2θ values of 9.8 and 20.4° (Figure 11). Chitosan in its free amino form (DD = 100%) exhibits characteristic peaks for angles 2θ = 10.4°, 19.8° and 22° which were named “tendon” hydrated polymorph [255]. Chitosan in its hydrochloride form has been reported to obtain spectra with lower intensity and slightly lower diffraction angles [256]. The latter is in agreement to the peak observed at 2θ value of 9.8° as supposed to 10.4°. XRPD diffraction patterns confirm an amorphous state of drug-loaded and free films. Interestingly while F2 displayed an overall amorphous pattern a peak at a 2θ value of 11° which is not present in clonidine raw material was observed. This can be most likely contributed to influences of the sample holder or other impurities.

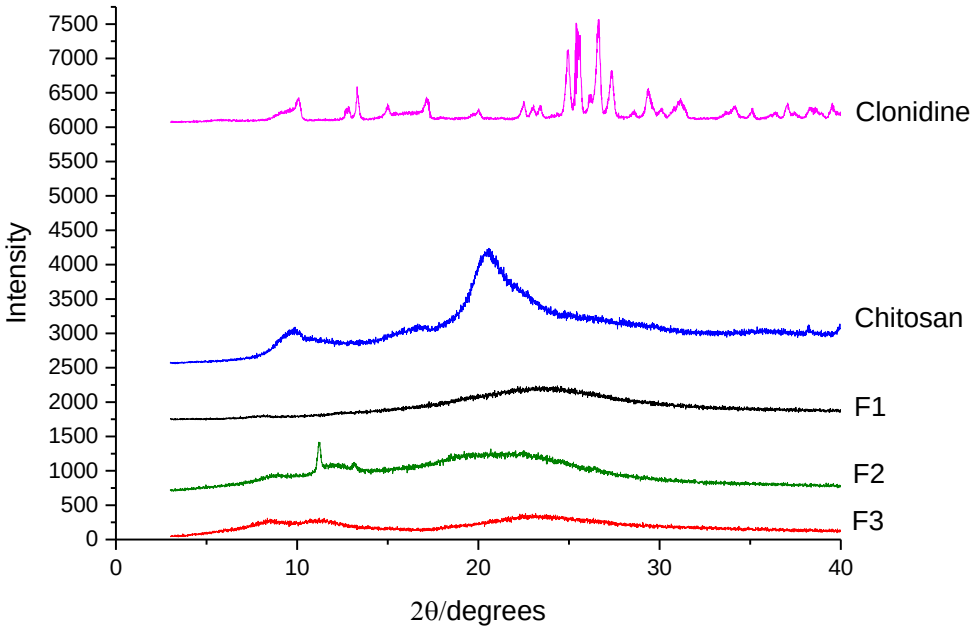

Figure 11: XRPD patterns of raw materials clonidine, chitosan and films termed F1, F2 and F3. Samples are stacked by y offsets. Measurements confirmed a crystalline state of clonidine as well as amorphous state of chitosan, F1, F2 and F3. Data was collected using a step size of 0.01°, speed of 10°/min over a range of 3 to 40°.

F1 displayed a similar pattern to drug free film (F3) and appears amorphous. This was expected given the low drug load. Again it is worth noting that due to the low drug load in F1 it is likely that possible recrystallinization is not detectable using XRPD. This provides further evidence of difficulties detecting such low concentrations let alone the physical state of materials.

5.6 Dynamic vapor sorption (DVS)

Relatively low water uptake was measured at RH values < 30% and a more significant increase in water sorption was seen as the RH value reached 40% (Figure 12A). This may be because at the beginning water sorption is predominantly based on surface adsorption whereas at higher RH values bulk absorption dominates. Figure 12B shows a symmetrical course of the curve indicating a reversible sorption-desorption process. Hence it is likely that only surface water was involved in the process. In the range of 40 to 90% RH a linear correlation between the increase in mass and the RH value can be observed. An increase to 90% RH resulted in an increase in weight change of 20% (w/w). Water uptake at 60% RH was around 10% (w/w). Initial water content was calculated by measuring weight loss (% w/w) after exposing films to 0% RH for 120 min resulting in 6.25 ± 0.71%. Overall F1 contains a large amount of chitosan which is known to absorb water slowly [241], therefore water sorption is largely dependent on the polymer present in films.

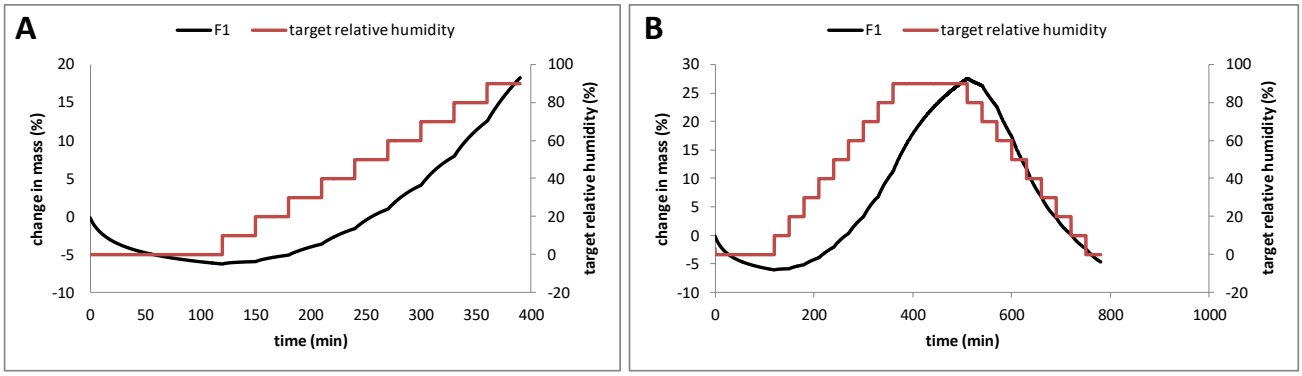

Figure 12: Time course curve of film F1 exposed to relative humidity (DVS measurements). A: exposed to RH from 0 to 90% (sorption, n = 3). B: exposed to RH from 0 to 90% and 90 to 0% (desorption, n = 1). The symmetrical curve in B indicates that changes in mass are most likely associated to surface water rather than bulk absorption.

5.7 Thermal characterization

Moisture content of F1 and F3 were determined at 9.1 ± 1.6% and 8.1 ± 1.9% (w/w), respectively (Table 4) by TGA at a temperature range of 30°C to 125°C. These values are close to the determined 8.2 ± 0.1% (w/w) of chitosan powder. Differences between F1 and F3 are within the measured standard deviation and not contributed by the API but room conditions when casting. Degradation onset temperatures of raw materials, F1 and F3 occurred in the range of 250 to 260°C. Films which were stored for 48 h at 25°C and 60% RH showed significant higher water content.

Table 4: TGA of clonidine, chitosan and films F1 and F3. F1*: stored for 48 h in climate chamber at 60% RH and 25°C. Water loss respectively moisture content was measured in the temperature range from 30 to 125°C. n = 3

Sample	Water loss % (w/w)	Degradation $_{onset}$ (°C)
Clonidine powder	0.4 ± 0.2	248.8 ± 15.0
Chitosan powder	8.2 ± 0.1	257.6 ± 0.2
F1	9.3 ± 1.8	258.7 ± 0.9
F1*	14.6 ± 0.3	258.0 ± 2.8
F3	8.1 ± 1.9	256.8 ± 0.4

Determination of water content in films is of high importance for its stability and packaging in particular. Moreover moisture content is known to potentially cause changes in mechanical properties such as flexibility and folding endurance [7].

Table 5: (MT)DSC measurements of clonidine and F3. TA high sensitive pinholed aluminium pan with 5 to 10 mg samples. DSC conditions: 10°C/min; MTDSC conditions: 2°C/min, amplitude of ±0.212°C over a period of 40 s. n = 3

Formulation	$T_{m\ onset}$ (°C)	$T_{m\ peak}$ (°C)	$\Delta H_{melting}$ (J/g)	T_g (°C)	ΔC_p (J/g°C)
Clonidine	305.9 ± 3.7	307.6 ± 4.8	207.8 ± 42.6	-	-
F3	-	-	-	182.4°C	0.184

Using conventional DSC to determine the melting temperature (T_m) of clonidine provided values of a $T_{m\ onset}$ of 305.9 ± 3.7 °C and $T_{m\ peak}$ of 307.6 ± 4.8 °C (Table 5 and Figure 13). An exothermic peak with an onset temperature of 311.6 ± 5.3°C and peak value of 315.7 ± 4.4°C was measured and assigned to its degradation temperature. These findings are in agreement to the literature with its melting point reported at 305.0°C [157] and confirmed that melting of clonidine is quickly followed by its degradation. One MTDSC measurement of F3 showed a distinct T_g obtained at 182.4°C.

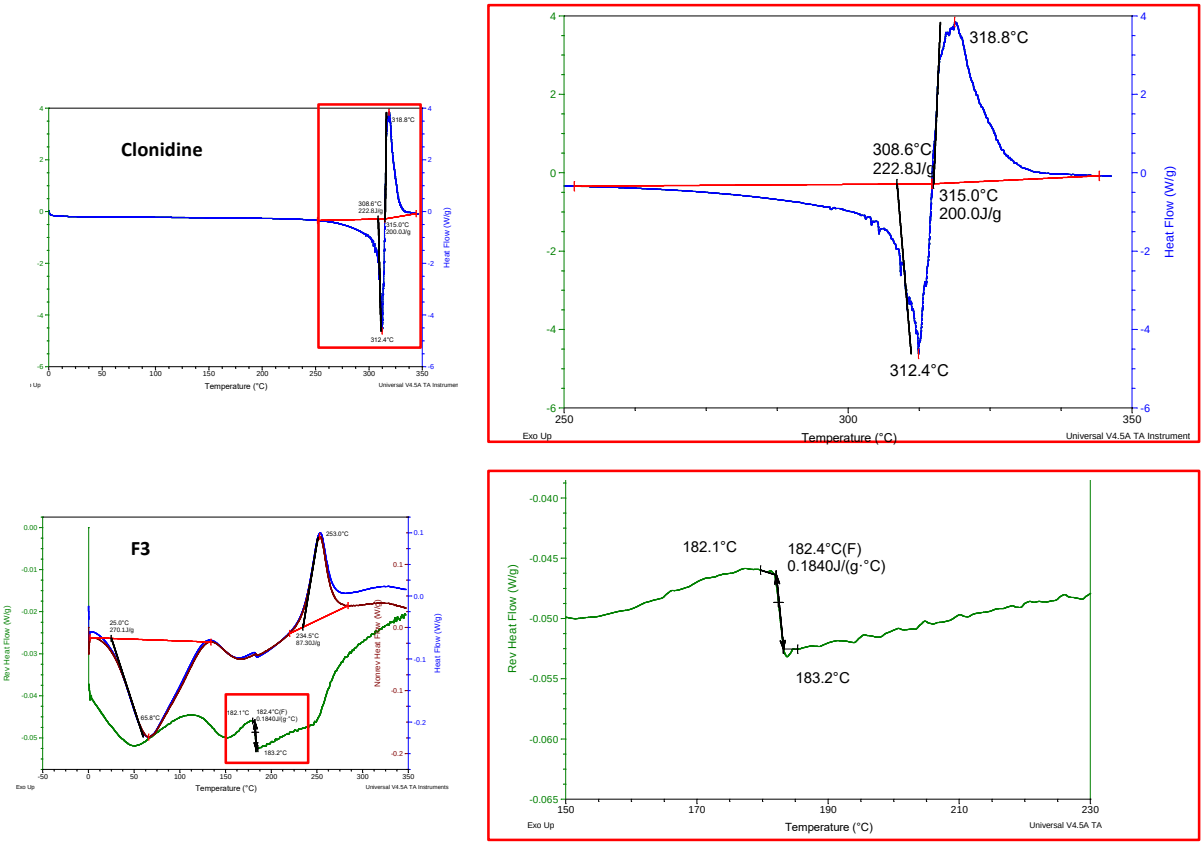

Figure 13: DSC and MTDSC analyses of clonidine powder and F3, respectively. TA high sensitive pinholed aluminium pan with 5 to 10 mg samples. DSC conditions: 10°C/min; MTDSC conditions: 2°C/min, amplitude of ±0.212°C over a period of 40 s. n = 3 for clonidine, n = 1 for F3.

There have been a number of studies that focused on detecting chitosan's T_g with apparent discrepancies and highlighted the importance of water content in these films [184, 232]. Therefore chitosan powder, F1 and F3 were all measured several times to reproduce and verify the measured T_g of 182.4°C. The results between these three samples differed only slightly as excepted (Figure 14). Measurements were unsuccessful as no distinct T_g was analyzed. F3 shows an endothermic event between 0 and 135°C (T_{peak} = 66.1°C, ΔH = 190.0 J/g) which can be assigned to water loss. Degradation occurred between 237.0 and 300°C (T_{peak} = 254.1°C, ΔH = 92.5 J/g). Water loss and degradation measured using MTDSC was in agreement with the data obtained by TGA.

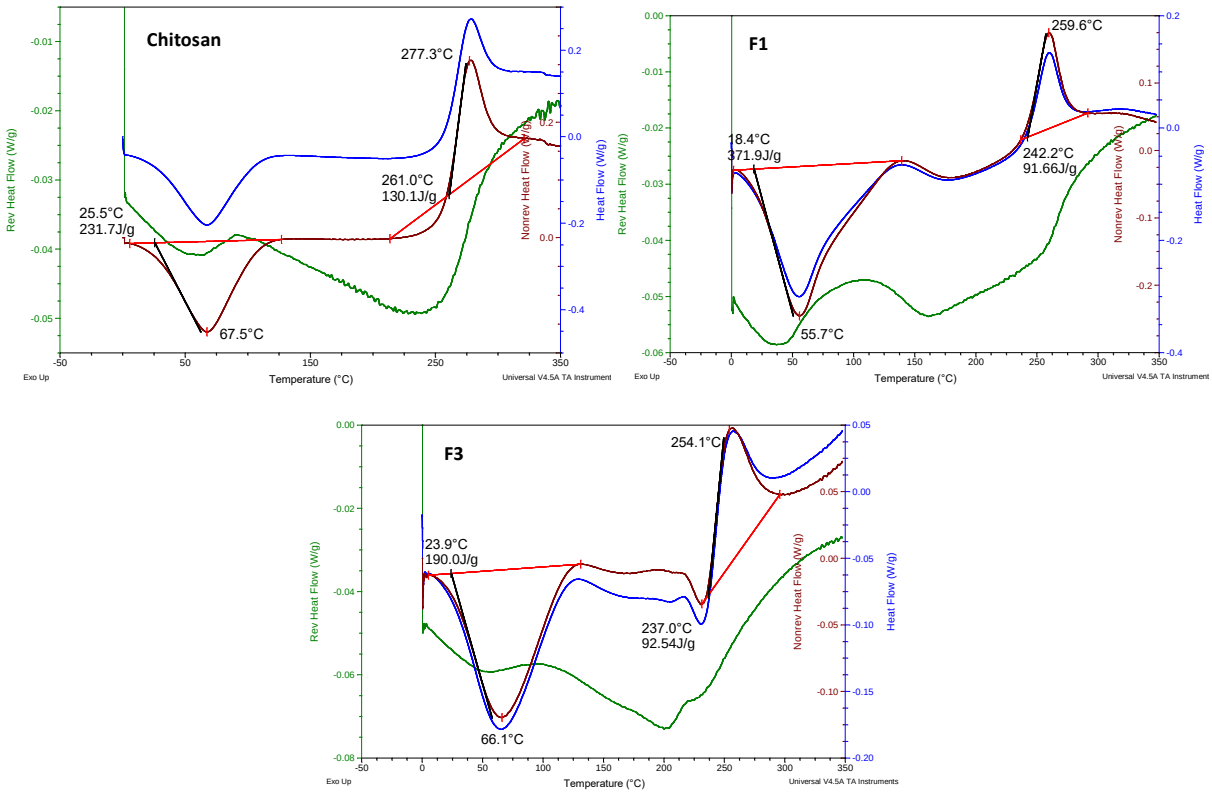

Figure 14: MTDSC analyses of chitosan powder, F1 and F3. TA high sensitive pinholed aluminium pan with 5 to 10 mg samples. MTDSC conditions: 2°C/min, amplitude of ±0.212°C over a period of 40 s. n = 3.

Overall several different sample sizes in the range of 5 to 20 mg were analyzed. Films were cut into different sizes as well as casted directly in highly sensitive pinholed aluminium pans. MTDSC measurements with and without heating-cooling cycles were carried out to confirm if water loss was overlapping with the T_g of chtiosan. Temperature ramps for heating and cooling were increased to enhance sensitivity. Moreover glycerol was also added to the film formulation to lower the T_g of chitosan due to its plasticizing effect [257]. Although one distinct T_g of chitosan was measured (Figure 13), this result was not reproducible highlighting its complexity (Figure 14).

Dhawade et al. confirmed an increase in crystallinity of chitosan and its oligomers due to an decrease in water content and increase in depolymerisation [242]. These problems have been contributed to difficulties in sample preparation and chitosan's hygroscopicity [232]. The latter leads to hydrogen bond formation [258] which affects its thermal and mechanical properties and leads to a depression of the glass transition temperature [259]. This confirms the plasticizing effect of water content in chitosan [184]. Higher water content correlates with lower DD [259]. Although contrary findings were reported [232]. As a matter of fact T_g values of -37°C, -43°C [260], 61°C, 118°C [242], 140 to 150°C [232] and 203°C [261] have been analyzed. Additonal studies were unable to detect a distinct T_g, despite the presence of

amorphous content [260, 262]. This led to conclusions that T_g of chitosan is located at temperatures beyond its degradation, preventing T_g detection [242].

In this study degradation onset temperatures of F3 of 256.8 ± 2.8°C and 239.4 ± 3.8°C were measured using TGA and DSC, respectively. These results were in accordance with degradation temperatures of 225, 246 and 255°C found in literature [260]. Dong et al. emphasized on the intricacy of thermal characterization of chitosan using 4 different techniques [232]. It has been assumed that MTDSC measurements are not sensitive enough to detect relaxation temperatures of polysaccharides. This is in agreement with our findings as a distinct T_g measurement was not reproducible using MTDSC. It is worth noting that Dong et al. implemented physical aging to increase sensitivity due to enthalpy relaxation [232]. Moreover higher casting temperatures were used and casted films were rinsed with diethylether and subsequently dried under reduced pressure to ensure thorough solvent evaporation.

5.8 Dynamic mechanical thermal analysis (DMTA)

In F3 the T_g was determined as peak of tan δ with values of 154.95 ± 0.47°C (Figure 15). F1 displayed nearly identical results as F3. The peak observed at around 92°C was assigned to water induced relaxations based on chitosan's hygroscopicity. F2 displayed a T_g value of 166.47 ± 2.31°C which was assigned to chitosan. This increase of chitosan's T_g in comparison to F1 and F3 is most likely attributed to the higher drug concentration in F2. For non-plasticized analyses a peak maximum for tan δ of 265.73 ± 1.53°C and 258.98°C were observed in F1 and F2, respectively (Figure 16). These temperatures were assigned to the degradation temperature of chitosan. TGA measurements of degragadation onset temperatures of chitosan in the range of 250 to 260°C confirm these results. As expected no water induced relaxations were measured.

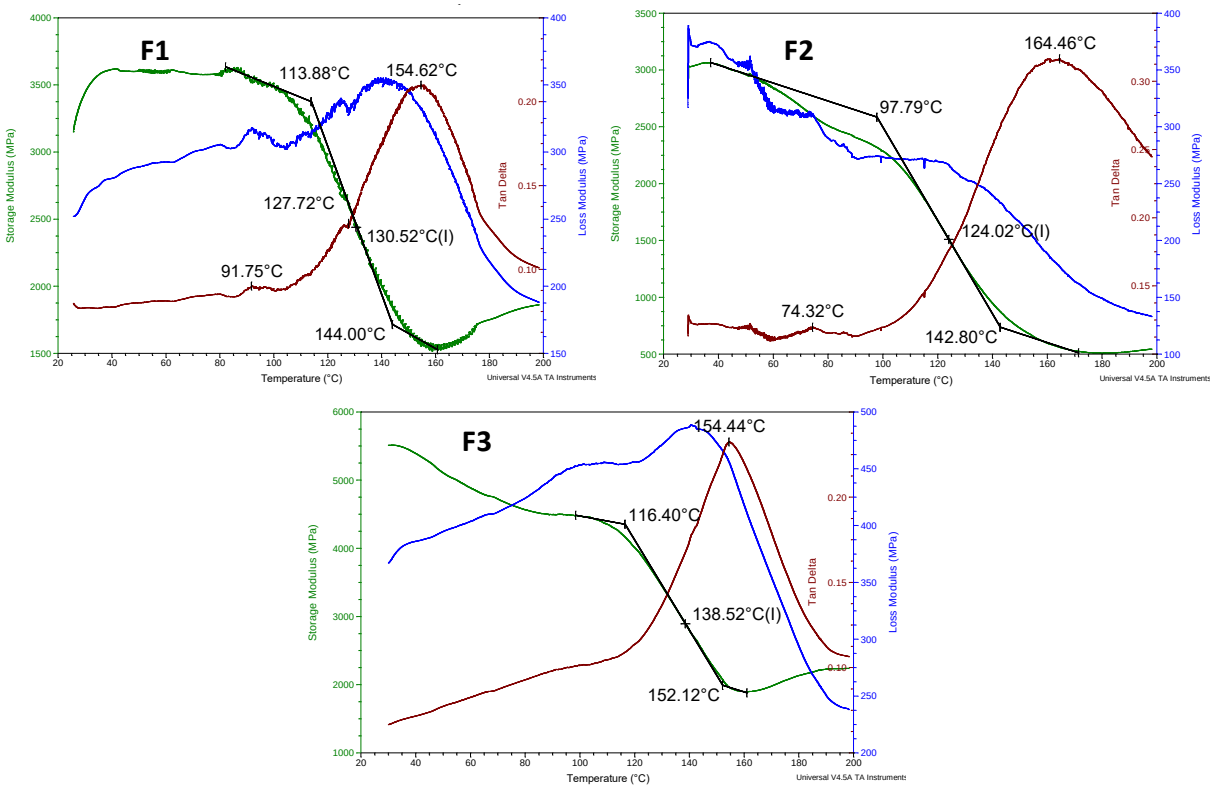

Figure 15: DMTA measurements of F1, F2 and F3. Heating rate of 2°C/min from 30 to 200°C. Oscillating frequency of 1 Hz. n = 3

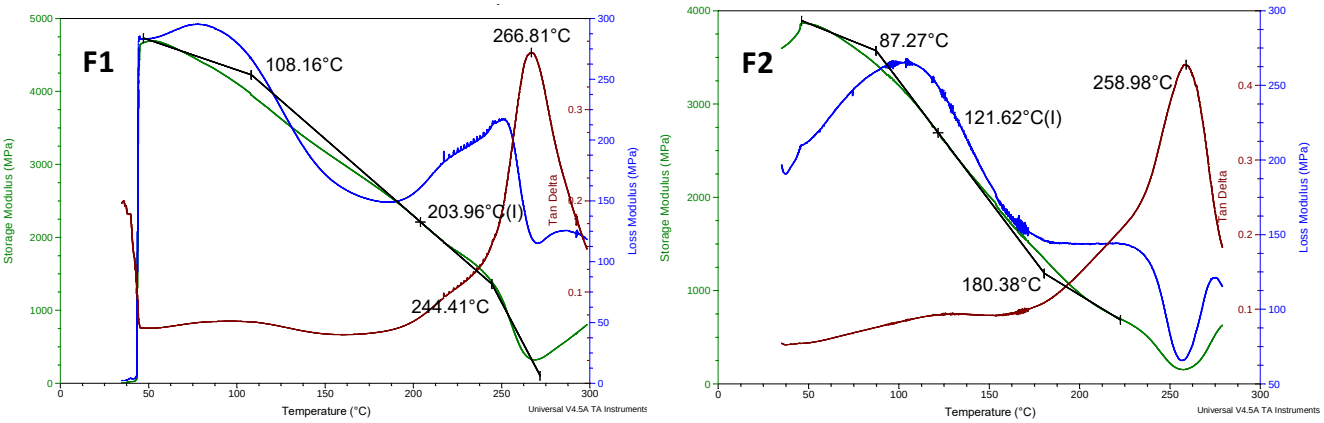

Figure 16: Reheated DMTA measurements of F1 and F2 (non-plasticized). Second heating cycle from 30 to 250°C. Heating rate of 2°C/min, oscillating frequency of 1 Hz. n = 3.

DMTA was confirmed as a promising alternative to MTDSC to measure T_g. This is based on its sensitivity to detect small changes in a polymeric structures [184, 232]. The T_g was determined by the signal maximum of tan δ (quotient of storage and loss moduli). It can also be calculated by the inflection point of storage modulus decrease [223]. Results obtained in this study were in agreement with T_g measurements verified by several techniques [232]. While DMTA provided great results in this study unsuccessful T_g analyses on chitosan films

have been reported in the past [263]. In particular problems connected to low heating rates, subsequent water loss and brittleness of films do not allow T_g analysis [174].

5.9 Chromatographic separation and content uniformity test (CUT)

Quantification of clonidine required separation using HPLC as conventional UV-Vis spectroscopy would not allow differentiation of clonidine, chitosan and acetic acid which all absorb at 220 nm. Identification and separation of analytes was carried out according to ICH guideline Q2(R1) [264]. Discrimination between compounds was achieved and validated by a comparison between samples containing clonidine and negative samples which did not contain the analyte. Moreover mixtures of compounds were anaylzed to observe potential interferences. Overall chromatographic separation of compounds, namely chitosan, acetic acid and clonidine, was achieved within 10 minutes using an isocratic method (Figure 17).

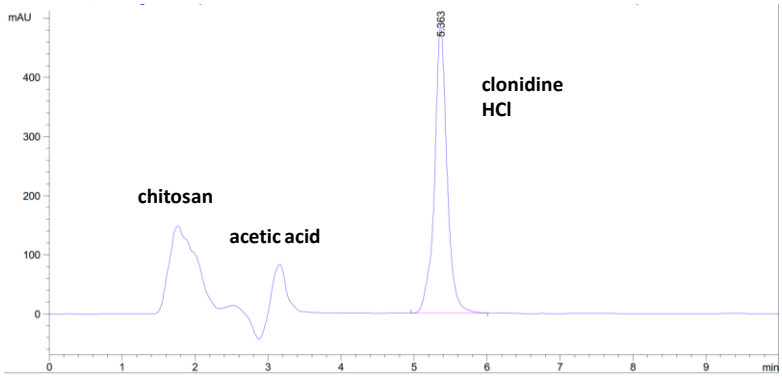

Figure 17: Chromatographic separation of chitosan, acetic acid and clonidine hydrochloride. Mobile phase: 0.1% (v/v) trifluoroacetic acid in water and acetonitrile (80:20 v/v). Measurements were done at a flow rate of 1.0 mL/min, 40°C, absorbance of 220 nm and injection volume of 10 µL. C-12 Phenomenex SynergyMax column (250 mm x 4.6 mm x 4 µm).

Besides identification, according to ICH guideline Q2(R1) [264] a linear relationship must be evaluated. This was confirmed over a range of 0 to 120 µg/mL with a linear response of R^2 = 0.9995 (Figure 18). LOD (6) and LOQ (7) were expressed according to ICH.

$$\mathrm{LOD} = \frac{3.3\ \sigma}{S} \qquad \textbf{(6)}$$

$$\mathrm{LOQ} = \frac{10\ \sigma}{S} \qquad \textbf{(7)}$$

σ is the standard deviation of the response, S is the slope of the calibration curve

The used range provides the requirement for CUT of using a minimum of 5 concentrations covering a minimum of 70 to 130% of the test concentration of 90 µg [264]. 1 mg/mL clonidine was diluted by a series dilution and a limit of detection (LOD) was measured at 1.85 µg/mL and a limit of quantification (LOQ) was found at 5.60 µg/mL.

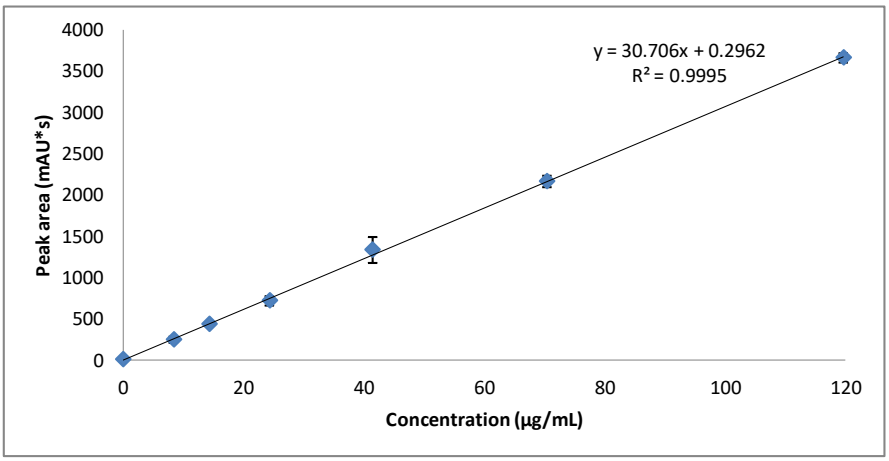

Figure 18: Linear relationship of clonidine hydrochloride dissolved in 1% (v/v) acetic acid. Calibration curve was carried out using a series dilution resulting in concentrations of 119.7, 70.4, 41.4, 24.4, 14.3, 8.4 and 0 µg clonidine per mL. n = 3

Depending upon the dosage form and dose of the drug substance either weight variation or content uniformity is necessary to be tested. In this study content uniformity was required and was determined by calculating the acceptance value (AV) according to Ph. Eur. The requirement of content uniformity was fulfilled with an AV value of 14.4 and standard deviation of 6.00 (n = 10) (Figure 19). The AV value is dependent on the difference between the measured mean and reference value ($|\mathrm{M} - \overline{\mathrm{X}}|$) and width of the tolerance interval (ks). Hence, the requirement is influenced by the width of this interval and the obtained standard deviation ($|\mathrm{M} - \overline{\mathrm{X}}| + \mathrm{ks}$) [265].

Film	Content uniformity (%)	Film weight (mg)	Film thickness (µm)
1	109.26	14.55	60.0
2	102.13	13.83	50.0
3	99.83	13.37	52.0
4	96.46	13.23	53.5
5	100.14	13.39	52.0
6	97.81	13.27	55.5
7	88.63	11.62	52.0
8	108.78	14.32	58.0
9	102.82	13.30	57.5
10	98.08	13.24	53.0
Mean	100.40	13.41	54.35
SD	6.00	0.79	3.24
RSD	5.98	5.88	5.96

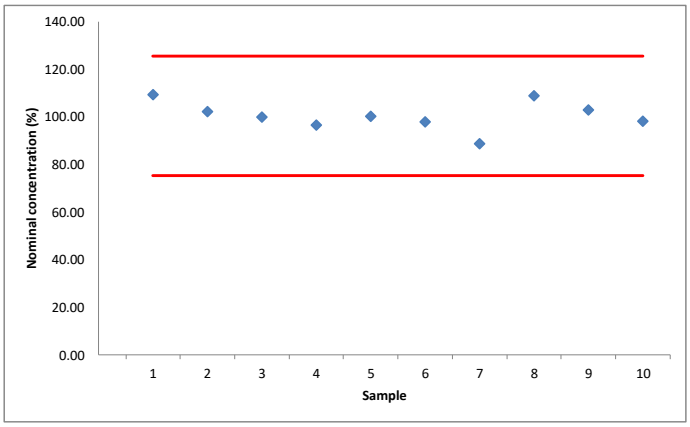

Figure 19: Uniformity of content of film F1. Red lines indicate "maximum allowed range for deviation of each dosage unit tested from the calculated value of M" [266]. SD = standard deviation, RSD = relative standard deviation, n = 10

While low drug load is desirable for films it causes difficulties in detection and even more quantification. Insufficient uniformity of content is a known problem for OTFs in general [47–49] which increases with low solution viscosity [3, 6, 236] and decreases with high solution viscosity [267]. However this is generally a bigger challenge in large scale than small scale production [6]. In small scale, high viscosity might cause problems when transferring the solution into casting apparatus due to impeded pouring [268].

Insufficient uniformity of content on laboratory scale is mostly contributed to thickness fluctuations. Therefore in research content uniformity is often calculated based on either area or weight but not according to Ph. Eur. Dissolving a known film weight for analysis has been postulated as erroneous since in research films are cut by area [269]. On production scale it is preferred cutting films by weight as film stretching is inevitable when cutting by length [6]. On laboratory scale solvent casting is the most utilized technique which is more prone to thickness and therefore weight fluctuations. These fluctuations most likely occur due to surface tension, unleveled hot plates, dust, etc. Also drop formation due to condensation on petri dish walls and subsequent trickle down leads to thicker film edges. Additionally polystyrene petri dishes are lighter and more flexible than glass and therefore might deform slightly when using higher temperatures and subsequently lose contact to the hot plates. This leads to irregular heat transfer and casting occurs under unleveled conditions. This can be circumvented by weighing petri dishes down. Finally if room conditions such as RH and temperature are not controlled, batch-to-batch variability is inevitable. This is particularly important to achieve the desired viscosity of the solution [7] which in turn affects content uniformity. In that regard it is worth noting that while the obtained AV value was within the norm all selected films were casted in one petri dish. In other words content uniformity varies

when casting several petri dishes from one batch. Moreover rectangular film dimensions made cutting areas close to petri dish edges impossible.

Based on the above mentioned difficulties when using solvent casting and known reported content uniformity problems for OTFs [47], a lot of effort has been put in sample preparation and solvent casting itself. Above all, insufficient uniformity of content, weight and thickness of oromucosal films consisting solely of chitosan are known [241]. Correspondingly, impurities were thoroughly separated, chitosan solution was stirred over night and entrapped air bubbles were removed thoroughly. Moreover hot plates were precisely leveled and weighed down to the hot plate to ensure constant contact and uniform heat transfer. Finally to ensure desired film dimension, films were cut using a referenced sized carton fixed with mini magnets.

5.10 Mapping of homogenous drug distribution using SEM-EDS

Figure 20 confirmed homogenous API distribution with low (F1) and high drug load (F2). In both films at least 3 areas were analyzed with each providing an area over 1 mm^2. The number of measurements and the chosen area provide further evidence of homogenous drug distribution within each film. Therefore these results are in agreement with the confirmed homogenous drug distribution as analyzed by the CUT according to Ph. Eur. Moreover areas of 300 x 300 µm were zoomed out to confirm homogenous drug distribution in areas analyzed by TTM (5.11).

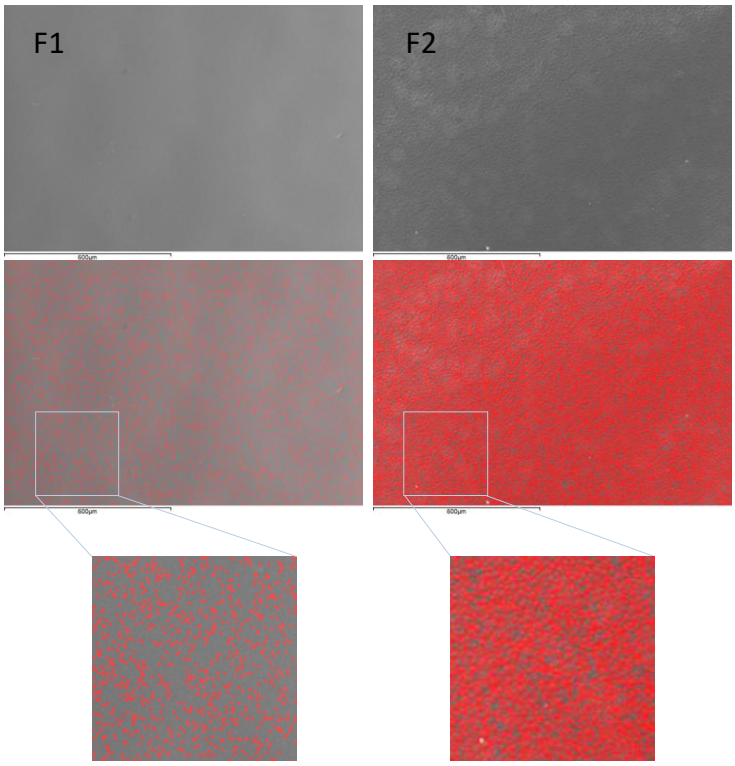

Figure 20: SEM-EDS analyses of films F1 and F2. Map resolution: 256 x 256, EDS analysis operated at 20 kV, 10.0 mm working distance and 100 s counting time. Zoomed areas: 300 x 300 µm. n = 3.

In addition F1 and F2 were semi-quantitative analyzed. Concentrations of 0.35 ± 0.02% (w/w) for F1 and 8.73 ± 0.91% (w/w) for F2 were detected. These results have to be observed carefully as firstly the clonidine concentration of F1 is most likely located close to the instrument's LOD for chlorine. Secondly this set-up allowed only a semi-quantitative analysis of a chemical composition relative to a standard. Thirdly different sample preparation methods can be used such as carbon coating to improve accuracy.

Clonidine, containing two chlorine groups, made its detection using SEM-EDS possible. In connection with the flat film surface, SEM-EDS analysis is a promising technique to map and analyze quite large areas of oromucosal films semi-quantitatively. Analyses can be done quickly and the results revealed the feasibility to detect theoretical concentrations below 0.9% (w/w) in F1. Moreover SEM itself provides information on the film morphology. In conclusion mapping should be especially considered in case content uniformity is not reached as this technique provides the possibility to detect consistent patterns of inhomogeneities within the dosage forms (e.g. caused by adsorption).

5.11 Mapping of homogenous drug distribution using TTM

The machine set up was calibrated up to 250°C. For that purpose, the probe deflection is monitored over an applied voltage range until the known T_m of three polymers is reached and melting occurs (Figure 21).

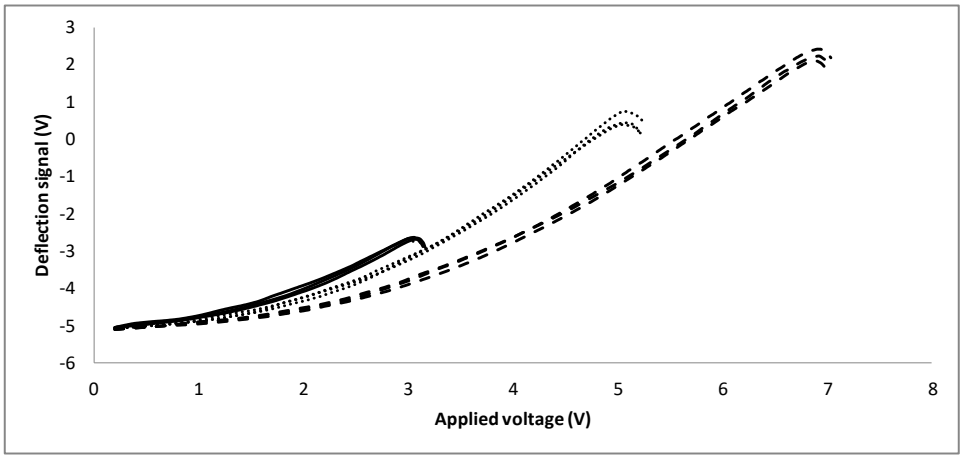

Figure 21: Temperature calibration of TTM. Calibration was done using distinct melting temperatures of polycaprolactone (T_m = 55°C; –), polyethylene (T_m = 116°C; ···) and polyethylene terepthalate (T_m = 235°C; - - -). n = 3

Due to the measured T_m (307.6 ± 4.8 °C) of clonidine powder by DSC, the probe was heated up to its maximum of 350°C. While there is no knowledge on a clearly defined LOD the provided drug load in F1 is most likely too low to detect as numerous trials were unsuccessful and provided the same histogram as the drug free F3 (Figure 22). In both films no distinct peaks were obtained that could be assigned to either chitosan or clonidine. Most measurements were not assigned to a transition at all or to transitions occurring at temperatures far beyond 250°C. The latter is not within the calibrated range of the set up. Moreover TGA measurements of chitosan powder, clonidine powder and F1 revealed degradation temperatures of around 250°C. Therefore it is likely that these measurements were due to degradation instead of T_m or T_g. F2 showed a broad peak with a clear Gaussian distribution with a mean value of 162°C. This temperature is in agreement with T_g values of chitosan reported in the past [232]. Additionally this value lies close to the measured DMTA value of 166.47 ± 2.31°C in this study. However the obtained TTM result is skewed as F1 and F3, containing (almost) solely chitosan, did not reveal a similar pattern at this temperature range. Additionally the peak broadness might be a sign of inhomogeneity [229].

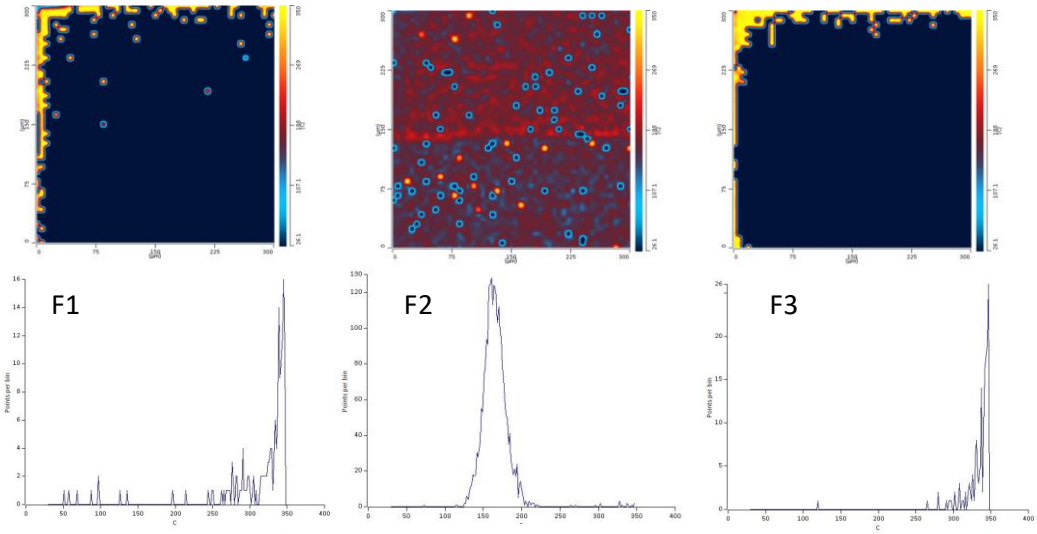

Figure 22: TTM maps and corresponding histograms of films F1, F2 and F3. Heating rate of 10°C/s (600°C/min) at 30 to 350°C. Measurements were done at 300 x 300 µm film areas with a resolution of 6 µm. n = 2

Due to the low drug load in F1 a high number of measurements and consequently high resolution was inevitable in order to detect the API. To obtain a statistically good representation of drug distribution in relation to the actual film area (2 cm^2) an area of 300 x 300 µm with a maximum resolution of 6 µm was chosen. Under these settings a single TTM analysis took up to 30 h. SEM-EDS analyses were carried out prior to TTM measurements to verify the presents of clonidine within the areas measured. SEM-EDS analyses confirmed the presence of clonidine and more importantly homogenous drug distribution within 300 x 300 µm areas. While in theory films are very suitable for TTM due to their flat and more importantly smooth surface. Their susceptibility to humidity provided a challenge. Depending on RH, films are either sticky or brittle and change their mechanical properties drastically. Moreover water absorption will affect its thermal characteristics. To conclude such long analysis under unregulated room conditions might affect the results. Therefore addressing these concerns requires further method optimization of TTM but could potentially provide a successful technique utilized for pharmaceutical purposes [229, 230].

Based on the known difficulties in measuring the T_g of chitosan due to its hygroscopicity [232] and film susceptibility to RH it is not surprising that only one clear transitions was measured in F2. Moreover thermal characterization of chitosan might require heating-cooling cycles which cannot be achieved using TTM.

5.12 *In vitro* drug release (dissolution test)

As with the CUT, ICH guideline Q2(R1) [264] requires to validate the HPLC method used for dissolution test. A linear relationship was evaluated across the range of 0 to 120 µg/mL with a linear response of R^2 = 0.9999 (Figure 23). This provides the ICH requirement for

dissolution testing of using a minimum of 5 concentrations covering a minimum of ± 20% over the specified range of the test concentration of 90 µg [264]. A limit of detection (LOD) was measured at 0.93 µg/mL and a limit of quantification (LOQ) was found at 2.81 µg/mL.

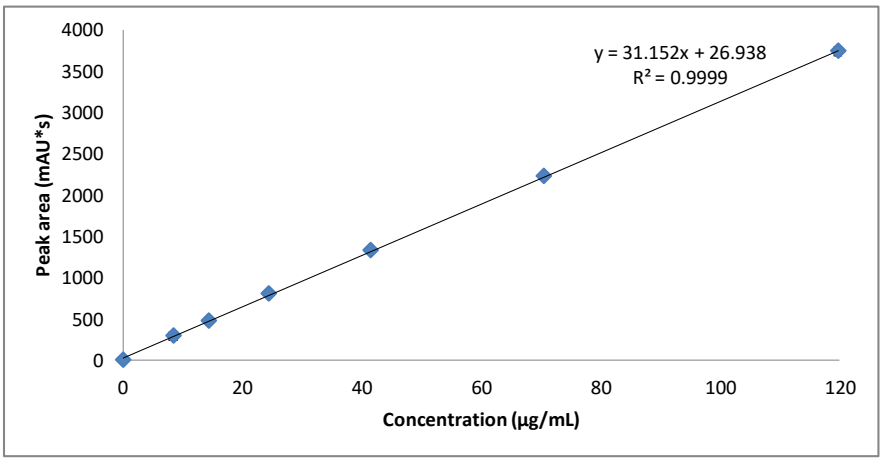

Figure 23: Linear relationship of clonidine hydrochloride dissolved in deionised water. Deionised water with a pH of 6.8 was used. Calibration curve was carried out using a series dilution resulting in concentrations of 119.7, 70.4, 41.4, 24.4, 14.3, 8.4 and 0 µg clonidine per mL. n = 3

In vitro drug release was tested in deionised water (pH: 6.8). Preformulation studies revealed a fast release of clonidine. Therefore time intervals of 1, 5, 15, 30, 60, 120, 180, 240, 300 and 360 min were analyzed. Obtained release profile showed a hyperbolic curve with more than 50% drug released ($t_{50\%}$) under 30 min (Figure 24). The release rate declined noticeable after 60 min (59% drug release) and a linear release rate between 60 and 360 min was observed. 80% drug release ($t_{80\%}$) was achieved after 240 min.

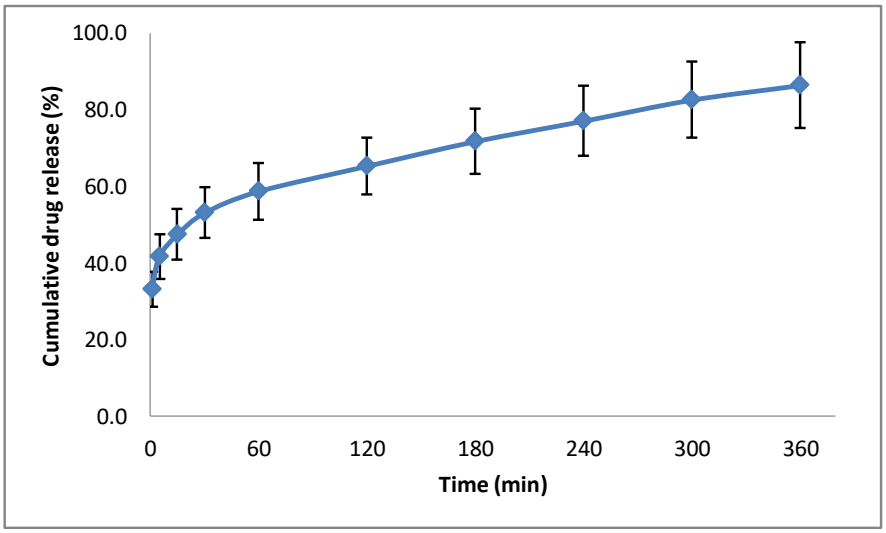

Figure 24: Dissolution profile of film F1. Dissolution medium: 5 mL deionised water (pH: 6.8; 37 ± 1°C) in petri dish, n = 3.

The sustained clonidine release of a chitosan oromucosal film is based on the polymer's hygroscopicity [241, 270]. The overall drug release of 86.36 ± 11.31% at the 360 min time point confirmed the feasibility of an intended oromucosal sustained release film. Contrary a high swelling degree and rapid water absorption of chitosan have been highlighted as sustained drug release limitation as this leads to fast drug release [271]. Incorporation of glycerol to chitosan films is related to higher viscosity and in turn to slower drug release [245]. Moreover the addition of water-soluble additives such as gelatin and polyvinyl pyrrolidone (PVP) proved to slow down drug release [241, 245] and provide options for release adaptations. The overall nonlinear release profile is in accordance to the literature. This is based on water swelling capabilities and matrix-like structure of films with its release rates typical following a profile between Fickian diffusion and zero order kinetics [6, 245, 272].

Conventional dissolution tests are not applicable for oromucosal films as low dissolution volumes are required for biorelevant purposes [49, 50, 73, 74]. In this study the low drug load of 90 µg per film and the desired slow drug release required low volumes anyway. Such low volumes are highly incluenced by replacing withdrawn volumes and are more prone to high standard deviations as observed in this study. Moreover weight fluctuations of the films used contributed to the high standard deviation measured. Interestingly besides the above mentioned drug release modification options, chitosan is degraded by lysoyzme [273, 274] present in human saliva [69, 110, 111]. Its degradation degree decreases with the DD in chitosan [275]. Furthermore β-1,4-linked D-glucosamine (GlcN) monomer segments are not accessible by lysoyzme's active site and chitosan is therefore not fully degraded [274]. This is often exploited to modify the release of drug loaded chitosan films [276, 277].

6 Conclusions

The main objective of this study was to optimize the characterization methodology for low drug loaded oromucosal films at various levels. Very low drug concentrations as used in this study are accompanied by analytical obstacles. We addressed these issues by detecting and quantifying such low API concentrations, studying its solid state and thermal properties. Moreover uniformity of content of a single batch and within single film areas as well as its drug release was studied. Therefore F2 was developed which served as benchmark as it surpasses the LOD of all methodologies used in this study. Additionally from a galenic point of view this drug load provides a feasible formulation. XRPD and FTIR measurements proved overall amorphous film content and compound interactions, respectively. However, limitations in detecting such low API concentrations in F1 were confirmed. In that regard, transition temperatures seemed promising as this allows highly specific identifications of analytes. Nevertheless, low drug concentrations in connection with a complex polymer such as chitosan, made thermal characterizations difficult. Conventional DSC measurements on T_m of clonidine were successful. Measurements of chitosan using MTDSC lacked reproducibility, requiring alternative methods. Follow-up measurements exploiting DMTA's high sensitivity led successfully to a distinct T_g of chitosan at 154.95 ± 0.47°C in F3.

A quick isocratic HPLC method allowed separation of clonidine, chitosan and acetic acid. Using chitosan as film forming polymer, content uniformity was successfully reached according to Ph.Eur. Next, SEM-EDS and TTM were utilized to verify homogenous API distribution. Analytical challenges are firstly based on the limited number of methodologies to detect, quantify and especially map APIs. Secondly, sampling introduces the biggest error in analysis, hence verifying the presence of analytes in samples is particularly important when dealing with such low concentrations. This was done using SEM-EDS and mapping areas of 300 x 300 µm that were equivalent to TTM sample areas. CUT essentially gives an insight on uniformity of content of one batch as a whole whereas SEM-EDS provided knowledge on the distribution of several film areas obtained by several batches. Due to the fast analysis, several sites of interest can be analyzed providing a good representation on laboratory scale. A combination of these methodologies might serve as a powerful tool to ensure quality control of content uniformity. The obtained TTM result of F2 with a mean value of 162°C was assigned to chitosan's T_g value. This is in agreement with the T_g values of chitosan reported in the past [232] and its value of 166.47 ± 2.31°C measured via DMTA in this study. While this result seems overall promising, F1 and F3 measurements failed to verify the measured T_g of chitosan. Moreover our results of F1 confirmed difficulties in detecting the low clonidine concentration. While further method optimizing is required to overcome analysis obstacles, theoretically TTM provides the advantage of mapping the API distribution and simultaneously obtaining information on its physical state (crystalline or amorphous) [229]. This indicates the

presence of a single or a multi-phase and makes TTM a novel method for pharmaceutics. Alternatives to assess API distribution include among others: raman spectroscopy, nuclear magnetic resonance (NMR) spectroscopy and time-of-flight secondary ion mass spectrometry (ToF-SIMS).

Moreover a dissolution test confirmed sustained release and provided additional evidence of its applicability for both cancer patients suffering from oral mucositis as well as postoperative analgesic and sedative in paediatric patients. To verify adequate drug release follow-up work such as permeability studies would be required. In that regard, animal studies are typically carried out using rabbits, pigs, dogs (especially beagle dogs) or monkeys as those animals contain a non-keratinized buccal mucosa similar to humans. Moreover the thickness of the buccal mucosa of these animals (rabbit: 600 µm [278], dog: 770 µm [87], pig: 770 µm [84], rhesus monkey: 1000 - 1200 µm [279]) is comparable to humans [55]. Porcine's oral mucosa seems as the most comparable animal model due to its distinct keratinization profile and lipid composition [35, 280].

Overall, we addressed general issues involved in solvent casting and uniformity of content when low drug load is desired. Additionally, extensive thermal analysis on chitosan's T_g using DMTA, MTDSC, TTM and TGA contributed additional knowledge on its sophisticated thermal history. To conclude, this study provides evidence for both clinical need and galenic feasibility of a low dose clonidine orormucosal film obtaining uniformity of content.

7 References

[1] A. F. Borges, C. Silva, J. F. J. Coelho, and S. Simoes, “Oral films: Current status and future perspectives II-Intellectual property, technologies and market needs,” *J. Control. Release*, vol. 206, pp. 108–121, 2015.

[2] A. F. Borges, C. Silva, J. F. J. Coelho, and S. Simões, “Oral films: Current status and future perspectives I - Galenical development and quality attributes,” *J. Control. Release*, vol. 206, pp. 1–19, 2015.

[3] M. Preis, C. Woertz, P. Kleinebudde, and J. Breitkreutz, “Oromucosal film preparations: classification and characterization methods.,” *Expert Opin. Drug Deliv.*, vol. 10, no. 9, pp. 1303–17, 2013.

[4] European Directorate for the Quality of Medicines (EDQM), “European Pharmacopoeia Comission. Oromucosal Preparations.,” in *European Pharmacopoeia.*, 8th ed., Strasbourg, 2014.

[5] European Directorate for the Quality of Medicines (EDQM), “European Pharmacopoeia Comission. Oromucosal Preparations,” in *European Pharmacopoeia.*, 7.4 editio., 2012, pp. 4257–9.

[6] R. Krampe *et al.*, “Oromucosal film preparations: points to consider for patient centricity and manufacturing processes,” *Expert Opin. Drug Deliv.*, vol. 13, no. 4, pp. 493–506, 2016.

[7] R. P. Dixit and S. P. Puthli, “Oral strip technology: Overview and future potential,” *J. Control. Release*, vol. 139, no. 2, pp. 94–107, 2009.

[8] M. D. N. Siddiqui, G. Garg, and P. K. Sharma, “A Short Review on: A Novel Approach in Oral Fast Dissolving Drug Delivery System and Their Patents,” *Adv. Biol. Res. (Rennes).*, vol. 5, no. 6, pp. 291–303, 2011.

[9] A. H. Shojaei, “Buccal mucosa as a route for systemic drug delivery: a review.,” *J Pharm Pharm Sci.*, vol. 1, no. 1, pp. 15–30, 1998.

[10] S. Gaisford, A. Verma, M. Saunders, and P. Royall, “Monitoring crystallisation of drugs from fast-dissolving oral films with isothermal calorimetry.,” *Int. J. Pharm.*, vol. 380, no. 1–2, pp. 105–11, 2009.

[11] J. Breitkreutz and J. Boos, “Paediatric and geriatric drug delivery.,” *Expert Opin Drug Deliv.*, vol. 4, no. 1, pp. 37–45, 2007.

[12] S. Bourgeois and C. Pailler-mattei, “Formulation of orodispersible films for paediatric therapy: investigation of feasibility and stability for tetrabenazine as drug model,” *J. Pharm. Pharmacol.*, pp. 1–11, 2016.

[13] R. Bala, P. Pawar, S. Khanna, and S. Arora, “Orally dissolving strips: A new approach to oral drug delivery system.,” *Int. J. Pharm. Investig.*, vol. 3, no. 2, pp. 67–76, 2013.

[14] D. A. El-Setouhy and N. S. Abd El-Malak, “Formulation of a Novel Tianeptine Sodium Orodispersible Film,” *AAPS PharmSciTech*, vol. 11, no. 3, pp. 1018–1025, 2010.

[15] Food and Drug Administration, “Revision of ‘Pediatric use’ Subsection in the Labeling; Final Rule,” *Specif. Requir. Content Format Labeling Hum. Prescr. Drugs*, vol. 59, no. 238, 1994.

[16] S. Stegemann *et al.*, “Geriatric drug therapy: Neglecting the inevitable majority,” *Ageing Res. Rev.*, vol. 9, no. 4, pp. 384–398, 2010.

[17] United States Government Accountability Office (GAO), “Pediatric Drug Research - Studies conducted under Best Pharmaceuticals for Children Act (GAO-07-557),” Washington D.C., 2007.

[18] I. Stoltenberg, G. Winzenburg, and J. Breitkreutz, “Solid oral dosage forms for children - Formulations, excipients and acceptance issues,” *J. Appl. Ther. Res.*, vol. 7, no. 4, pp. 141–146, 2010.

[19] A. Ali, N. Charoo, and D. Abdallah, “Pediatric drug development: formulation considerations.,” *Drug Dev Ind Pharm*, vol. 40, no. 10, pp. 1283–1299, 2014.

[20] European Medicines Agency (EMA), “Reflection paper: formulations of choice for the paediatric population (EMEA/CHMP/PEG/194810/2005),” London, 2006.

[21] M. K. Preis, “Oromucosal film preparations for pharmaceutical use – formulation development and analytical characterization,” Heinrich-Heine University Duesseldorf, 2014.

[22] WHO Headquarters, “Report of the Informal Expert meeting on Dosage Forms of Medicines for Children.,” Geneva, Switzerland, 2008.

[23] P. Clavé, V. Arreola, M. Romea, L. Medina, E. Palomera, and M. Serra-Prat, “Accuracy of the volume-viscosity swallow test for clinical screening of oropharyngeal dysphagia and aspiration,” *Clin. Nutr.*, vol. 27, no. 6, pp. 806–815, 2008.

[24] I. Strachan and M. Greener, “Medication-related swallowing difficulties may be more

common than we realise," *Pharm. Pract.*, vol. 15, no. 9, pp. 1–4, 2005.

[25] M. Serra-Prat *et al.*, "Prevalence of oropharyngeal dysphagia and impaired safety and efficacy of swallow in independently living older persons," *J. Am. Geriatr. Soc.*, vol. 59, no. 1, pp. 186–187, 2011.

[26] J. Vaupel, "Biodemography of human ageing," *Nature*, vol. 464, no. 7288, pp. 536–542, 2010.

[27] K. Christensen, G. Doblhammer, R. Rau, and J. W. Vaupel, "Ageing populations: the challenges ahead," *Lancet*, vol. 374, no. 9696, pp. 1196–1208, 2009.

[28] M. Eisenmenger, O. Pötzsch, and B. Sommer, "Germany's population by 2050 Results of the 11th coordinated population projection," Wiesbaden, Germany, 2006.

[29] C. Klaver, R. Wolfs, J. Vingerling, A. Hofman, and P. de Jong, "Age-specific prevalence and causes of blindness and visual impairment in an older population," *Ophatalmol.*, vol. 116, pp. 653–658, 1998.

[30] P. Atkin, T. Finnegan, S. Ogle, and G. Shenfield, "Functional ability of patients to manage medication packaging: a survey of geriatric inpatients," *Age Ageing*, vol. 23, no. 2, pp. 113–116, 1994.

[31] A. B. Gyllenstrand, "Medication management and patient compliance in old age.," Karolinska Institutet, 2007.

[32] S. Stegemann, "Colored capsules—a contribution to drug safety," *Pharm. Ind.*, vol. 67, no. 9, pp. 1088–1095, 2005.

[33] European Medicines Agency (EMA), "Guideline on pharmaceutical development of medicines for paediatric use (EMA/CHMP/QWP/805880/2012 Rev.2)," London, 2013.

[34] T. Caon, L. Jin, C. M. O. Simoes, R. S. Norton, and J. A. Nicolazzo, "Enhancing the buccal mucosal delivery of peptide and protein therapeutics," *Pharm. Res.*, vol. 32, no. 1, pp. 1–21, 2015.

[35] P. M. Castro, P. Fonte, F. Sousa, A. R. Madureira, B. Sarmento, and M. E. Pintado, "Oral films as breakthrough tools for oral delivery of proteins/peptides," *J. Control. Release*, vol. 211, pp. 63–73, 2015.

[36] A. Semalty, M. Semalty, R. Singh, S. Saraf, and S. Saraf, "Properties and Formulation of Oral Drug Delivery Systems of Protein and Peptides.," *Indian J. Pharm. Sci.*, vol. 69, pp. 741–747, 2007.

[37] R. Singh, S. Singh, and L. J. Jr, “Past, present, and future technologies for oral delivery of therapeutic proteins.,” *J Pharm Sci.*, vol. 97, no. 7, pp. 2497–523, 2008.

[38] A. Muheem *et al.*, “A review on the strategies for oral delivery of proteins and peptides and their clinical perspectives,” *Saudi Pharm. J.*, vol. 24, no. 4, pp. 413–428, 2016.

[39] U.S. Food and Drug Administration, “CY 2015 CDER New Molecular Entity (NME) Drug & Original BLA Calendar Year Approvals As of December 31, 2015,” Silver Spring, 2015.

[40] L. Z. Benet, “The role of BCS (biopharmaceutics classification system) and BDDCS (biopharmaceutics drug disposition classification system) in drug development,” *J. Pharm. Sci.*, vol. 102, no. 1, pp. 34–42, 2013.

[41] E. Russo *et al.*, “A focus on mucoadhesive polymers and their application in buccal dosage forms,” *J. Drug Deliv. Sci. Technol.*, vol. 32, pp. 113–125, 2016.

[42] J. C. Visser *et al.*, “Orodispersible films in individualized pharmacotherapy: The development of a formulation for pharmacy preparations,” *Int. J. Pharm.*, vol. 478, no. 1, pp. 155–163, 2015.

[43] M. Preis, J. Breitkreutz, and N. Sandler, “Perspective: Concepts of printing technologies for oral film formulations,” *Int. J. Pharm.*, vol. 494, no. 2, pp. 578–584, 2015.

[44] J. Pardeike *et al.*, “Nanosuspensions as advanced printing ink for accurate dosing of poorly soluble drugs in personalized medicines,” *Int. J. Pharm.*, vol. 420, no. 1, pp. 93–100, 2011.

[45] M. Preis *et al.*, “Design and evaluation of bilayered buccal film preparations for local administration of lidocaine hydrochloride,” *Eur. J. Pharm. Biopharm.*, vol. 86, no. 3, pp. 552–561, 2014.

[46] E. M. Hoffmann, A. Breitenbach, and J. Breitkreutz, “Advances in orodispersible films for drug delivery.,” *Expert Opin. Drug Deliv.*, vol. 8, no. 3, pp. 299–316, 2011.

[47] J. O. Morales and J. T. Mcconville, “Manufacture and characterization of mucoadhesive buccal films,” *Eur. J. Pharm. Biopharm.*, vol. 77, no. 2, pp. 187–199, 2011.

[48] V. A. Perumal, D. Lutchman, I. Mackraj, and T. Govender, “Formulation of monolayered films with drug and polymers of opposing solubilities,” *Int. J. Pharm.*, vol. 358, pp. 184–191, 2008.

[49] V. Garsuch and J. Breitkreutz, “Comparative investigations on different polymers for the preparation of fast-dissolving oral films,” *J Pharm Pharmacol.*, vol. 62, no. 4, pp. 539–545, 2010.

[50] R. Krampe, D. Sieber, M. Pein-Hackelbusch, and J. Breitkreutz, “A new biorelevant dissolution method for orodispersible films,” *Eur. J. Pharm. Biopharm.*, vol. 98, pp. 20–25, 2016.

[51] L. Collins and C. Dawes, “The surface area of the adult human mouth and thickness of the salivary film covering the teeth and oral mucosa.,” *J Dent Res.*, vol. 66, no. 8, pp. 1300–2, 1987.

[52] C. A. Squier and P. W. Wertz, “Permeability and the pathophysiology of oral mucosa,” *Adv. Drug Deliv. Rev.*, vol. 12, no. 1–2, pp. 13–24, 1993.

[53] N. V. Satheesh Madhav, R. Semwal, D. K. Semwal, and R. B. Semwal, “Recent trends in oral transmucosal drug delivery systems: an emphasis on the soft palatal route,” *Expert Opin. Drug Deliv.*, vol. 9, no. 6, pp. 629–647, 2012.

[54] S. I. Pather, M. J. Rathbone, and S. Senel, “Current status and the future of buccal drug delivery systems.,” *Expert Opin. Drug Deliv.*, vol. 5, no. 5, pp. 531–42, 2008.

[55] D. Harris and J. R. Robinson, “Drug Delivery via the Mucous Membranes of the Oral Cavity,” *J. Pharm. Sci.*, vol. 81, no. 1, pp. 1–10, 1992.

[56] S. Y. Chen and C. A. Squier, “The Ultrastructure of the Oral Epithelium,” in *The Structure and Function of Oral Mucosa.*, J. Meyer, C. A. Squier, and S. J. Gerson, Eds. Oxford: Pergamon Press, 1984, pp. 7–30.

[57] L. A. Tabak, M. J. Levine, I. D. Mandel, and S. A. Ellison, “Role of salivary mucins in the protection of the oral cavity.,” *J. Oral Pathol.*, vol. 11, no. 1, pp. 1–17, 1982.

[58] B. L. Slomiany, V. L. N. Murty, J. Piotrowski, and A. Slomiany, “Salivary mucins in oral mucosal defense,” *Gen. Pharmacol.*, vol. 27, no. 5, pp. 761–771, 1996.

[59] N. A. Peppas and P. A. Buri, “Surface, Inerfacial and Molecular Aspects of Polymer Bioadhesion on Soft Tissues,” *J. Control. Release*, vol. 2, pp. 257–275, 1985.

[60] C. Squier and M. Kremer, “Biology of oral mucosa and esophagus.,” *J. Natl. Cancer Inst. Monogr.*, vol. 52242, pp. 7–15, 2001.

[61] D. R. Tobergte and S. Curtis, “An Exhaustive Review on Recent Advancement in Pharmaceutical Bioadhesive Used for Systemic Drug Delivery Through Oral Mucosa

for Achieving Maximum Pharmacological Response and Effect," *J. Chem. Inf. Model.*, vol. 53, no. 9, pp. 1689–1699, 2013.

[62] R. B. Gandhi and J. R. Robinson, "Oral cavity as a site for bioadhesive drug delivery," *Adv. Drug Deliv. Rev.*, vol. 13, no. 1–2, pp. 43–74, 1994.

[63] V. F. Patel, F. Liu, and M. B. Brown, "Advances in oral transmucosal drug delivery," *J. Control. Release*, vol. 153, no. 2, pp. 106–116, 2011.

[64] M. J. Rathbone, B. K. Drummond, and I. G. Tucker, "The oral cavity as a site for systemic drug delivery," *Adv. Drug Deliv. Rev.*, vol. 13, no. 1–2, pp. 1–22, 1994.

[65] V. de Almeida Pdel, A. Grégio, M. Machado, A. de Lima, and L. Azevedo, "Saliva Composition and Functions: A comprehensive review," *J. Contemp. Dent. Pract.*, vol. 9, no. 3, pp. 72–80, 2008.

[66] N. Salamat-Miller, M. Chittchang, and T. P. Johnston, "The use of mucoadhesive polymers in buccal drug delivery," *Adv. Drug Deliv. Rev.*, vol. 57, no. 11, pp. 1666–1691, 2005.

[67] R. M. Nagler and O. Hershkovich, "Relationships between age, drugs, oral sensorial complaints and salivary profile," *Arch. Oral Biol.*, vol. 50, no. 1, pp. 7–16, 2005.

[68] H. Park and J. R. Robinson, "Physico-chemical properties of water insoluble polymers important to mucin/epithelial adhesion," *J. Control. Release*, vol. 2, no. C, pp. 47–57, 1985.

[69] M. Kaul, S. Verma, A. Rawat, and S. Saina, "An Overview on Buccal Drug Delivery System," *Int. J. Pharm. Sci. Res.*, vol. 2, no. 6, pp. 1303–1321, 2011.

[70] P. Gilles, F. A. Ghazali, and M. J. Rathbone, "Systemic oral mucosal drug delivery systems and delivery systems," in *Oral mucosal drug delivery*, M. J. Rathbone, Ed. New York: Marcel Dekker Inc., 1996, pp. 241–285.

[71] R. D. Mattes, "Physiologic responses to sensory stimulation by food: nutritional implications," *J. Am. Diet. Assoc.*, vol. 97, pp. 406–410, 1997.

[72] M. Sattar, O. M. Sayed, and M. E. Lane, "Oral transmucosal drug delivery - Current status and future prospects," *Int. J. Pharm.*, vol. 471, no. 1–2, pp. 498–506, 2014.

[73] H. . Batchelor, N. Fotaki, and S. Klein, "Paediatric oral biopharmaceutics: key considerations and current challenges," *Adv. Drug Deliv. Rev.*, vol. 73, pp. 102–126, 2014.

[74] S. Azarmi, W. Roa, and R. Löbenberg, “Current perspectives in dissolution testing of conventional and novel dosage forms.,” *Int. J. Pharm.*, vol. 328, no. 1, pp. 12–21, 2007.

[75] A. Bardow, J. Madsen, and B. Nauntofte, “The bicarbonate concentration in human saliva does not exceed the plasma level under normal physiological conditions,” *Clin. Oral Investig.*, vol. 4, pp. 245–253, 2000.

[76] N. Utoguchi, Y. Watanabe, T. Suzuki, J. Maehara, Y. Matsumoto, and M. Matsumoto, “Carrier-mediated transport of monocarboxylic acids in primary cultured epithelial cells from rabbit oral mucosa.,” *Pharm Res.*, vol. 14, no. 3, pp. 320–4, 1997.

[77] S. Senel, M. Kremer, K. Nagy, and C. Squier, “Delivery of bioactive peptides and proteins across oral (buccal) mucosa.,” *Curr Pharm Biotechnol.*, vol. 2, no. 2, pp. 175–86, 2001.

[78] E. Muschler, H. G. Schaible, and P. Vaupel, “Transport- und Regelprozesse,” in *Anatomie Physiologie Pathophysiologie des Menschen*, 6th ed., Stuttgart: Wissenschaftliche Verlagsgesellschaft mbH, 2007, pp. 59–72.

[79] J. Hao and P. W. S. Heng, “Buccal delivery systems.,” *Drug Dev. Ind. Pharm.*, vol. 29, no. 8, pp. 821–32, 2003.

[80] P. W. Wertz, D. C. Swartzendruber, and C. A. Squier, “Regional variation in the structure and permeability of oral mucosa and skin,” *Adv. Drug Deliv. Rev.*, vol. 12, no. 1–2, pp. 1–12, 1993.

[81] W. R. Galey, H. K. Lonsdale, and S. Nacht, “The In Vitro Permeability Of Skin And Buccal Mucosa To Selected Drugs And Tritiated Water,” *J. Invest. Dermatol.*, vol. 67, no. 6, pp. 713–717, 1976.

[82] Y. Rojanasakul, L. Y. Wang, M. Bhat, D. D. Glover, C. J. Malanga, and J. K. Ma, “The transport barrier of epithelia: a comparative study on membrane permeability and charge selectivity in the rabbit,” *Pharm. Res.*, vol. 9, no. 8, pp. 1029–1034, 1992.

[83] A. V. Gore, A. C. Liang, and Y. W. Chien, “Comparative biomembrane permeation of tacrine using yucatan minipigs and domestic pigs as the animal model,” *J. Pharm. Sci.*, vol. 87, no. 4, pp. 441–447, 1998.

[84] C. A. Squier and B. K. Hall, “The permeability of skin and oral mucosa to water and horseradish peroxidase as related to the thickness of the permeability barrier.,” *J Invest Dermatol.*, vol. 84, no. 3, pp. 176–9, 1985.

[85] C. A. Lesch, C. A. Squier, A. Cruchley, D. M. Williams, and P. Speight, “The permeability of human oral mucosa and skin to water,” *J. Dent. Res.*, vol. 68, pp. 1345–1349, 1989.

[86] C. A. Squier, “Keratinization of the Sulcular Epithelium - a Pointless Pursuit,” *J. Periodontol.*, vol. 52, no. 8, pp. 426–429, 1981.

[87] C. A. Squier and B. K. Hall, “The permeability of mammalian non-keratinized oral epithelia to horseraddish peroxidase applied in vivo and in vitro,” *Arch. Oral Biol.*, vol. 29, no. 1, pp. 45–50, 1984.

[88] M. J. Rathbone, *Oral Mucosal Drug Delivery*. New York: Marcel Dekker Inc., 1996.

[89] A. F. Hayward, “Membrane-coating granules.,” *Int Rev Cytol.*, vol. 59, pp. 97–127, 1979.

[90] C. A. Squier, “Membrane coating granules in nonkeratinizing oral epithelium.,” *J Ultrastruct Res.*, vol. 60, no. 2, pp. 212–20, 1977.

[91] A. G. Matoltsy, “Keratinization.,” *J Invest Dermatol.*, vol. 67, no. 1, pp. 20–5, 1976.

[92] C. A. Squier, “The permeability of oral mucosa.,” *Crit. Rev. oral Biol. Med.*, vol. 2, no. 1, pp. 13–32, 1991.

[93] R. M. Lavker, “Membrane coating granules,” *J Ultrastruct Res.*, vol. 55, pp. 79–86, 1976.

[94] C. A. Squier, R. A. J. Eady, and R. M. Hopps, “The Permeability of Epidermis Lacking Normal Membrane-Coating Granules: An Ultrastructural Tracer Study of Kyrle-Flegel Disease,” *J. Invest. Dermatol.*, vol. 70, no. 6, pp. 361–364, 1978.

[95] C. A. Squier, “The permeability of keratinized and nonkeratinized oral epithelium to horseradish peroxidase.,” *J. Ultrasructure Res.*, vol. 43, no. 1, pp. 160–177, 1973.

[96] C. A. Squier and L. Rooney, “The permeability of keratinized and nonkeratinized oral epithelium to lanthanum in vivo.,” *J Ultrastruct Res.*, vol. 54, no. 2, pp. 286–95, 1976.

[97] A. F. Hayward, A. I. Hamilton, and M. M. Hackemann, “Histological and ultrastructural observations on the keratinizing epithelia of the palate of the rat.,” *Arch. Oral Biol.*, vol. 18, no. 8, pp. 1041–57, 1973.

[98] C. A. Squier, “Zinc iodide-osmium staining of membrane-coating granules in keratinized and non-keratinized mammalian oral epithelium.,” *Arch. Oral Biol.*, vol. 27, no. 5, pp. 377–82, 1982.

[99] N. Washington, C. Washington, and C. Wilson, *Physiological Pharmaceutics: Barriers to Drug Absorption*, 2nd ed. London: CRC Press / Taylor & Francis, 2001.

[100] M. R. Tavakoli-Saberi and K. L. Audus, “Cultured buccal epithelium: an in vitro model derived from the hamster pouch for studying drug transport and metabolism.,” *Pharm. Res.*, vol. 6, no. 2, pp. 160–6, 1989.

[101] G. Wiseman, “Absorption of amino acids (section 6),” in *Handbook of Physiology*, C. F. Code, Ed. Washington D.C.: American Physiological Society, 1968, pp. 1277–1307.

[102] C. A. Squier and P. W. Wertz, “Structure and function of the oral mucosa and implications for drug delivery.,” in *Oral mucosal drug delivery*, New York: Marcel Dekker Inc., 1996, pp. 1–26.

[103] I. Diaz-Del Consuelo, Y. Jacques, G. P. Pizzolato, R. H. Guy, and F. Falson, “Comparison of the lipid composition of porcine buccal and esophageal permeability barriers,” *Arch. Oral Biol.*, vol. 50, no. 12, pp. 981–987, 2005.

[104] P. W. Wertz and C. A. Squier, “Cellular and molecular basis of barrier function in oral epithelium.,” *Crit Rev Ther Drug Carr. Syst.*, vol. 8, no. 3, pp. 237–69, 1991.

[105] S. Law, P. W. Wertz, D. C. Swartzendruber, and C. A. Squier, “Regional variation in content, composition and organization of porcine epithelial barrier lipids revealed by thin-layer chromatography and transmission electron microscopy,” *Arch. Oral Biol.*, vol. 40, no. 12, pp. 1085–1091, 1995.

[106] J. M. Lakkis, *Encapsulation and Controlled Release Technologies in Food Systems*. Oxford: John Wiley & Sons, Ltd, 2007.

[107] A. Yamamoto, E. Hayakawa, and V. H. Lee, “Insulin and proinsulin proteolysis in mucosal homogenates of the albino rabbit: implications in peptide delivery from nonoral routes.,” *Life Sci.*, vol. 47, no. 26, pp. 2465–74, 1990.

[108] S. D. Kashi and V. H. Lee, “Enkephalin hydrolysis in homogenates of various absorptive mucosae of the albino rabbit: similarities in rates and involvement of aminopeptidases.,” *Life Sci.*, vol. 38, no. 2, pp. 2019–28, 1986.

[109] H. Yamahara and V. H. L. Lee, “Drug metabolism in the oral cavity,” *Adv. Drug Deliv. Rev.*, vol. 12, no. 1–2, pp. 25–39, 1993.

[110] H. H. Chauncey, F. Lionetti, R. A. Winer, and V. F. Lisanti, “Enzymes of Human Saliva: I. the Determination, Distribution, and Origin of whole Saliva Enzymes,” *J. Dent. Res.*, vol. 33, no. 3, pp. 321–34, 1954.

[111] H. H. Chauncey, F. Lionetti, and V. F. Lisanti, “Enzymes of human saliva, II. Parotid saliva total esterases.,” *J. Dent. Res.*, vol. 36, no. 5, pp. 713–716, 1957.

[112] M. S. Burstone, “Esterase of the salivary glands.,” *J Histochem Cytochem.*, vol. 4, no. 2, pp. 130–9, 1956.

[113] H. H. Chauncey, “Salivary enzymes.,” *J Am Dent Assoc.*, vol. 63, pp. 360–8, 1961.

[114] L. Lindqvist and K. B. Augustinsson, “Esterases in human saliva.,” *Enzyme*, vol. 20, no. 5, pp. 277–91, 1975.

[115] S. G. Tan, “Human saliva esterases: genetic studies.,” *Hum Hered.*, vol. 26, no. 3, pp. 207–16, 1976.

[116] L. Lindqvist, C. E. Nord, and P. O. Soder, “Origin of esterases in human whole saliva.,” *Enzyme*, vol. 22, no. 3, pp. 166–75, 1977.

[117] J. R. Robinson and X. Yang, “Absorption enhancers,” in *Encyclopedia of pharmaceutical technology*, B. J. C. Swarbrick J., Ed. New York: Marcel Dekker Inc., 2001, pp. 1–27.

[118] G. F. Walker, N. Langoth, and A. Bernkop-Schnürch, “Peptidase activity on the surface of the porcine buccal mucosa,” *Int. J. Pharm.*, vol. 233, no. 1–2, pp. 141–147, 2002.

[119] L. L. Christrup and H. Bundgaard, “Saliva-catalyzed hydrolysis of a ketobemidone ester prodrug: Factors influencing human salivary esterase activity,” *Int. J. Pharm.*, vol. 88, pp. 221–227, 1992.

[120] V. H. Lee, “Peptidase activities in absorptive mucosae.,” *Biochem Soc Trans.*, vol. 17, no. 5, pp. 937–40, 1989.

[121] S. Rossi, G. Sandri, and C. M. Caramella, “Buccal drug delivery: A challenge already won?,” *Drug Discov. Today Technol.*, vol. 2, no. 1, pp. 59–65, 2005.

[122] P. Chinna Reddy, K. S. C. Chaitanya, and Y. Madhusudan Rao, “A review on bioadhesive buccal drug delivery systems: current status of formulation and evaluation methods.,” *Daru*, vol. 19, no. 6, pp. 385–403, 2011.

[123] H. P. Merkle and G. Wolany, “Buccal delivery for peptide drugs,” *J. Control. Release*, vol. 21, no. 1–3, pp. 155–164, 1992.

[124] V. L. Bykov, “The tissue and cell defense mechanisms of the oral mucosa.,” *Morfologiia*, vol. 110, no. 6, pp. 14–24, 1996.

[125] J. R. Robinson and B. Li, “Preclinical Assessment of Oral Mucosal Drug Delivery Systems,” in *Drug Delivery to the Oral Cavity. Molecules to Market*, Boca Raton, FL: CRC Press, 2005, pp. 41–66.

[126] S. J. Pimlott and M. Addy, “A study into the mucosal absorption of isosorbide dinitrate at different intraoral sites,” *Oral Surg. Oral Med. Oral Pathol.*, vol. 59, pp. 145–148, 1985.

[127] L. Schenkels, T. L. Gururaja, and M. J. Levine, “Salivary mucins: their role in oral mucosal barrier function and delivery,” in *Oral Mucosal Drug Delivery*, M. J. Rathbone, Ed. New York: Marcel Dekker Inc., 1996, pp. 191–220.

[128] M. Hill, “Cell renewal in oral epithelia,” in *The Structure and Function of Oral Mucosa.*, C. A. Squier and S. J. Gerson, Eds. New York: Permagon, 1984, pp. 53–81.

[129] F. Veuillez, Y. N. Kalia, Y. Jacques, J. Deshusses, and P. Buri, “Factors and strategies for improving buccal absorption of peptides.,” *Eur. J. Pharm. Biopharm.*, vol. 51, no. 2, pp. 93–109, 2001.

[130] J. F. Forstner, “Intestinal mucins in health and disease.,” *Digestion*, vol. 17, no. 3, pp. 234–63, 1978.

[131] C. Lehr, F. Poelma, H. Junginger, and J. Tukker, “An estimate of turnovertime of intestinalmucusgellayer in the rat in situ loop,” *Int. J. Pharm.*, vol. 70, no. 3, pp. 235–240, 1991.

[132] N. F. H. Ho, C. L. Barsuhn, P. S. Burton, and H. P. Merkle, “(D) Routes of delivery: Case studies: (3) Mechanistic insights to buccal delivery of proteinaceous substances,” *Adv. Drug Deliv. Rev.*, vol. 8, no. 2–3, pp. 197–236, 1992.

[133] A. K. Mitra, H. H. Alur, and T. P. Johnston, “Peptides and Proteins: Buccal Absorption,” in *Encyclopedia of Pharmaceutical Technology*, 3rd ed., J. Swarbrick, Ed. New York: Informa Healthcare Inc, 2007, pp. 2664–2677.

[134] T. P. Johnston, “Background and Rationale of Oral Mucosal Drug Delivery,” in *Oral Mucosal Drug Delivery and Therapy*, M. J. Rathbone, S. Senel, and I. Pather, Eds. New York: Springer, 2015, pp. 1–2.

[135] A. Puratchikody, V. V Prasanth, S. T. Mathew, and B. A. Kumar, “Development and characterization of mucoadhesive patches of salbutamol sulfate for unidirectional buccal drug delivery,” *Acta Pharm.*, vol. 61, no. 2, pp. 157–70, 2011.

[136] B. K. Satishbabu and B. P. Srinivasan, “Preparation and Evaluation of Buccoadhesive

Films of Atenolol," *Indian J. Pharm. Sci.*, vol. 70, no. 2, pp. 175–179, 2008.

[137] N. A. Nafee, F. A. Ismail, N. A. Boraie, and L. M. Mortada, "Mucoadhesive buccal patches of miconazole nitrate: in vitro/in vivo performance and effect of ageing," *Int. J. Pharm.*, vol. 264, pp. 1–14, 2003.

[138] B. M. A. Silva, A. F. Borges, C. Silva, J. F. J. Coelho, and S. Simoes, "Mucoadhesive oral films: The potential for unmet needs," *Int. J. Pharm.*, vol. 494, no. 1, pp. 537–551, 2015.

[139] J. Breitkreutz, "Schnell zerfallende orale Arzneiformen," in *Innovative Arzneiformen*, Stuttgart: Wissenschaftliche Verlagsgesellschaft mbH, 2010, pp. 37–52.

[140] A. H. Shojaei, "Buccal mucosa as a route for systemic drug delivery: a review," *J Pharm Pharm Sci.*, vol. 1, no. 1, pp. 15–30, 1998.

[141] Z. Antosova, M. Mackova, V. Kral, and T. Macek, "Therapeutic application of peptides and proteins: parenteral forever?," *Trends Biotechnol.*, vol. 27, no. 11, pp. 628–635, 2009.

[142] M. J. Humphrey and P. S. Ringrose, "Peptides and related drugs: a review of their absorption, metabolism, and excretion.," *Drug Metab Rev.*, vol. 17, no. 3–4, pp. 283–310, 1986.

[143] C. McMartin, L. Hutchinson, R. Hyde, and G. Peters, "Analysis of structural requirements for the absorption of drugs and macromolecules from the nasal cavity.," *J Pharm Sci.*, vol. 76, no. 7, pp. 535–40, 1987.

[144] M. D. Donovan, G. L. Flynn, and G. L. Amidon, "Absorption of polyethylene glycols 600 through 2000: the molecular weight dependence of gastrointestinal and nasal absorption.," *Pharm Res.*, vol. 7, no. 8, pp. 863–8, 1990.

[145] G. Camenisch, J. Alsenz, H. Van De Waterbeemd, and G. Folkers, "Estimation of permeability by passive diffusion through Caco-2 cell monolayers using the drugs' lipophilicity and molecular weight," *Eur. J. Pharm. Sci.*, vol. 6, no. 4, pp. 313–319, 1998.

[146] J. O. Morales and J. T. McConville, "Manufacture and characterization of mucoadhesive buccal films," *Eur. J. Pharm. Biopharm.*, vol. 77, no. 2, pp. 187–199, 2011.

[147] A. H. Beckett and A. C. Moffat, "Correlation of partition coefficients in n-heptane-aqueous systems with buccal absorption data for a series of amines and acids.," *J*

Pharm Pharmacol., vol. 21(suppl.), pp. 144–150, 1969.

[148] S. Sasaki *et al.*, “Kinetics of buccal absorption of propafenone single oral loading dose in healthy humans,” *Gen. Pharmacol.*, vol. 31, no. 4, pp. 589–591, 1998.

[149] M. J. Rathbone, I. Pather, and S. Senel, “Overview of Oral Mucosal Delivery,” in *Oral Mucosal Drug Delivery and Therapy*, M. J. Rathbone, I. Pather, and S. Senel, Eds. New York: Springer, 2015, pp. 17–30.

[150] M. J. Rathbone and J. Hadgraft, “Absorption of drugs from the human oral cavity.,” *Int. J. Pharm.*, vol. 74, no. 1, pp. 9–24, 1991.

[151] S. Şenel and A. A. Hincal, “Drug permeation enhancement via buccal route: Possibilities and limitations,” *J. Control. Release*, vol. 72, no. 1–3, pp. 133–144, 2001.

[152] S. Senel, M. Cansiz, and M. J. Rathbone, “Buccal delivery of biopharmaceuticals: vaccines and allergens.,” in *Mucosal delivery of biopharmaceuticals.*, J. das Neves and B. Sarmento, Eds. New York: Springer, 2014, pp. 149–168.

[153] V. M. Patel, B. G. Prajapati, J. K. Patel, and M. M. Patel, “Physicochemical characterization and evaluation of buccal adhesive patches containing propranolol hydrochloride.,” *Curr Drug Deliv.*, vol. 3, no. 3, pp. 325–31, 2006.

[154] M. Jackson and A. Lowey, “Clonidine hydrochloride oral liquid,” in *Handbook of Extemporaneous Preparation: A guide to pharmaceutical compounding*, M. Jackson and A. Lowey, Eds. London: Pharmaceutical Press, 2010, p. 146.

[155] L. Trissel, “Clonidine hydrochloride,” in *Trissel’s Stability of Compounded Formulations*, 3rd ed., L. Trissel, Ed. Washington D.C.: American Pharmaceutical Association, 2005, p. 113.

[156] C. Hansch and A. Leo, *Partition Coefficient Data Bank*. Claremont, CA, USA: Pomona College, 1985.

[157] M. Williams, *The Merck Index: An Encyclopedia of Chemicals, Drugs, and Biologicals*, 15th ed. Cambridge: John Wiley & Sons, Ltd, 2013.

[158] P. York, “Partition coefcient and pKa,” in *Aulton’s Pharmaceutics - The Design and Manufacture of Medicines*, 4th ed., M. E. Aulton and K. Taylor, Eds. Edinburgh: Churchill Livingstone Elsevier, 2013, p. 30.

[159] T. P. Johnston, “Anatomy and Physiology of the Oral Mucosa,” in *Oral Mucosal Drug Delivery and Therapy*, M. J. Rathbone, S. Senel, and I. Pather, Eds. New York:

Springer, 2015, pp. 1–16.

[160] E. M. Aulton, “Properties of solutions,” in *Aulton’s pharmaceutics: the design and manufacture of medicines.*, 4th ed., E. M. Aulton and K. Taylor, Eds. Edinburgh: Churchill Livingstone Elsevier, 2013, p. 43.

[161] European Medicines Agency (EMA), “Revised priority list for studies on off-patent paediatric medicinal products (EMA/PDCO/98717/2012),” London, 2012.

[162] R. J. Levick, Ed., “Control of blood vessels,” in *An Introduction to Cardiovascular Physiology*, 3rd ed., London: Butterworth & Co Ltd, 1991, pp. 178–202.

[163] D. J. Reis and J. E. Piletz, “The imidazoline receptor in control of blood pressure by clonidine and drugs,” *Am. J. Physiol.*, vol. 273, no. 5 Pt 2, pp. 1569–1571, 1997.

[164] F. E. Cunningham, V. L. Baughman, J. Peters, and C. E. Laurito, “Comparative pharmacokinetics of oral versus sublingual clonidine,” *J. Clin. Anesth.*, vol. 6, no. 5, pp. 430–433, 1994.

[165] Z. P. Khan, C. N. Ferguson, and R. M. Jones, “Alpha-2 and imidazoline receptor agonistsTheir pharmacology and therapeutic role,” *Anaesthesia*, vol. 54, no. 2, pp. 146–65, 1999.

[166] J. Eisenach, D. Detweiler, and D. Hood, “Hemodynamic and analgesic actions of epidurally administered clonidine.,” *Anesthesiology*, vol. 78, no. 2, pp. 277–287, 1993.

[167] T. Kimura, T. Nishikawa, K. Sato, and K. Wada, “Oral clonidine reduces thiamylal requirement for induction of anesthesia in adult patients.,” *J. Anesth.*, vol. 10, no. 1, pp. 1–4, 1996.

[168] K. Mikawa, N. Maekawa, K. Nishina, Y. Takao, H. Yaku, and H. Obara, “Efficacy of oral clonidine premedication in children.,” *Anesthesiology*, vol. 79, no. 5, pp. 926–931, 1993.

[169] K. S. Umiya *et al.*, “Sedation and plasma concentration of clonidine hydrochloride for pre-anesthetic medication in pediatric surgery.,” *Biol Pharm Bull.*, vol. 26, no. 4, pp. 421–423, 2003.

[170] T. Goyagi and T. Nishikawa, “Oral Clonidine Premedication Enhances the Quality of Postoperative Analgesia by Intrathecal Morphine.,” *Anesth. Analg.*, vol. 82, pp. 1192–6, 1996.

[171] Y. Sinha and N. E. Cranswick, “Clonidine poisoning in children: a recent experience,” *J*

Paediatr Child Heal., vol. 40, no. 12, pp. 678–80, 2004.

[172] F. R. Sallee, “The role of alpha2-adrenergic agonists in attention-deficit/hyperactivity disorder.,” *Postgr. Med*, vol. 122, no. 5, pp. 78–87, 2010.

[173] H. Bergendahl, P. A. Lönnqvist, and S. Eksborg, “Clonidine in paediatric anaesthesia: Review of the literature and comparison with benzodiazepines for premedication,” *Acta Anaesthesiol. Scand.*, vol. 50, no. 2, pp. 135–143, 2006.

[174] A. B. M. Buanz, C. C. Belaunde, N. Soutari, C. Tuleu, M. O. Gul, and S. Gaisford, “Ink-jet printing versus solvent casting to prepare oral films: Effect on mechanical properties and physical stability,” *Int. J. Pharm.*, vol. 494, no. 2, pp. 611–618, 2015.

[175] M. Homma, K. Sumiya, Y. Kambayashi, S. Inomata, and Y. Kohda, “Assessment of Clonidine Orally Disintegrating Tablet for Pre-anesthetic Medication in Pediatric Surgery,” *Biol Pharm Bull.*, vol. 29, no. 2, pp. 321–323, 2006.

[176] J. Greciet, “Positive Phase II preliminary results of Validive®,” *Onxeo*, 2014. [Online]. Available: http://www.onxeo.com/site/wp-content/uploads/2014/10/141030EN-Validive-Preliminary-Results.pdf. [Accessed: 06-Nov-2016].

[177] J. Giralt *et al.*, “Compliance and Patient Acceptability of Clonidine Mucoadhesive Buccal Tablet (Clonidine Lauriad) to Prevent Severe Radiomucositis in Head and Neck Cancer Patients,” *Int. J. Radiat. Oncol. Biol. Phys.*, vol. 93, no. 3, p. 213, 2015.

[178] E. M. Gamper *et al.*, “Taste alterations in breast and gynaecological cancer patients receiving chemotherapy: prevalence, course of severity, and quality of life correlates.,” *Acta Oncol.*, vol. 51, no. 4, pp. 490–6, 2012.

[179] S. Steinbach *et al.*, “Qualitative and quantitative assessment of taste and smell changes in patients undergoing chemotherapy for breast cancer or gynecologic malignancies.,” *J Clin Oncol.*, vol. 27, no. 11, pp. 1899–905, 2009.

[180] K. I. Coa *et al.*, “The Impact of Cancer Treatment on the Diets and Food Preferences of Patients Receiving Outpatient Treatment,” *Nutr Cancer.*, vol. 67, no. 2, pp. 339–53, 2015.

[181] A. Boltong *et al.*, “A Prospective Cohort Study of the Effects of Adjuvant Breast Cancer Chemotherapy on Taste Function, Food Liking, Appetite and Associated Nutritional Outcomes,” *PLoS One*, vol. 9, no. 7, p. e103512, 2014.

[182] S. Cafaggi, R. Leardi, B. Parodi, G. Caviglioli, E. Russo, and G. Bignardi, “Preparation and evaluation of a chitosan salt-poloxamer 407 based matrix for buccal drug

delivery," *J. Control. Release*, vol. 102, no. 1, pp. 159–169, 2005.

[183] H. S. Kaş, "Chitosan: properties, preparations and application to microparticulate systems.," *J. Microencapsul.*, vol. 14, no. 6, pp. 689–711, 1997.

[184] P. Ferreira, J. F. J. Coelho, K. S. C. R. dos Santos, E. I. Ferreira, and M. H. Gil, "Thermal Characterization of Chitosan-Grafted Membranes to be Used as Wound Dressings," *J. Carbohydr. Chem.*, vol. 25, pp. 233–251, 2006.

[185] J. Berger, M. Reist, J. M. Mayer, O. Felt, and R. Gurny, "Structure and interactions in chitosan hydrogels formed by complexation or aggregation for biomedical applications," *Eur J Pharm Biopharm.*, vol. 57, no. 1, pp. 35–52, 2004.

[186] M. Dash, F. Chiellini, R. M. Ottenbrite, and E. Chiellini, "Chitosan — A versatile semi-synthetic polymer in biomedical applications," *Prog. Polym. Sci.*, vol. 36, no. 8, pp. 981–1014, 2011.

[187] Y.-W. Cho, J. Jang, C. R. Park, and S.-W. Ko, "Preparation and Solubility in Acid and Water of Partially Deacetylated Chitins," *Biomacromolecules*, vol. 1, pp. 609–614, 2000.

[188] R. Hejazi and M. Amiji, "Chitosan-based gastrointestinal delivery systems," *J. Control. Release*, vol. 89, no. 2, pp. 151–165, 2003.

[189] L. Hu, Y. Sun, and Y. Wu, "Advances in chitosan-based drug delivery vehicles.," *Nanoscale*, vol. 5, no. 8, pp. 3103–11, 2013.

[190] D. T. N. Chen, Q. Wen, P. A. Janmey, J. C. Crocker, and A. G. Yodh, "Rheology of Soft Materials," *Annu. Rev. Condens. Matter Phys.*, vol. 1, pp. 301–322, 2010.

[191] M. A. Meyers and K. K. Chawla, "Elasticity and Viscoelasticity," in *Mechanical behavior of materials*, M. A. Meyers and K. K. Chawla, Eds. Upper Saddle River, NJ: Prentice Hall, 1999, pp. 98–103.

[192] J. Goldstein *et al.*, *Scanning Electron Microscopy and X-ray Microanalysis*, 3rd ed. New York: Springer, 2003.

[193] R. Mishra and A. Amin, "Formulation development of taste-masked rapidly dissolving films of cetirizine hydrochloride," *Pharm Technol*, vol. 33, no. 2, pp. 48–56, 2009.

[194] European Directorate for the Quality of Medicines (EDQM), "European Pharmacopeia Comission. Tablets," in *European Pharmacopoeia.*, Strasbourg, 2008.

[195] FDA U.S. Food and Drug Administration, "Guidance for Industry - Orally Disintegrating

Tablets," Silver Spring, 2008.

[196] C. M. Corniello, "Quick-dissolve strips: from concept to commercialization," *Drug Deliv Technol*, vol. 6, no. 2, pp. 68–71, 2006.

[197] S. D. Barnhart, "Thin film oral dosage forms," in *Modified release drug delivery technology*, 2nd ed., M. J. Rathbone, J. Hadgraft, M. Roberts, and M. Lane, Eds. London: Informa Healthcare Inc, 2008, pp. 209–16.

[198] K. . Peh and C. F. Wong, "Polymeric fils as vehicle for buccal delivery: swelling, mechanical, and bioadhesive properties," *J. Pharm. Pharm. Sci.*, vol. 2, no. 2, pp. 53–61, 1999.

[199] V. Garsuch, "Preparation and characterization of fast-dissolving oral films for pediatric use," Heinrich Heine University, Dusseldorf, 2009.

[200] V. Garsuch and J. Breitkreutz, "Novel analytical methods for the characterization of oral wafers," *Eur. J. Pharm. Biopharm.*, vol. 73, no. 1, pp. 195–201, 2009.

[201] B. C. Smith, *Fundamentals of Fourier Transform Infrared Spectroscopy*, 2nd ed. Boca Raton: CRC Press / Taylor & Francis, 2011.

[202] M. Tasumi, Ed., *Introduction to Experimental Infrared Spectroscopy: Fundamentals and Practical Methods*. Chichester: John Wiley & Sons, Ltd, 2015.

[203] P. R. Griffiths, J. A. de Haseth, and J. D. Winefordner, Eds., *Fourier Transform Infrared Spectrometry*, 2nd ed. New Jersey: Wiley, 2007.

[204] Brian C. Smith, *Infrared Spectral Interpretation: A Systematic Approach*. Boca Raton, FL: CRC Press / Taylor & Francis, 1999.

[205] M. Lee, *X-Ray Diffraction for Materials Research: From Fundamentals to Applications*. Boca Raton: Apple Academic Press, 2016.

[206] B. D. Cullity, *Elements of X-Ray Diffraction*, 2nd ed. Reading: Addison-Wesley, 1978.

[207] D. J. Burnett, F. Thielmann, and T. D. Sokoloski, "Investigating carbamazepine-acetone solvate formation via Dynamic gravimetric Vapor Sorption," *J. Therm. Anal. Calorim.*, vol. 89, no. 3, pp. 693–698, 2007.

[208] J. S. Boateng, A. D. Auffret, K. H. Matthews, M. J. Humphrey, H. N. E. Stevens, and G. M. Eccleston, "Characterisation of freeze-dried wafers and solvent evaporated films as potential drug delivery systems to mucosal surfaces," *Int. J. Pharm.*, vol. 389, no. 1–2, pp. 24–31, 2010.

[209] S. E. Hogan and G. Buckton, “The application of near infrared spectroscopy and dynamic vapor sorption to quantify low amorphous contents of crystalline lactose.,” *Pharm Res.*, vol. 18, no. 1, pp. 112–6, 2001.

[210] J. Sun, “The Use of Dynamic Vapor Sorption Method in the Determination of Water Sorption Limit and Setting Specification for Drug Substance,” *Am. Pharm. Rev.*, vol. 14, no. 6, 2011.

[211] G. Zhou *et al.*, “Determination and differentiation of surface and bound water in drug substances by near infrared spectroscopy,” *J. Pharm. Scienes*, vol. 92, no. 5, pp. 1058–1065, 2003.

[212] D. Q. M. Craig and M. Reading, *Thermal analysis of pharmaceuticals*. London: CRC Press / Taylor & Francis, 2007.

[213] A. W. Coats and J. P. Redfern, “Thermogravimetric Analysis: A Review,” *Analyst*, vol. 88, no. 1053, pp. 906–924, 1963.

[214] V. L. Hill, D. Q. M. Craig, and L. C. Feely, “Characterisation of spray-dried lactose using modulated differential scanning calorimetry,” *Int. J. Pharm.*, vol. 161, no. 1, pp. 95–107, 1998.

[215] P. G. Royall, D. Q. M. Craig, and C. Doherty, “Characterisation of the glass transition of an amorphous drug using modulated DSC,” *Pharm. Res.*, vol. 15, no. 7, pp. 1117–1121, 1998.

[216] P. G. Royall, D. Q. M. Craig, and C. Doherty, “Characterisation of moisture uptake effects on the glass transitional behaviour of an amorphous drug using modulated temperature DSC,” *Int. J. Pharm.*, vol. 192, no. 1, pp. 39–46, 1999.

[217] N. Soutari, A. B. M. Buanz, M. O. Gul, C. Tuleu, and S. Gaisford, “Quantifying crystallisation rates of amorphous pharmaceuticals with dynamic mechanical analysis (DMA),” *Int. J. Pharm.*, vol. 423, no. 2, pp. 335–340, 2012.

[218] S. Matsuoka, *Relaxation Phenomena in Polymers*. New York: Hanser Gardner Publications, 1992.

[219] W. Brostow and R. D. Corneliussen, *Failure of Plastics*. New York: Hanser Gardner Publications, 1986.

[220] K. P. Menard, *Dynamic Mechanical Analysis - A Practical Introduction*, 2nd ed. Boca Raton: CRC Press / Taylor & Francis, 2008.

[221] M. McCrum, B. Williams, and G. Read, *Anelastic and Dielectric Effects in Polymeric Solids*. New York: Dover, 1991.

[222] R. Bird, C. Curtis, R. Armstrong, and O. Hassenger, *Dynamics of Polymeric Liquids, Volume 2: Kinetic Theory*, 2nd ed. New York: Wiley, 1987.

[223] N. Gontard and S. Ring, “Edible Wheat Gluten Film: Influence of Water Content on Glass Transition Temperature,” *J. Agric. Food Chem.*, vol. 44, pp. 3474–3478, 1996.

[224] V. R. Meyer, *Praxis der Hochleistungs-Flüssigchromatographie*, 9. Auflage. Weinheim: Wiley-VCH, 2004.

[225] F. Lottspeich and J. W. Engels, *Bioanalytik*, 3. Auflage. Berlin: Springer Spektrum, 2012.

[226] J. Calvert, “Glossary of atmospheric chemistry terms (Recommendations 1990),” *Pure Appl. Chem.*, vol. 62, no. 11, pp. 2167–2219, 2009.

[227] B. Magnusson and U. Örnemark, “Eurachem Guide: The Fitness for Purpose of Analytical Methods – A Laboratory Guide to Method Validation and Related Topics,” 2014.

[228] European Medicines Agency (EMA), “Guideline on bioanalytical method validation,” London, 2011.

[229] X. Dai, J. G. Moffat, J. Wood, and M. Reading, “Thermal scanning probe microscopy in the development of pharmaceuticals,” *Adv. Drug Deliv. Rev.*, vol. 64, no. 5, pp. 449–460, 2012.

[230] N. Scoutaris *et al.*, “Development and Biological Evaluation of Inkjet Printed Drug Coatings on Intravascular Stent,” *Mol Pharm.*, vol. 13, no. 1, pp. 125–33, 2016.

[231] S. Khan, V. Trivedi, and J. Boateng, “Functional physico-chemical, ex vivo permeation and cell viability characterization of omeprazole loaded buccal films for paediatric drug delivery,” *Int. J. Pharm.*, vol. 500, no. 1–2, pp. 217–226, 2016.

[232] Y. Dong, Y. Ruan, H. Wang, Y. Zhao, and D. Bi, “Studies on Glass Transition Temperature of Chitosan with Four Techniques,” *J. Appl. Polym. Sci.*, vol. 93, pp. 1553–1558, 2004.

[233] Kumar M.N.V.R, “A review of chitin and chitosan applications.,” *React. Funct Polym*, vol. 46, pp. 1–27, 2000.

[234] B. Abu-Jdayil and D. A. Fara, “Modification of the Rheological Behaviour of Sodium

Alginate by Chitosan and Multivalent Electrolytes," *Ital. J. Food Sci.*, vol. 25, no. 2, pp. 196–201, 2013.

[235] D. Raafat and H. Sahl, "Chitosan and its antimicrobial potential – a critical literature survey," *Microb Biotechnol.*, vol. 2, no. 2, pp. 186–201, 2009.

[236] D. Park *et al.*, "Development of chitosan-based ondansetron buccal delivery system for the treatment of emesis," *Drug Dev. Ind. Pharm.*, vol. 38, no. 9, pp. 1077–83, 2012.

[237] R. H. Chen and M. L. Tsaih, "Effect of temperature on the intrinsic viscosity and conformation of chitosans in dilute HCl solution," *Int J Biol Macromol*, vol. 23, no. 2, pp. 135–141, 1998.

[238] A. K. Singla and M. Chawla, "Chitosan: some pharmaceutical and biological aspects--an update.," *J Pharm Pharmacol.*, vol. 53, no. 8, pp. 1047–1067, 2001.

[239] P. Mura, G. Corti, M. Cirri, F. Maestrelli, N. Mennini, and M. Bragagni, "Development of Mucoadhesive Films for Buccal Administration of Flufenamic Acid: Effect of Cyclodextrin Complexation," *J. Pharm. Sci.*, vol. 99, no. 7, pp. 3019–3029, 2010.

[240] A. B. Dhanikula and R. Panchagnula, "Development and Characterization of Biodegradable Chitosan Films for Local Delivery of Paclitaxel," *AAPS J.*, vol. 6, no. 3, pp. 88–99, 2004.

[241] A. Abruzzo, F. Bigucci, T. Cerchiara, F. Cruciani, B. Vitali, and B. Luppi, "Mucoadhesive chitosan/gelatin films for buccal delivery of propranolol hydrochloride," *Carbohydr. Polym.*, vol. 87, pp. 581–588, 2012.

[242] P. P. Dhawade and R. N. Jagtap, "Characterization of the glass transition temperature of chitosan and its oligomers by temperature modulated differential scanning calorimetry," *Adv Appl Sci Res*, vol. 3, no. 3, pp. 1372–1382, 2012.

[243] R. Anders and H. P. Merkle, "Evaluation of laminated muco-adhesive patches for buccal delivery," *Int. J. Pharm.*, vol. 49, pp. 231–240, 1989.

[244] M. J. Rathbone, B. K. Drummond, and I. G. Tucker, "The oral cavity as a site for systemic drug delivery," *Adv. Drug Deliv. Rev.*, vol. 13, no. 1–2, pp. 1–22, 1994.

[245] N. A. Nafee, N. A. Boraie, F. A. Ismail, and L. M. Mortada, "Design and characterization of mucoadhesive buccal patches containing cetylpyridinium chloride," *Acta Pharm.*, vol. 53, pp. 199–212, 2003.

[246] L. Panigrahi, S. Pattnaik, and S. K. Ghosal, "Design and characterization of

mucoadhesive buccal patches of salbutamol sulphate.," *Acta Pol Pharm.*, vol. 61, no. 5, pp. 351–60, 2004.

[247] S. A. Yehia, O. N. El-Gazayerly, and E. B. Basalious, "Fluconazole mucoadhesive buccal films: in vitro/in vivo performance.," *Curr Drug Deliv.*, vol. 6, no. 1, pp. 17–27, 2009.

[248] E. de Souza Costa-Junior, M. M. Pereira, and H. S. Mansur, "Properties and biocompatibility of chitosan films modified by blending with PVA and chemically crosslinked," *J. Mater. Sci. Mater. Med.*, vol. 20, pp. 553–561, 2009.

[249] T. Yoshioka, R. Hirano, T. Shioya, and M. Kako, "Encapsulation of mammalian cell with chitosan-CMC capsule.," *Biotechnol Bioeng.*, vol. 35, no. 1, pp. 66–72, 1990.

[250] F. G. Pearson, R. H. Marchessault, and C. Y. Liang, "Infrared spectra of crystalline polysaccharides. V. Chitin," *J. Polym. Sci.*, vol. 43, no. 141, pp. 101–116, 1960.

[251] T. Sannan, K. Kurita, and Y. Iwakura, "Studies on chitin. 2. Effect of deacetylation on solubility," *Makromol. Chem.*, vol. 177, pp. 3589–3600, 1976.

[252] T. Sannan, K. Kurita, K. Ogura, and Y. Iwakura, "Studies on chitin: (7) IR spectroscopic determination of degree of deacetylation," *Polymer (Guildf).*, vol. 19, pp. 458–459, 1978.

[253] T. Wang, M. Turhan, and S. Gunasekaran, "Selected properties of pH-sensitive, biodegradable chitosan–poly(vinyl alcohol) hydrogel," *Polym. Int.*, vol. 53, pp. 911–918, 2004.

[254] L. J. Bellamy, *The Infrared Spectra of Complex Molecules: Volume Two Advances in Infrared Group Frequencies*, 2nd ed. London: Chapman and Hall, 1980.

[255] K. Ogawa, "Effect of Heating an Aqueous Suspension of Chitosan on the Crystallinity and Polymorphs," *Agric. Biol. Chem.*, vol. 55, no. 9, pp. 2375–2379, 1991.

[256] E. Belamie, A. Domard, and M.-M. Giraud-Guille, "Study of the Solid-State Hydrolysis of Chitosan in Presence of HCl," *J. Polym. Sci.*, vol. 35, pp. 3181–3191, 1997.

[257] A. P. Martínez-camacho, M. O. Cortez-rocha, J. M. Ezquerra-brauer, and A. Z. Graciano-verdugo, "Chitosan composite films: Thermal, structural, mechanical and antifungal properties," *Carbohydr. Polym.*, vol. 82, pp. 305–315, 2010.

[258] M. Mucha and A. Pawlak, "Thermal analysis of chitosan and its blends," *Thermochim. Acta*, vol. 427, no. 1–2, pp. 69–76, 2005.

[259] A. Lazaridou and C. G. Biliaderis, “Thermophysical properties of chitosan, chitosan-starch and chitosan-pullulan Films near the glass transition,” *Carbohydr. Polym.*, vol. 48, pp. 179–190, 2002.

[260] Z. Zong, Y. Kimura, M. Takahashi, and H. Yamane, “Characterization of chemical and solid state structures of acylated Chitosans,” *Polymer (Guildf).*, vol. 41, pp. 899–906, 2000.

[261] K. Sakurai, T. Maegawa, and T. Takahashi, “Glass transition temperature of chitosan and miscibility of chitosan/poly(N-vinyl pyrrolidone) blends,” *Polymer (Guildf).*, vol. 41, pp. 7051–7056, 2000.

[262] F. S. Kittur, K. V Harish Prashanth, K. Udaya Sanka, and R. N. Tharanathan, “Characterization of chitin, chitosan and their carboxymethyl derivatives by differential scanning calorimetry,” *Carbohydr. Polym.*, vol. 49, no. 2, pp. 185–193, 2002.

[263] D. de Britto, S. P. Campana-Filho, and O. B. G. de Assis, “Mechanical Properties of N,N,N-trimethylchitosan Chloride Films,” *Polímeros Ciência e Tecnol.*, vol. 15, no. 2, pp. 142–145, 2005.

[264] ICH Harmonised Tripartite Guideline, “International Conference on Harmonisation of Technical Requirements for Registration of Pharmaceuticals for Human Use (ICH), Validation of analytical Procedures: Text and methodology Q2(R1),” 2005.

[265] B. Banfai, K. Ganzler, and S. Kemeny, “Content uniformity and assay requirements in current regulations,” *J. Chromatogr.*, vol. 1156, pp. 206–212, 2007.

[266] The United States Pharmacopeial Convention, “Uniformity of Dosage Units,” 2011.

[267] C. Woertz and P. Kleinebudde, “Development of orodispersible polymer films with focus on the solid state characterization of crystalline loperamide,” *Eur J Pharm Biopharm.*, vol. 94, pp. 52–63, 2015.

[268] C. F. Wong, K. H. Yuen, and K. K. Peh, “Formulation and evaluation of controlled release Eudragit buccal patches,” *Int J Pharm*, vol. 178, pp. 11–22, 1999.

[269] V. A. Perumal, T. Govender, D. Lutchman, and I. Mackraj, “Investigating a New Approach to Film Casting for Enhanced Drug Content Uniformity in Polymeric Films,” *Drug Dev. Ind. Pharm.*, vol. 34, no. 10, pp. 1036–1047, 2008.

[270] I. Pather and C. S. Kolli, “Chitosan,” in *Oral Mucosal Drug Delivery and Therapy*, M. J. Rathbone, S. Senel, and I. Pather, Eds. New York: Springer, 2015, pp. 37–52.

[271] J. Desbrieres, “Biomedical Applications of Amphiphilic Systems,” in *Polymeric Biomaterials: Structure and Function, Volume 1*, S. Dumitriu and V. Popa, Eds. Boca Raton, FL: CRC Press, 2013, p. 256.

[272] J. O. Morales, R. Su, and J. T. Mcconville, “The Influence of Recrystallized Caffeine on Water-Swellable Polymethacrylate Mucoadhesive Buccal Films,” *AAPS PharmSciTech*, vol. 14, no. 2, pp. 475–484, 2013.

[273] R. J. Verheul, M. Amidi, M. J. van Steenbergen, E. van Riet, W. Jiskoot, and W. E. Hennink, “Influence of the degree of acetylation on the enzymatic degradation and in vitro biological properties of trimethylated chitosans.,” *Biomaterials*, vol. 30, no. 18, pp. 3129–35, 2009.

[274] K. Tomihata and Y. Ikada, “In vitro and in vivo degradation of films of chitin and its deacetylated derivatives.,” *Biomaterials*, vol. 18, no. 7, pp. 567–75, 1997.

[275] L. Wei, C. Cai, J. Lin, L. Wang, and X. Zhang, “Degradation controllable biomaterials constructed from lysozyme-loaded Ca-alginate microparticle/chitosan composites,” *Polymer (Guildf).*, vol. 52, pp. 5139–5148, 2011.

[276] S. H. Pangburn, P. V Trescony, and J. Heller, “Lysozyme degradation of partially deacetylated chitin , its films and hydrogels,” *Biomaterials*, vol. 3, pp. 105–108, 1982.

[277] C. Yomota, T. Komuro, and T. Kimura, “Studies on the degradation of chitosan films by lysozyme and release of loaded chemicals,” *Yakugaku Zasshi.*, vol. 110, no. 6, pp. 442–8, 1990.

[278] S.-Y. Chen, “Comparison of the fine structure of the mucosa of cheek and hard palate in the rabbit,” University of Illinois Medical Center, 1970.

[279] M. Mehta, B. W. Kemppainen, and R. G. Stafford, “In vitro penetration of tritium-labelled water (THO) and [3H]PbTx-3 (a red tide toxin) through monkey buccal mucosa and skin.,” *Toxicol. Lett.*, vol. 55, no. 2, pp. 185–194, 1991.

[280] A. D. van Eyk and P. van der Bijl, “Comparative permeability of various chemical markers through human vaginal and buccal mucosa as well as porcine buccal and mouth floor mucosa,” *Arch. Oral Biol.*, vol. 49, no. 5, pp. 387–392, 2004.